

ABSTRACT

Title of dissertation: DEVELOPMENT OF A SIMULATION AND OPTIMIZATION
TOOL FOR HEAT EXCHANGER DESIGN

Haobo Jiang, Doctor of Philosophy, 2003

Dissertation directed by: Professor Reinhard Radermacher
Department of Mechanical Engineering

Heat exchangers have been used extensively and play an important role in the capital cost, energy efficiency and physical size of refrigeration and air conditioning systems. In this dissertation, a simulation and optimization tool to improve effectiveness and efficiency in design, rating, and analysis of air to refrigerant heat exchangers including conventional finned tube coils and emerging microchannel heat exchangers, Coil Designer, is developed and investigated using a general-purpose modeling concept and user-friendly interface. It is applicable to design of condensers, evaporators, and heating and cooling coils under any operating conditions.

A network viewpoint was adopted to establish the general-purpose model and allow for analysis of arbitrary tube circuitry and mal-distribution of fluid flow inside the tubes. Comprehensive evaluation of solutions to the highly nonlinear system of equations in the local thermal/hydraulic performance within the tube network was conducted and a new solution method to successively approximate the physics of heat and fluid flow was developed to enhance the solution convergence capability.

A segment-by-segment approach within each tube was implemented, to account for two-dimensional non-uniformity of air distribution across the exchanger, and heterogeneous refrigerant flow patterns through a tube. A further sub-dividable-segment model was created in order to address the significant change of properties and heat transfer coefficients in the single-phase and two-phase regime when a segment experiences flow regime change. The effectiveness-NTU method for cross-flow configuration was used also for combined heat and mass transfer problem under dehumidification, by defining equivalent thermal resistance and heat capacity.

Object-oriented programming techniques were applied in developing Coil Designer to facilitate flexible and customizable design platform and building graphic user-friendly interface. Coupled heat exchangers with multiple fluids inside different subsets of tubes can be modeled and analyzed simultaneously. A

wide variety of working fluids and correlations of heat transfer and pressure drop are available at the user's choice. The tabular and graphic representation of performance simulation results provides convenience in comprehensive and detailed parametric analysis.

The model prediction with Coil Designer was verified against experimentally determined data collected from a number of sources. The simulation tool was shown to be able to predict the heat transfer rate for a variety of coils with good accuracy. Parametric studies were conducted to confirm the capability of the program in exploring all aspects of heat exchanger performance under a wide variation of design and operating conditions.

A genetic algorithm is introduced and integrated with the simulation tool for single and multi-objective optimization design of heat exchanger to accomplish the following goals quickly and accurately: achieve optimum circuitry selection, minimize volume, minimize the amount of material utilized in the coil and thus minimize overall cost of the coil while achieving the best possible performance.

DEVELOPMENT OF A SIMULATION AND OPTIMIZATION TOOL FOR HEAT
EXCHANGER DESIGN

by

Haobo Jiang

Dissertation submitted to the Faculty of the Graduate School of the
University of Maryland at College Park in partial fulfillment
of the requirements for the degree of
Doctor of Philosophy
2003

Advisory Committee:

Professor Reinhard Radermacher, Chair/Advisor
Professor Henry King
Associate Professor Jungho Kim
Associate Professor Tien-Mo Shih
Assistant Professor Steven Buckley

DEDICATION

Dedicated
to
my parents

ACKNOWLEDGEMENT

I would first like to thank my advisor Dr. Reinhard Radermacher for providing me the opportunity and support to pursue advanced education and research at the University of Maryland, College Park. His invaluable guidance and encouragement will go a long way in shaping my future both in my professional and personal development. My appreciation also goes to the other committee members, Drs. S. Buckley, J. Kim, H. King, and T. Shih, for serving on my dissertation committee and reviewing my dissertation.

I am indebted to my father and mother, my wife and son, my sister and brother, who believe in me, and support me to do my best. I would also like to extend a warm thanks to my colleagues, Vikrant Aute, Dave Richardson, Dr. Yunho Hwang, and Hans-Joachim Huff, for their continuous help and cooperation.

TABLE OF CONTENTS

TABLE OF CONTENTS	iv
LIST OF TABLES	vii
LIST OF FIGURES	viii
LIST OF ABBREVIATIONS	xiii
INTRODUCTION	1
1.1 Overview	1
1.2 Motivation	3
1.3 Heat Exchanger Models and Simulation Tools	4
1.4 Heat Exchanger Optimization	9
1.5 Summary of Literature Review	12
1.6 Objectives of Research	13
HEAT EXCHAHNEGR MODELING	20
2.1 Junction and Junction-Tube Connectivity Matrix	22
2.1.1 Definition	22
2.1.2 JTA Validation	23
2.1.3 Junction Numbering	24
2.2 Tube Numbering and Location	24
2.3 Tube Segmentation	25
2.4 Tube Direction	25
2.5 Multiple Working Fluids	26
2.6 Non-Uniform Air Distribution and Fin Spacing	27
2.7 Modeling Assumption	27
2.8 Input and Output	28
2.9 Refrigerant Side Modeling	29
2.10 Modeling of Heat Transfer between Refrigerant and Air	33
2.10.1 Dry Surface Condition	33
2.10.2 Wet Surface Condition	36
2.11 Air Side Mass, Energy Flow and Pressure Drop	42
2.12 Sub-Dividable Segment in Case of Flow Regime Change within the Segment	43
2.13 Solution Methodology	46
2.14 Heat Transfer, Pressure Drop and Fin Efficiency Correlations	48
MODEL VALIDATION	63
3.1 Model Agreement with Experimental Data in Literature	63
3.2 Model Agreement with Experimental Data in Laboratory	65
3.2.1 A-Type Coil	65
3.2.2 Micro-channel Heat Exchanger	67
3.3 Model Agreement with Test Data of Commercial Products	68
3.3.1 A Coil for Refrigerator Application	68
3.3.2 An Integrated Absorber/Condenser Coil	69

SIMULATION STUDY	86
4.1 Modeling of a Coil with Arbitrary Circuitry	86
4.2 Model Improvement Results	88
4.2.1 Subdivided Segments.....	88
4.2.2 ϵ -NTU Method versus Arithmetic Average Temperature Difference Method	89
4.3 Examples of Tube-Level and Segment-Level Analysis	89
4.3.1 Comparison of Cross-counter Flow and Cross-parallel Flow.....	89
4.3.2 Refrigerant Side Heat Transfer Coefficients at Segments	90
4.3.3 Latent and Sensible Heat Duty at Tubes	91
4.4 Non-uniform Air Flow and Fin Spacing	91
4.4.1 Non-uniform Air Flow.....	91
4.4.2 Non-uniform Fin Spacing.....	92
4.5 ϵ -NTU Relationship Study.....	93
4.6 Effect of Air Flow Rate and Humidity on the Latent Heat Ratio.....	94
DESIGN OPTIMIZATION CASE STUDY	107
5.1 Introduction	107
5.2 An Overview of Genetic Algorithms	110
5.3 Constraint Handling and Multi-Objective Optimization	112
5.3.1 Constraint Handling.....	112
5.3.2 Multi-Objective Optimization.....	114
5.4 PGAPack and MOGA	116
5.4.1 Introduction.....	116
5.4.2 Key GA Parameters.....	116
5.5 Single Objective Optimization	117
5.5.1 Single Objective Optimization without Constraints	117
5.5.2 Heat Transfer Surface Area Minimization.....	120
5.5.3 Volume Minimization	122
5.6 Two-Objective Optimization	124
5.6.1 Area and Volume Minimization of the Benchmark Water Coil	124
5.6.2 Minimal Fan Power and Maximal Heat Duty of a Heat Pipe Heat Exchanger	127
5.6.3 Minimal Fan Power and Weight Design of a Condenser	130
5.7 Circuitry Optimization of an Interlaced Heat Exchanger.....	131
GRAPHIC USER INTERFACE.....	146
6.1 Introduction	146
6.2 Entering Data and Setup of a Heat Exchanger	147
6.2.1 Geometric Size and Dimensions	147
6.2.2 Working Fluids.....	148
6.2.3 Heat Transfer Coefficients and Pressure Drop.....	149
6.2.4 Tube Circuitry Design.....	150
6.2.5 Unit System	151
6.3 Output Data Processing.....	152
CONCLUSIONS	166

7.1 Development of a Comprehensive Simulation Tool	166
7.2 Validation of Results from Coil Designer	170
7.3 Parametric Studies Using Coil Designer	170
7.4 Optimization using Genetic Algorithms with Coil Designer.....	171
FUTURE WORK.....	172
Appendix	173
REFERENCES	179

LIST OF TABLES

Table 2.1 Junction-Tube Connectivity Matrix.....	51
Table 2.2 Summary of System of Hydraulic/Energy Equations	52
Table 3.1 Specifications and Operating Conditions of the McQuiston Coils	72
Table 3.2 Specifications and Operating Conditions of the Indoor A-Type Coils .	73
Table 3.3 Specifications and Operating Conditions of Gas Cooler	74
Table 3.4 Specifications and Operating Conditions of A Commercial Coil	75
Table 5.1 Specifications of a Benchmark Coil	133
Table 5.2 Area Minimization of the Benchmark Water Coil	133
Table 5.3 Tube Diameters, Tube Patterns and Fin Pitch Available	134
Table 5.4 Optimization Results for Minimizing Volume of a Water Coil	134
Table 5.5 Area/Volume Minimization of the Benchmark Water Coil	135
Table 5.6 Heat Pipe Heat Exchanger Optimization Results	136
Table 5.7 Design Optimization Results for a Condenser	137

LIST OF FIGURES

Figure 1.1 Water/Glycol/Brine Coils.....	15
Figure 1.2 Evaporator Coils.....	15
Figure 1.3 Condenser Coils.....	16
Figure 1.4 Steam Coils.....	16
Figure 1.5 In-Stock Multi-Purpose Coil.....	16
Figure 1.6 An OEM Coil.....	17
Figure 1.7 Special Coils.....	17
Figure 1.8 Commercial Fin-and-Tube Coils.....	18
Figure 1.9 OEM Fin-and-Tube Coils and Microchannel Heat Exchangers for HVAC & R Application.....	18
Figure 1.10 Directions of Air Flow into Coils.....	18
Figure 1.11 Coils with Different Circuitries.....	19
Figure 2.1a Schematic Diagram of a General Cross Flow Heat Exchanger.....	53
Figure 2.1b Flat Tubes with Microchannels.....	54
Figure 2.2 Schematic to Explain Junction-Tube Connectivity Matrix (JTA).....	54
Figure 2.3 Tube Numbering and Location.....	55
Figure 2.4 Tube Segmentation Example.....	55
Figure 2.5 Refrigerant Flow Directions inside Tubes.....	56
Figure 2.6 Non-uniform Fin Spacing.....	57
Figure 2.7 Refrigerant Side Mass and Energy Flow in a Tube Network.....	57

Figure 2.8 Bend Length Dependent on Tube Configuration	58
Figure 2.9 Segment as a Single Heat Exchanger.....	58
Figure 2.10 Linearized Air Dehumidification Process on the Psychometric Chart	59
Figure 2.11 Air Side Mass and Energy Flow	60
Figure 2.12 Schematic Diagram of Sub-Divided Segment	61
Figure 2.13 Flow Chart of the Solution Methodology.....	62
Figure 3.1 Water Coils McQuiston Tested.....	76
Figure 3.2 Heat Duty Comparison with the Experimental Data of McQuiston's Coils	77
Figure 3.3 Outlet Air Dry Bulb Temperature Comparison with the Experimental Data of McQuiston's Coils	77
Figure 3.4 Outlet Air Wet Bulb Temperature Comparison with the Experimental Data of McQuiston's Coils	78
Figure 3.5 An A Type Indoor Coil	79
Figure 3.6 Comparison of Outlet Air Temperature of the A Type Coil in Cooling Mode	80
Figure 3.7 Comparison of Outlet Air Temperature of the A Type Coil in Heating Mode	80
Figure 3.8 A Carbon Dioxide Gas Cooler	81
Figure 3.9 Comparison of Carbon Dioxide Outlet Temperature of the Gas Cooler	82

Figure 3.10 Comparison of Air Outlet Temperature of the Gas Cooler.....	82
Figure 3.11 A Commercial Coil for Refrigerator Application	83
Figure 3.12 Heat Duty Comparison of the Commercial Coil	83
Figure 3.13 An Intertwined Absorber/Condenser Coil	84
Figure 3.14 Comparison of the Temperatures along the Condenser Circuit.....	84
Figure 3.15 Comparison of the Temperatures along the Absorber Circuit.....	85
Figure 4.1 A Coil with Arbitrary Circuitry.....	95
Figure 4.2 Air Side Enthalpy Residual	96
Figure 4.3 Mass Flow Rate Residual at Junctions.....	96
Figure 4.4 Mass Flow Rate of Each Tube in Coil with Arbitrary Circuitry.....	97
Figure 4.5 Comparison of Heat Duty w/o Sub-divided Segment Model.....	97
Figure 4.6 Comparison of ϵ -NTU and Average Temperature Difference Method	98
Figure 4.7 Cross-Counter and Cross-Parallel Flow	98
Figure 4.8 Refrigerants and Air Temperature	99
Figure 4.9 Heat Capacity of Each Tube.....	99
Figure 4.10 Local Heat Transfer Coefficients of Refrigerant Side.....	100
Figure 4.11 Local Temperature of Refrigerant.....	100
Figure 4.12 Sensible and Latent Heat of Tubes	101
Figure 4.13 Refrigerant Temperature Profile with Non-Uniform Air Flow.....	101
Figure 4.14 Air Temperature Profile with Non-Uniform Fin Spacing	102
Figure 4.15 Air Temperature Profile with Uniform Fin Spacing.....	103
Figure 4.16 Cross-counter Flow Configuration	104

Figure 4.17 Effect of Tubes per Row on Exchange Effectiveness	104
Figure 4.18 Effect Number of Rows on Exchange Effectiveness.....	105
Figure 4.19 Effect of Circuitry (Configuration) on Exchange Effectiveness	105
Figure 4.20 Effect of Humidity and Air Flow on Latent Heat Ratio.....	106
Figure 5.1 Flowchart of Genetic Algorithm	138
Figure 5.2 Graphic Representations of the Design Variables	139
Figure 5.4 Schematic Diagram of a Benchmark Water Coil	140
Figure 5.5 Schematic of a Multi-Stream Coil	141
Figure 5.6 Pareto Optima Front in a Population	141
Figure 5.7 Schematic of a Heat Pipe Heat Exchanger	142
Figure 5.8 Pareto Solutions of Heat Pipe Heat Exchanger Design.....	143
Figure 5.9 Pareto Solutions of Condenser Design.....	143
Figure 5.10 Basic Circuitry Comparison in Terms of Heat Duty	144
Figure 5.11 Circuitry Optimization on an Interlaced Heat Exchanger	145
Figure 5.12 Uniform vs. Non-Uniform Air Distribution.....	145
Figure 6.1 Setup of a New Heat Exchanger	153
Figure 6.2 GUI for Specifying Tube Parameters.....	154
Figure 6.3 GUI for Specifying Fin Types and Parameters	155
Figure 6.4 GUI for Specifying Working Fluid inside the Tube	155
Figure 6.5 GUI for Choosing Heat Transfer Coefficient (or Pressure Drop)	156
Figure 6.6 The Main Interface for Fin-and-Tube Coil Construction.....	157

Figure 6.7 The Main Interface for Micro-Channel Heat Exchanger Construction	158
Figure 6.8 GUI for Specifying Inlet Stream Properties.....	159
Figure 6.9 GUI for Specifying Inlet Air Properties.....	160
Figure 6.10 GUI for Editing Tube Connection.....	161
Figure 6.11 Output Window of the Predicted Performance	162
Figure 6.12 Output Window of the Working Fluid Properties (Quality)	162
Figure 6.13 Output to MS Excel Spreadsheet	163
Figure 6.14 Window for Parametric Analysis.....	164
Figure 6.15 Parametric Analysis of the Heat Exchanger Performance.....	165

LIST OF ABBREVIATIONS

A	Area
a	A coefficient
b	A coefficient
b	Allele
b	Allele
c	A coefficient
C, c	Constants, Heat Capacity
c_p	Specific heat capacity
D, d	Diameter
DP	Pressure drop
f	Objective function name
g	Gravity constant
g,G	Inequality Constraint function
h	Specific enthalpy, convective heat transfer coeff.
h	Equality Constraint function
h_d	Mass transfer coefficient
h_{fg}	Evaporation heat (latent heat)
i,j	Index for junction or tube numbering, location
iCircuitry	An integer represent a particular circuitry
JTA	Junction-tube connectivity matrix

k	Index of segment, thermal conductivity
k	Integer
l	Length
L	Length
l	Length of bits
L	Lower limit of a decimal number
L	Function
Le	Lewis number
\dot{m}	Mass flow rate
m	A parameter
N	Number of segments, tubes, rows, columns
n	Number of variables
N_{col}	Number of columns of the tube array
N_{row}	Number of rows of the tube array
NTU	Number of transfer units
P	Pressure, Circumference
P	Fan Power
pop	Population size
Q	Heat transfer rate, heat duty
q	Heat flux
R	Heat transfer resistance
r	A coefficient

s	Fin spacing
s	<i>Stream</i>
S_l	Tube horizontal spacing
S_t	Tube vertical spacing
T	Temperature
t	Tube
T_{col}	Index of tube location at the column of tube array
T_{dir}	Index indicating direction of fluid flow inside tubes
T_{row}	Index of tube location at the row of tube array
U	Upper limit of a decimal number
UA	Overall heat transfer conductance
V	Velocity
V	Volume
x	Horizontal coordinate
x	Fraction of length
x	Variable
y	Vertical coordinate

Greek

ε	<i>Heat transfer effectiveness</i>
ε	A small number
η	<i>Fin efficiency</i>

η_m	Fin efficiency of combined heat and mass transfer
η_{ms}	Surface effectiveness of combined heat and mass transfer
η_s	<i>Surface effectiveness</i>
θ	<i>Angle</i>
ρ	<i>Density</i>
ϕ	<i>Relative humidity</i>
ω	Humidity ratio

Subscript

∞	Mainstream
a	Air
a	Acceleration
av	Average
c	Fin-tube Contact
c	Cross-sectional
env	Environment
f	Fouling, friction, fin
g	Gravitation
i	Index of tube
in	Inlet, inside
j	Index of tube

k	Index of segment
out	Outlet, outside
ref	Refrigerant
res	Residual
s	Surface
sat	Saturated
w	Wall

Chapter 1

INTRODUCTION

1.1 Overview

As energy costs become very important in today's industrial, residential, and commercial settings, the rational use of energy is now a primary design and management objective. The air-conditioning, refrigeration, and heating equipment consume a large part of electrical energy on a global level. For example, almost 20% of the total US energy consumption is in HVAC & R applications (DOE, 1998, 1999, 2001). The research and progress have been going a long way toward improving the energy efficiency of the systems, by means of innovative system and component design.

In dealing with the high-energy costs, simulation and optimization of the energy-consuming equipment and systems and its operating conditions, with the aid of computer, has been becoming increasingly popular and gaining great momentum. On the other side, many of today's manufacturers of thermal/fluid products such as heat exchangers, refrigerators, heat pumps, and air conditioners are challenged with reducing the time to market, reducing the cost of design, and achieving designs that perform as expected on the first try. They are

making increased use of “virtual prototyping” where a computer model is replacing the physical prototype.

Plate-fin-tube and microchannel heat exchangers (often referred to as “coil”) made of copper, aluminum, steel, and other materials, are the major components of the HVAC & R systems. They are also used in a wide range of other applications, such as food processing, commercial laundry, petrochemical, transportation, textile, pulp and paper, ammonia, plastic and pharmaceutical industries, to transfer heat between air and fluid (refrigerant, water, water-glycol, ammonia-water, or oil), and they play a vital role in the manufacturing cost and energy consumption of the systems. Figures 1.1 through 1.9 illustrate graphically a large assortment of heat exchanging coils according to their functionality and applications, whereas Figure 1.10 and Figure 1.11 exemplify different air flow arrangement and fluid circuitry respectively. Due to the complexity in terms of geometry, tube arrangement, circuitry, non-uniformity of airflow, thermal and hydraulic phenomena in multi-phase flow, and variety of the working fluids, it appears infeasible to accurately and rapidly predict the performance of these coils by analytical or graphic design approaches as described in many conventional heat exchanger and HVAC handbooks.

In this thesis, Coil Designer, a simulation and optimization tool for design of air-to-fluid heat exchangers, is introduced. It distinguishes itself by providing

the greatest generality and flexibility, providing a user-friendly graphical interface, and integrating genetic algorithm for optimization of designs.

1.2 Motivation

In recent decades, a number of mathematical models and simulation tools have been developed for design and rating of thermal/fluid components and systems, including heat exchangers. However, the usage of these models and tools is restricted by the fact that they are tailored to very specific existing systems or component applications. The lack of flexibility and generality of these models makes it time-expensive to develop new products.

Nonetheless, commercially available software tools for simulation of general thermal/fluid systems and components are now emerging. Some of them are sophisticated in their models and solution philosophy, but lack graphical user interfaces, and require considerable time and effort to learn how to use. The user is expected to do some programming as a necessary part of the entire modeling system. Thus, the building of models is time consuming and expensive.

Manufacturers are demanding an integrated approach to the simulation and optimization of both components and systems. A flexible modular modeling environment, which allows the user to specify components and then construct a thermal system by linking the components in a certain order on the computer

screen, will have the benefits of fast evaluation of many design alternatives, and more options to evaluate and find optimal designs. The heat exchanging coil, when considering the finned tube as a component, and the circuitry and the air passage as the link between components, is a sub-thermal system and should be modeled with great generality.

Moreover, a built-in optimization program will help the designer to meet cost, compactness, and heat duty requirement, by optimizing the geometry parameters and operating conditions of the heat exchangers.

The development of a universally applicable software package for simulation of air-cooled heat exchangers, has been motivated by the growing need of the market and the user.

1.3 Heat Exchanger Models and Simulation Tools

Computer models and simulation tools have been developed for heat exchanger design and optimization since the 1980s, with increasing complexity of the calculation procedure, detail of the coil parameter input, and range of working fluids.

Domanski (1991) developed a Fortran simulation model EVSIM for plate-fin-tube evaporator in residential air conditioning. It accounted for the non-

uniform velocity distribution of the one-dimensional air flow at the frontal face, as well as the non-uniform distribution of the refrigerant flow among individual circuits after splitting at a particular location in the coil. Certain correlations were used to calculate the heat transfer coefficients and pressure drops on both the refrigerant side and air side. A tube-by-tube approach is used to analyze the performance of each tube separately. Individual refrigerant property and mass flow rate as well as air property and mass flow rate are assigned to each tube and calculated in a proper order depending on the refrigerant circuitry and air stream. Coil data is input from a data file. A major shortcoming is that the air flow mal-distribution can only be addressed on a tube level (one-dimensional), whereas in real life the air distribution is almost always two-dimensional non-uniform.

Based on his simulation models EVSIM, Domanski (1999, 2003) further introduced a software package EVAP-COND for finned-tube evaporator and condenser, using graphic user interface with the overall performance shown in tabular form. No choice for correlations of heat transfer and pressure drop is available. The circuitry design is limited to typical evaporator or condenser configuration.

Kempiak (1992) developed a three-zone (desuperheating, condensing, and subcooling) model for a condenser tested in a mobile air conditioning

system. The overall heat transfer coefficients of the three zones and the friction factor were determined from a least-square analysis of experimental data.

In his PhD research, Mirth (1993) fundamentally studied the heat transfer on chilled-water cooling coils under dehumidifying condition. There were three models developed respectively for the tube surface and fin surface, based on either single potential or dual potential drive for the heat transfer between the air stream and the coil surface. Linear relationships between the temperature (dry bulb, wet bulb) and the humidity/enthalpy of the moist air were assumed in order to determine the fin temperature distribution and fin efficiency. One of the models can account for partially condensing fin when the fin base temperature is less than whereas the fin tip temperature is higher than the dew point temperature of the free air stream.

Ragazzi (1995) implemented three combined heat and mass transfer models (namely, discretized differential equations model, thermal resistance model, and equivalent effectiveness model) in simulation and thermodynamic optimization of evaporators with zeotropic refrigerant mixtures. He found that in case of moisture removal, only the discretized differential equations model properly accounted for the sensible heat ratio.

The computational model presented by Bensafi (1997) discretizes plate-fin-tube coil into tube elements and solves the associated governing equations of each element with local values of temperature, pressure and heat transfer coefficient. The working fluids include water, R22, R134a, and some refrigerant mixtures. The coil geometry and circuitry, and operating parameters are given thorough an input file. The computation algorithm starts at the inlet tube and tracks the refrigerant flow to the exit. The outlet air temperature/humidity and refrigerant temperature/quality of each element are repeatedly calculated and updated until the difference of the successive values of these properties are within a pre-specified tolerance. When there are multiple circuits in a coil, the refrigerant flows in each branch are calculated iteratively to yield the same pressure drop.

In a procedure for the performance prediction of chilled water coils, Vardhan (1998) calculated the local heat transfer at each tube segment with effectiveness-NTU method. Under wet conditions, parallel flow is assumed instead of cross flow as the coolant heat capacity is much larger than that of air.

Corberan (1998) made a comparative study of a number of correlations for both heat transfer and pressure drop on the refrigerant side, in modeling of the plate finned tube of evaporators and condensers working with R134a. An experimental study was made to validate the model. The pressure drop of the

two-phase flow is expressed as the sum of the frictional, momentum, gravitational, and local (at the 180° bends) pressure drops.

Liang (2001) used a hierarchical system consisting of branch, tube, and control volume to develop a general program that can simulate evaporator coils with splitting and joining. To balance the increase of the heat transfer coefficient and pressure drop in the high vapor quality region and reduce the pressure gradient in the superheating region, the author suggested using a suitable refrigerant flow circuitry changing the refrigerant mass velocity along its flow path to improve the coil performance.

Oliet (2002) presented his model of dehumidifying coils based on the analysis and solution of mass and energy balance of the dry air, water vapor and water condensate film in each control volume within the coil. He also considered the heat conduction through the fins by a two-dimensional discretization of the fins.

Commercially available simulation tools are now emerging in response to the growing demand for design and optimization of heat exchangers. HTFS offers heat exchanger design software depending on the types of the heat exchangers, such as air-cooled, shell and tube, and plate-fin heat exchangers (AEA Technology Engineering Software Hyprotech, 2001). ACX and STX are

software packages for the designing, rating and evaluation of air-cooled heat exchangers and shell and tube heat exchangers, respectively (Heat Transfer Consultants, 2001).

1.4 Heat Exchanger Optimization

Optimization of heat exchanger design has been a long-existing research topic since 1950's, especially in the chemical processing industry (Bulck, 1991, Fax, 1957, Hedderich, 1982, Jegede, 1992, Kovarik, 1989), where analytical solutions for the performance of the heat exchanger are adopted and conventional gradient-based optimization methods are used. The relationship between the area of the heat exchangers and the power requirement of both sides of the fluid streams was explicitly derived by simplified assumption.

Hedderich(1982) developed a model for analysis of air-cooled heat exchangers, which was coupled with a numerical optimization program to produce an automated heat exchanger design. A general iteration-free approximation method was used for the analysis, which calculated the mean overall heat transfer coefficient and overall pressure drop for many flow arrangements. Under given tube arrangement (number of tubes, number of rows, number of passes), the continuous variables such as tube diameter, tube length, fin spacing, and tube pitch were optimized to meet requirement of minimum

volume, heat transfer area, air horsepower, or tube side pressure drop, subject to a given heat transfer rate between air and water.

Bulck(1991) theoretically investigated optimal design of cross-flow heat exchangers based on his observation that the transfer area is not effectively used due to non-uniform distribution of the heat transfer across the body of the exchanger. He suggested that along the diagonal of the exchanger denser surface should be used, while less compact area surfaces are used for the other parts. A substantial saving on the transfer area and reduced pressure drop can be achieved following his perspective design guideline.

Ragazzi (1995, 1996) conducted thermodynamic optimization of evaporators with zeotropic refrigerant mixtures, based on computer simulation model. The entropy generation associated with the heat transfer and pressure drop of both the refrigerant side and the air side is the objective function to be minimized. The effect of number of coil rows and tube diameter on the overall heat exchanger performance is investigated.

Ragazzi and Pederson (Ragazzi, 1996) looked into tube diameters and numbers of rows that minimized HX irreversibility in wet and dry evaporators using a tube-by-tube approach. Two circuits with smooth tubes were assumed.

The heat transfer was found to be the dominant source of irreversibility, over pressure drop and tube arrangement.

In optimization analysis of a micro-channel condenser design, Heun and Dunn (1996) found that for a given port diameter, the pressure drop effect provided an optimum relationship between the number of parallel refrigerant passages and the heat exchanger length. The cross-flow heat exchanger effect interacted with pressure drop effect. There existed an optimum combination of the number of ports and the number of tubes that minimized condenser volume for a given port diameter.

Reneaume (2000) used a sizing procedure to evaluate the objective function and the constraints, and HSQP algorithm to optimize plate fin heat exchangers. The program allows optimization of the fins, the core and the distributor, under given design and operating constraints such as pressure drops, maximum stacking height, to minimize capital cost, total volume or other objectives of the heat exchangers.

Thermodynamic optimization of heat exchangers, based on second law analysis, aims to irreversibility loss minimization, has been studied since 1970s (Bejan, 1977, London, 1983, Vargas, 2001, Zubair, 1987). The entropy generation due to heat transfer can be decoupled from that due to fluid friction,

and the effect of the dimensional and operating parameters on the irreversibility can be analyzed for heat exchanger design purpose.

Recently there is an increasing interest in applying genetic algorithms (GA) to the heat exchanger optimization. Schmit et al (1996) used GA to improve both the thermal and hydraulic performance of a high intensity cooler by optimizing a mix of discrete and continuous design variables. Aimed at minimizing heat transfer area required for a given heat duty, Tayal et al (1999) adopted GA to solve a large-scale, combinatorial and discrete optimization problem involving a black-box shell-and-tube heat exchanger model. The tube length, number of shells and baffles, tube and shell orientation, and other variables are optimized with considerable computational savings.

1.5 Summary of Literature Review

Heat exchanger design is becoming more dependent on performance prediction and parametric study with computational models and tools. Air-cooled fin-and-tube (including micro-channel tube) heat exchanger, as a common component of the refrigeration system, has been an object of simulation study using computer procedures for years together with emerging commercial modeling tools. Researchers adopt either phase-zone analysis, or tube-by-tube approach, or distributed model, in developing their simulation programs. Most of the models are geared toward a particular tube configuration and circuitry, fixed refrigerant,

and uniform air distribution, with particular correlations or empirical values of heat transfer and pressure drop on the air side and refrigerant side. The agreement between the predicted heat duty and the experimental data are usually much better than those for pressure drop. The uncertainty or negligence of the pressure drop owing to bends, headers, circuit splitting, change of momentum, gravitation, and impact of compressor oil, leads to considerable deviation of the predicted pressure drop from the measured values. Of the simulation programs, the input and output of the parameters are typically generated within data files, short of graphic user interface.

Heat exchanger optimization is mostly carried out on the basis of analytical solution of the performance as function of the continuous variables. Gradient-based optimization programs are widely used due to small scale of computation cost and analytical solution space.

1.6 Objectives of Research

The primary objective of this dissertation is to develop a general-purpose and comprehensive simulation tool, Coil Designer, to design air-to-refrigerant heat exchangers (including finned tube coils and micro-channel heat exchangers) based on prediction of their thermal and hydraulic performance. It is the further objective to integrate an optimization program with this tool to address any

combination of design requirements and improve speed and efficiency in design, rating, and analysis of heat exchangers in a single package.

More specifically, there are four major objectives in this study to be achieved:

1. Develop a powerful simulation tool with the major features as below.
 - Convenience for circuitry design.
 - Allowing for multiple working fluids in interlaced heat exchangers.
 - Accounting for two-dimensional non-uniform air distribution, fin spacing, and mal-distribution of refrigerant flow.
 - Flexibility in using correlations of heat transfer and pressure drop.
 - Abundant choice of working fluids.
 - Highly efficient and intuitive graphical user interface for engineering use.
2. Validate the simulation tool with experimental data collected from a number of sources.
3. Conduct parametric studies with the simulation tool to confirm its capability in exploring all aspects of heat exchanger performance and design.
4. Integrate optimization programs with the simulation tool to achieve optimal design variables, meet single or multi design objectives given any constraints, in an efficient way.

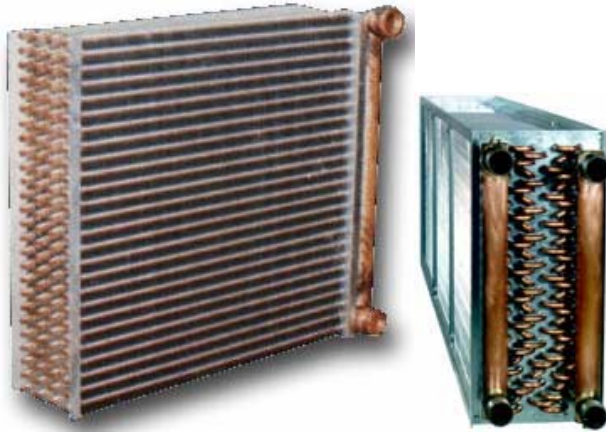


Figure 1.1 Water/Glycol/Brine Coils

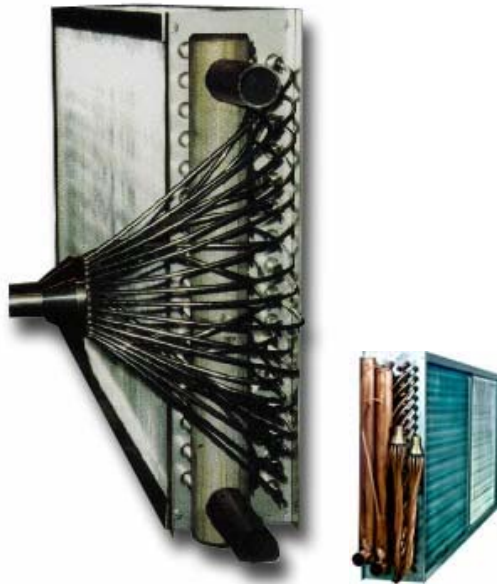


Figure 1.2 Evaporator Coils



Figure 1.3 Condenser Coils



Figure 1.4 Steam Coils



Figure 1.5 In-Stock Multi-Purpose Coil

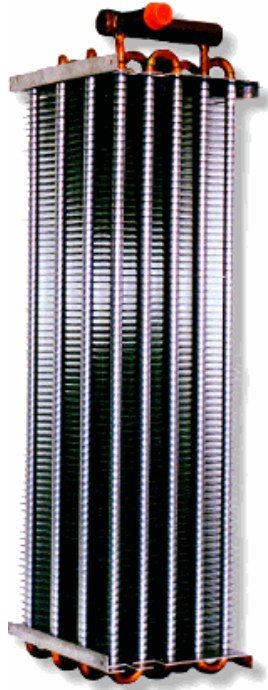


Figure 1.6 An OEM Coil

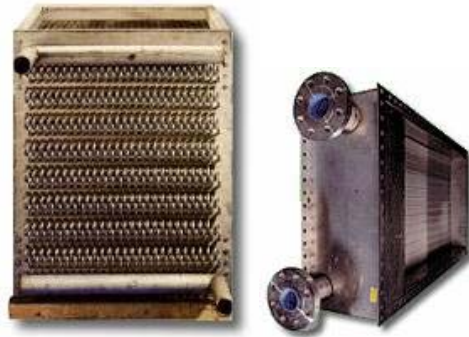


Figure 1.7 Special Coils



Figure 1.8 Commercial Fin-and-Tube Coils



Figure 1.9 OEM Fin-and-Tube Coils and Microchannel Heat Exchangers for HVAC & R Application

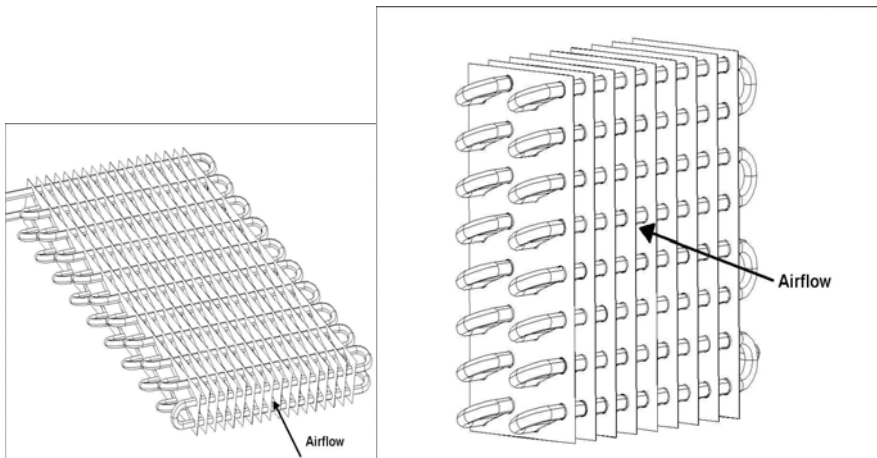


Figure 1.10 Directions of Air Flow into Coils

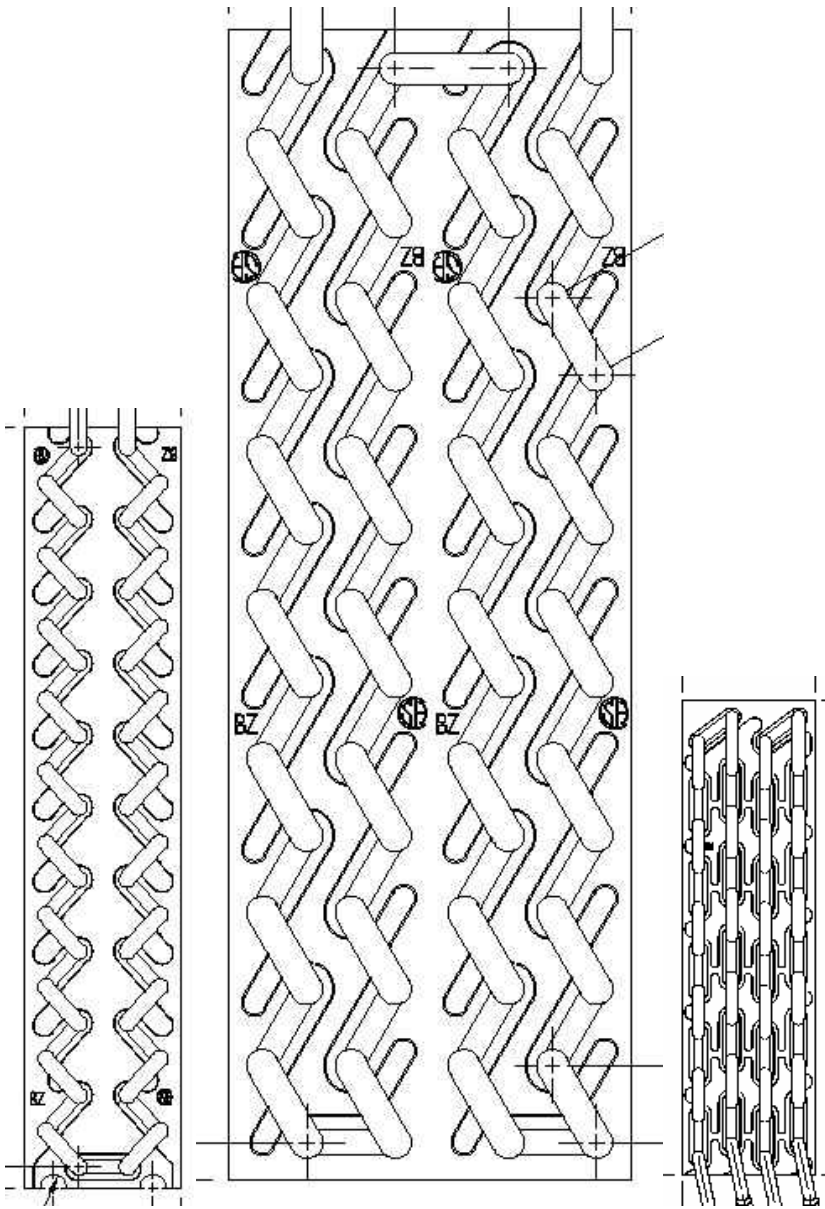


Figure 1.11 Coils with Different Circuitries

Chapter 2

Comment [RR1]: Overall, the chapter is a really good start, but it still needs a lot of work. Please be careful with the English! Your English is much better than that of other Chinese students, but it still can use improvement...

HEAT EXCHANGER MODELING

Comment [RR2]: USE SPELLCHECK!!!!!! Before you give me something, this is not acceptable

Finned tube coils are frequently used in the air conditioning, heat pumping, and refrigeration industries. The air passes between the fin plates while the refrigerants or coolants flow through the tubes. Parallel flow aluminum microchannel heat exchangers with their increased heat-transfer coefficients, smaller heat exchanger sizes, and increased design flexibility, are finding a wide range of applications to transfer heat between air and fluid.

Figure 2.1a shows a schematic diagram of a “general” finned tube coil. In designing a coil to cool or heat the air and the chosen refrigerant to required temperatures, one needs to specify geometry parameters, refrigerant flow circuitry (the way tubes are connected), and consider heat transfer resistance due to fouling and tube-fin contact. The geometry parameters include number of rows, number of tubes per row, tube diameter, tube length, tube spacing (the distance between centers of neighboring tubes in horizontal and vertical directions), fin thickness, fin spacing (the distance between neighboring fins). A general-purpose simulation tool for heat exchanger design should accommodate for all the following variables and operating conditions.

- All the geometry parameters stated above can be specified and input.

- Allow for arbitrary refrigerant flow circuitry design.
- Allow for multiple refrigerants in interlaced heat exchangers.
- Account for two-dimensional non-uniform air flow distribution.
- Account for varying properties of the fluid flowing in tubes.
- Allow for non-uniform fin spacing design.
- Allow for choice of refrigerants.
- Flexible in using correlations of heat transfer and pressure drop on both air side and refrigerant side, and fin efficiency.
- Allow for gas, liquid, condensation or evaporation fluid flow inside tubes for either heating or cooling purposes.

Comment [RR3]: You need to explain what you mean with these terms and show more examples of the various heat exchangers, this part really belongs into the introduction/background section

Figure 2.1b shows the cross-sectional view of tubes with ports in microchannel heat exchangers. There are many similarities in terms of the variables and working conditions between microchannel heat exchangers and finned tube coils, and simulation program can be developed simultaneously for both of them.

The following sections will discuss the details in developing the general-purpose heat exchanger model.

2.1 Junction and Junction-Tube Connectivity Matrix

2.1.1 Definition

The term “junction” is defined as the intersection where two or more than two tubes are joined together. To facilitate programming, a junction-tube connectivity matrix is defined and created, to describe the location relationship between junctions and tubes:

$JTA[i,j]=1$: junction i is upstream and connected to tube j

$JTA[i,j]=-1$: junction i is downstream and connected to tube j

$JTA[i,j]=0$: junction i is not connected to tube j

As an example, the junction-tube connectivity matrix is demonstrated in Figure 2.2 for a heat exchanger constructed of 8 tubes with 6 junctions. The left side of this figure is the cross-sectional view of the coil. Each circle stands for a tube. The crossed circle represents that the refrigerant flows into the page, and the dotted circle means the refrigerant flows out of the page. The solid line between the two circles indicates the two tubes are connected at the frontal side, whereas the dashed line means the two tubes are connected at the back side.

Comment [RR4]: Twice the same?
BE CAREFUL PROOF READ

The right side of the figure is an electric-circuit-like representation of the coil in terms of the tube connections. Each rectangle represents a tube. Each dot is a junction. Then the connectivity matrix (JTA) is shown in Table 2.1.

From the information of the junction-tube connectivity matrix, it is can be decided:

- The passage of the refrigerant flow from inlet of the coil to the outlet of the coil
- The tube direction in terms of the refrigerant flow into the page or out of the page
- When there are different working fluids (independent streams) in the same coil, the circuit that contains the same working fluid can be distinguished.

2.1.2 JTA Validation

The junction-tube connectivity matrix is automatically generated from the user interface (UI) when the user connects the tube ends to design the circuitry. Validation of the connectivity is implemented to avoid errors that may occur during circuitry design on the interface. The algorithm for validating a junction-tube connectivity matrix is described next.

Each inlet tube has only one junction connected to it and the junction is downstream to it. Each outlet tube has only one junction connected to it and the junction is upstream to it. Each internal tube has only two junctions connected to it, one of which is upstream to the tube, and the other one is downstream to the tube. Each junction has at least one tube connected to it from the upstream side, and at least one tube connected to it at the downstream side.

2.1.3 Junction Numbering

A junction is generated from the interface. It is numbered in order it is generated when the user joins two or more than two tubes. Thus it is not necessarily numbered in the order in which the fluid flows from the inlet to the outlet.

2.2 Tube Numbering and Location

After the user specifies the number of rows N_{col} and the number of tubes in each row N_{row} on the user interface, the tubes are automatically numbered N_T in order of left row to right row, top to bottom in each row, as shown in Figure 2.3.

Tube location in the coil is described in terms of a 2-D array.

If $N_T \leq N_{row}$

$$T_{col} = 1 \quad (2.1)$$

$$T_{row} = N_T \quad (2.2)$$

else

$$T_{col} = (N_T - 1) / N_{row} + 1 \quad (2.3)$$

$$T_{row} = N_T - N_{row} (T_{col} - 1) \quad (2.4)$$

where T_{col} is the index of the tube indicating at which column of the tube array the tube is located, and T_{row} indicates at which row the tube is located within a given row. The division of one integer by another integer obeys the rule set in the computer language.

Comment [RR5]: Better not use T, this stands for temperature and will be confused!

Comment [RR6]: What does this have to do with anything?

The right side of Figure 2.3 shows the tube location represented by the 2-D array. By knowing the tube location, the predecessor - successor relationship of two tubes in the airflow direction can be determined, and the length of the connecting bend between any two tubes can be calculated.

2.3 Tube Segmentation

To account for non-uniform air distribution and fin spacing, air cross flow effect on the temperature difference between the refrigerant, and heterogeneous properties and heat transfer coefficients of the refrigerant, each finned tube is divided into a number of segments. The segment is numbered in the order in which the refrigerant flows through the tube as shown in Figure 2.4.

Comment [RR7]: Needs to be explained better

Comment [RR8]: Sentence needs to be shorter, use several ones

Comment [RR9]: explain, when are the sections numbered? Before or after the inlet and outlet is defined?

2.4 Tube Direction

The tube direction in terms of the refrigerant flowing into the page or out of the page is necessary to determine the predecessor and successor segments of the neighboring tubes for the energy and mass conservation analysis on the air side. As shown in Figure 2.5, the direction of the tube(s) upstream to a junction is reversed to that of the tube(s) downstream to the junction.

Comment [RR10]: I better say refrigerant flow directions!?

$$T_{dir} \Big|_{JTA(j,i)=-1} = -T_{dir} \Big|_{JTA(j,i)=1} \quad (2.5)$$

where T_{dir} is an integer to indicate the tube direction. When $T_{dir}=1$, the refrigerant in the tube flows into the page; when $T_{dir}=-1$, the refrigerant in the tube flows out of the page.

Once the inlet tubes and their direction are specified, by using the above algorithm, the direction of each tube in the coil is determined. When two neighboring tubes i, j are in the same **direction**, the k^{th} segment of the tube i is next to the k^{th} segment of the tube j ; otherwise, the k^{th} segment of the tube i is neighbored with the $(N-k+1)^{\text{th}}$ segment of the tube j , as shown in Figure 2.5.

Comment [RR11]: The tubes cannot be in the same direction, only the refrigerant flow!

2.5 Multiple Working Fluids

In some cases, in interlaced heat exchangers, there are two or more working fluids flowing in the subsets of tubes. Assuming they are not mixed anywhere, the individual circuits they flow through can be determined with the junction-tube connectivity matrix JTA .

The working fluids at the inlet tubes are **specified by the user**. **Tracking from each inlet tube i_{inlet} , the junction j that is connected to this tube is known by verifying if**

Comment [RR12]: Is this part of the interface?

Comment [RR13]: Text is not clear!

$$JTA(j, i_{inlet}) = -1 \quad (2.6)$$

The tube(s) i that are connected to this junction j are known by checking if

$$JTA(j, i) = 1 \quad (2.7)$$

So on, the tubes that belong to the same independent circuit with the same working fluid flowing through can be identified.

2.6 Non-Uniform Air Distribution and Fin Spacing

Two-dimensional non-uniform air distribution at the frontal face of the heat exchanger is accounted for by assigning individual air temperature, relative humidity, and velocity to the segments of the tubes in the frontal row.

The non-uniform fin spacing is addressed by specifying individual fin spacing to each segment of the tubes in the heat exchanger as shown in Figure 2.6.

2.7 Modeling Assumption

In developing the heat transfer model for the heat exchanger, the following assumptions are made:

- 1.) Each segment is treated as the minimum unit of heat transfer, without considering the conduction heat transfer through the fin plates between tubes.
- 2.) When the air flow velocity at the face of the heat exchanger is non-uniform (different air velocity at different segments of the tubes in the frontal face row), the air velocity at the segments in the air flow direction across the heat exchanger remains the same as that at the segment in the frontal face. The air side heat transfer coefficient for each segment is calculated based on the individual air velocity at that segment.

- 3.) When dehumidification occurs, the heat transfer resistance due to the water film on the surface of the tube and the fin, is either neglected or can be accounted for by adding a certain value of resistance to the fin-tube contact resistance.

2.8 Input and Output

For the entire heat exchanger, the input parameters for the internal fluid are the pressure P_{in} and inlet enthalpy h_{in} at each inlet tube, and pressure P_{out} at each outlet tube. The input for the air side is the environmental temperature T_{env} , environmental relative humidity ϕ and air velocity V_{air} at each tube segment of the frontal row. The input for the geometry data of the heat exchanger includes the number of rows, the number of tubes in each row, the tube diameters, tube length, fin thickness, tube spacing, fin spacing, together with the refrigerant flow circuitry that is designed on the user interface by connecting tube ends with mouse clicks.

Comment [RR14]: Better say inlet air temperature, because it does not have to be environmental air

For the tube or the tube segment, the input for the internal fluid is the inlet pressure P_{in} , inlet enthalpy h_{in} , and outlet pressure P_{out} . The input for the air side is air enthalpy h_{airin} , humidity ratio ω , and air flow rate \dot{m}_a .

Comment [RR15]: I thought velocity not mass flow rate?

For the tube and the tube segment, the output values are the latent heat load, sensible heat load, refrigerant charge, mass flow rate, outlet enthalpy of the internal fluid, and the leaving air enthalpy and humidity ratio.

For the entire heat exchanger, the output is the total heat load, total latent heat load, total sensible heat load, total charge of the internal fluid, outlet temperature(s) of the internal fluid(s), the exit temperature and humidity value of the air stream, and the air side pressure drop. All values are reported on a segment level, on tube level, and for entire heat exchanger.

2.9 Refrigerant Side Modeling

In order to simulate a heat exchanger without restriction on the tube connection and flow circuitry, an analogy of the coil to an electric circuit network can be made. The finned tube in a coil is like the resistor in an electric circuit, the mass flow rate through a tube is analogous to the electric current, and the pressure is analogous to the electric potential. While the electric current via a resistor can be considered as a linear function of the potentials at the two ends of the resistors, the mass flow rate through a tube is a highly nonlinear function and determined by several variables including inlet pressure, inlet enthalpy and outlet pressure of the refrigerant and the surrounding air condition, plus the dimensions of the tube and the fins. The inlet enthalpy of the refrigerant is determined by the heat transfer of upstream fluids which increases the complexity of the **problem**.

Comment [RR16]: The reader expects now that you explain how you address this problem! Say that it is presented in Chapter#....

Figure 2.7 shows how the equations of mass and energy conservation are formulated at a particular junction. The mass flow entering a junction j is equal to the mass flow leaving the junction j . The energy flow entering the junction is equal to the energy flow leaving the junction (Lindsay, 2000). The enthalpy h_j at the inlet of each tube downstream to the junction j is the mass flow weighted average enthalpy of the fluid mixed at the junction from the upstream tubes.

$$\sum_{JTA[j][i]=-1} \dot{m}_i = \sum_{JTA[j][i]=1} \dot{m}_i \quad (2.8)$$

where

$$\dot{m}_i = f_i(P_{i,in}, h_{i,in}, P_{i,out}, h_{i,out}) \quad (2.9)$$

$$\sum_{JTA[j][i]=-1} \dot{m}_i h_{i,out} = \sum_{JTA[j][i]=1} \dot{m}_i h_{i,in} \quad (2.10)$$

where,

$$h_{i,out} = \varphi_i(\dot{m}_i, h_{i,in}, \text{air side condition}) \quad (2.11)$$

$$h_{i,in} = h_j = \frac{\sum_{JTA[j][i]=-1} \dot{m}_i h_i}{\sum_{JTA[j][i]=-1} \dot{m}_i} \quad (2.12)$$

The subscript j and i denotes junction and tube respectively.

The fluid pressure drop over the segment k of tube i can be expressed in a hydraulic equation,

$$P_{i,k,in} - P_{i,k,out} = \Delta P_f + \Delta P_a + \Delta P_g \quad (2.13)$$

where ΔP_f is the friction term, and can be calculated in the form,

$$\Delta P_f = c \frac{2l}{\pi \rho D^3} \dot{m}_i^2 \quad (2.13a)$$

ΔP_a is the accelerational term,

$$\Delta P_a = \frac{16\dot{m}_i^2}{\pi^2 d^4} \left(\frac{1}{\rho_{i,k,out}} - \frac{1}{\rho_{i,k,in}} \right) \quad (2.13b)$$

and ΔP_g is the gravitational term,

$$\Delta P_g = 0.5(\rho_{i,k,in} + \rho_{i,k,out})gl \sin \theta \quad (2.13c)$$

Among the three pressure drop components in equation 2.13, the frictional term is the most dominant, while the accelerational term does not exceed 1-5% (Paliwoda, 1989) or 10% (Jung, 1999) at typical operational conditions of refrigeration and heat pump systems, and the gravitational term is negligible for horizontal tube orientation which is often used in practice.

Various correlations and empirical equations exist in obtaining the frictional pressure drop in the form of equation 2.13a, both for single phase and two phase flow, depending on the flow pattern, working fluids, tube type, heat and mass flux, and other operating conditions.

The tubes in the heat exchanger are connected to each other via 180° bends. The pressure drop in the tube bend is usually higher than that in a straight tube of the same length. The enhancing effect of the bend curvature is normally accounted for with a multiplier or an additional term. Coil Designer as a general tool allowing arbitrary circuitry design, is capable of calculating the length of an arbitrary tube bend. Figure 2.8 shows the length of a tube bend depending on

the locations of the tubes associated with this bend, as described in Section 2.2, and the tube configuration of the coil.

$$l = \frac{\pi}{2} \sqrt{(x_1 - x_2)^2 + (y_1 - y_2)^2} \quad (2.14)$$

where,

$$x_1 = (j_1 - 1)S_t \quad (2.15)$$

$$x_2 = (j_2 - 1)S_t \quad (2.16)$$

For inline tube configuration,

$$y_1 = (N_{row} - i_1)S_t \quad (2.17)$$

$$y_2 = (N_{row} - i_2)S_t \quad (2.18)$$

For staggered tube configuration, if the tube is at the odd column, y_1 and/or y_2 are calculated using equations 2.17 and 2.18; if the tube is at the even column:

for convergent configuration,

$$y_1 = (N_{row} - i_1 - 0.5)S_t \quad (2.19)$$

$$y_2 = (N_{row} - i_2 - 0.5)S_t \quad (2.20)$$

for divergent configuration,

$$y_1 = (N_{row} - i_1 + 0.5)S_t \quad (2.21)$$

$$y_2 = (N_{row} - i_2 + 0.5)S_t \quad (2.22)$$

Appropriate correlations are also available for calculating pressure drop in the bends.

2.10 Modeling of Heat Transfer between Refrigerant and Air

As the minimum unit of heat transfer, each segment of a tube can be analyzed as a single heat exchanger (Figure 2.9). The air across the finned segment is assumed to be the unmixed fluid, and the refrigerant throughout the segment is the mixed fluid.

2.10.1 Dry Surface Condition

When the average wall/fin temperature of the tube segment is higher than the dew temperature of the air flowing across the segment, no water vapor condensation occurs. The segment operates under dry surface condition.

To calculate the heat transfer amount of a given segment, the refrigerant mass flow rate and the inlet pressure and specific enthalpy of the refrigerant and the mass flow rate and the specific enthalpy and humidity ratio of the inlet air are given or guessed as the known variables. The outlet conditions are the unknown variables to be calculated. The equations of heat transfer between air and refrigerant, and energy balance are,

$$Q = \frac{\Delta T_m}{R} = \frac{f(T_{air,in}, T_{air,out}, T_{ref,in}, T_{ref,out})}{R} \quad (2.23)$$

$$Q = \dot{m}_{air} (h_{air,in} - h_{air,out}) \quad (2.24)$$

$$Q = \dot{m} (h_{ref,out} - h_{ref,in}) \quad (2.25)$$

where,

$$R = \frac{1}{h_{ref} A_{t,in}} + \frac{(D_{out} - D_{in})}{k(A_{t,in} + A_{t,out})} + \frac{R_c}{A_{t,out}} + \frac{R_f}{A_{t,out}} + \frac{1}{h_{air} A_{total} \eta_0} \quad (2.26)$$

and under dry surface condition,

$$\dot{m}_{air} (h_{air,in} - h_{air,out}) = \dot{m}_{air} c_{p,air} (T_{air,in} - T_{air,out}) \quad (2.27)$$

The log-mean temperature difference (LMTD) method involves the outlet conditions of both the refrigerant and air, forming transcendental equations, and increasing the computational effort. The arithmetic average temperature difference method, on the other hand, could lead to violation of the second thermodynamic law in some extreme conditions. The ε -NTU method, based on the inlet conditions that are known, for cross-flow configuration with one fluid mixed and the other unmixed, is therefore applied to calculate the heat transfer rate between the air and the refrigerant in an iterative free way (Kays, London, 1984).

$$C_{unmixed} = \dot{m}_{air} c_{p,air} \quad (2.28)$$

$$C_{mixed} = \dot{m} c_{p,ref} \quad (2.29)$$

$$NTU = \frac{UA}{C_{min}} \quad (2.30)$$

where \dot{m}_{air} is the air flow rate across the whole segment, \dot{m}_{ref} is the refrigerant flow rate, U is the overall heat transfer coefficient, and A is the whole segment area.

$$UA = \frac{1}{\frac{1}{h_{ref} A_{t,in}} + \frac{(D_{out} - D_{in})}{k(A_{t,in} + A_{t,out})} + \frac{R_c}{A_{t,out}} + \frac{R_f}{A_{t,out}} + \frac{1}{h_{air} A_{total} \eta_s}} \quad (2.31)$$

Here the heat transfer coefficients on the refrigerant side h_{ref} and on the air side h_{air} , are calculated by employing appropriate correlations, or empirical equations or values. The surface effectiveness η_s by definition is

$$\eta_s = \frac{A_{t,out} + \eta A_f}{A_{total}} \quad (2.32)$$

where the fin efficiency η is calculated in similar ways as for the heat transfer coefficients.

For $C_{max} = C_{unmixed}$,

$$\varepsilon = 1 - \exp\left(-\frac{C_{max}}{C_{min}}(1 - \exp(-NTU \cdot C_{min}/C_{max}))\right) \quad (2.33)$$

$$\varepsilon = \frac{T_{in} - T_{out}}{T_{in} - T_{airin}} \quad (2.34)$$

For $C_{max} = C_{mixed}$,

$$\varepsilon = \frac{C_{max}}{C_{min}} \left(1 - \exp(-(1 - \exp(-NTU))C_{min}/C_{max})\right) \quad (2.35)$$

$$\varepsilon = \frac{T_{airout} - T_{airin}}{T_{in} - T_{airin}} \quad (2.36)$$

When the refrigerant in the segment is in condensation or evaporation,

$$\frac{C_{min}}{C_{max}} = 0 \quad (2.37)$$

$$\varepsilon = 1 - \exp(-NTU) \quad (2.38)$$

Which of the above equation for calculating the heat transfer effectiveness ε and the outlet temperature of air or refrigerant is used for each segment depends on

the magnitude of C_{\max} and C_{\min} , and whether the refrigerant is in single phase or two-phase in the segment.

The thermodynamic properties and the transport properties, and the quality of the refrigerant, used to calculate the heat transfer coefficient and the pressure drop of the refrigerant, are calculated according to the inlet condition P and h .

2.10.2 Wet Surface Condition

When the heat transfer surface is at a temperature below the dew point of the passing air stream, condensation of vapor occurs and introduces latent heat transfer in addition to the sensible heat transfer, between the moist air and the wet surface, which becomes wet in the process.

$$q = h_{air}(T_{air,\infty} - T_s) + h_d h_{fg}(\omega_{air,\infty} - \omega_s) \quad (2.39)$$

where T_s and ω_s are the temperature and humidity ratio of the saturated air at the wet surface.

In analysis of the dehumidification process, the mass transfer coefficient h_d is usually related to the air side sensible heat transfer coefficient h_{air} with the Colburn analogy (McQuiston, 1994),

$$\frac{h_{air}}{c_{p,air} h_d} = L_e^{2/3} \quad (2.40)$$

where the Lewis number L_e ranges from 0.81 to 0.86 over the range of temperatures of 10°C to 60°C and is valid for average from completely dry to saturated air (McQuiston, 1994).

From a strict point of view, for a finite-length finned tube segment, it is possible that only a part of the outside surface is wetted in either the radial direction or axial direction or in both directions. Identification of surface area below or above the dew point both along the primary surface (tube) and the associated extended surface (fin) appears to be difficult due to the uncertainty affecting the temperature profile, and may be impractical in a general heat exchanger simulation program. In the current model, a segment is assumed to be either completely dry or wet, based on the mean tube/fin surface temperature \bar{T}_s calculated under dry surface condition or assumption,

$$\bar{T}_s = \eta_s (\bar{T}_w - \bar{T}_{air}) + \bar{T}_{air} \quad (2.41)$$

where the average wall base temperature \bar{T}_w is

$$\bar{T}_w = Q \left(\frac{1}{h_{ref} A_{t,in}} + \frac{(D_{out} - D_{in})}{k(A_{t,in} + A_{t,out})} + \frac{R_c}{A_{t,out}} + \frac{R_f}{A_{t,out}} \right) + 0.5(T_{in} + T_{out}) \quad (2.42)$$

The governing equations of heat and mass transfer, and energy balance over a wetted segment become,

$$Q = \dot{m}_{air} (h_{air,in} - h_{air,out}) - \dot{m}_{air} (\omega_{in} - \omega_{out}) h_{water} \quad (2.43)$$

$$Q = \dot{m} (h_{ref,out} - h_{ref,in}) \quad (2.25)$$

$$Q = \frac{\bar{T}_w - \bar{T}_{ref}}{\frac{1}{h_{ref} A_{t,in}} + \frac{(D_{out} - D_{in})}{k(A_{t,in} + A_{t,out})} + \frac{R_c}{A_{t,out}} + \frac{R_f}{A_{t,out}}} \quad (2.44)$$

$$Q = h_{air} A_{total} (\bar{T}_{air} - \bar{T}_s) + h_d A_{total} h_{fg} (\bar{\omega}_{air} - \bar{\omega}_s) \quad (2.45)$$

where the mean surface temperature \bar{T}_s is given by

$$\bar{T}_s = \eta_{ms} (\bar{T}_w - \bar{T}_{air}) + \bar{T}_{air} \quad (2.46)$$

A number of dehumidification models have been developed and reviewed (Threlkeld, 1970, Oskarsson, 1990, Domanski, 1991, Hill, 1991, Mirth, 1993, McQuiston, 1994, Ragazzi, 1995), in respects of the driving potentials, the relationship between h_{air} and h_d , overall heat transfer coefficient and fin efficiency, mean enthalpy difference of cross-flow fluid streams, and equivalent effectiveness. The major difference of these models is in the assumption of the specific linear relationship between the temperature and humidity ratio or specific enthalpy of the moist air, in order to reduce the number of unknown variables and obtain the fin temperature distribution.

In deducing the overall fin efficiency η_{ms} in equation 2.46 with combined heat and mass transfer, a differential equation accounting for the energy balance on a finite fin element can be expressed as follows (McQuiston, 1994),

$$\frac{d^2 T}{dx^2} = \frac{P}{kA_c} [h_{air} (T - T_{air,\infty}) + h_d h_{fg} (\omega - \omega_{air,\infty})] \quad (2.47)$$

Assuming a simple relationship between the specific enthalpy and the dew point temperature of the moist air exists (McQuiston, 1994),

$$\omega - \omega_{air,\infty} = C(T - T_{air,\infty}) \quad (2.48)$$

where C is a constant. In most cases C vary less than 10 percent from inlet to exit, and an average value should be used (McQuiston, 1994). Equation 2.47 then becomes,

$$\frac{d^2T}{dx^2} = m^2(T - T_{air,\infty}) \quad (2.49)$$

where

$$m^2 = \frac{P}{kA_c}(h_{air} + Ch_d h_{fg}) \quad (2.50)$$

Equation 2.49 is identical in the form to classic differential equation for calculating dry surface fin efficiency, and therefore the overall fin efficiency for a wet fin surface can be obtained in a similar form,

$$\eta_m = \frac{\tanh(mL)}{mL} \quad (2.51)$$

and the surface effectiveness can be expressed by

$$\eta_{ms} = \frac{A_{t,out} + \eta_m A_f}{A_{total}} \quad (2.51a)$$

This solution can be applied to plate-fin surface with L and m replaced by appropriate quantities as for the dry surface fin efficiency.

Assuming the linearization of the air dehumidification process path from inlet to outlet, and the condensate surface as the intersection between the

saturated curve and an extension of the straight line of the air process path on the psychometric chart (Regazzi, 1995), as shown in Figure 2.10,

$$\omega_{air} = a + bT_{air} \quad (2.52)$$

$$\omega_s = a + bT_s \quad (2.53)$$

therefore,

$$\bar{\omega}_{air} - \bar{\omega}_s = b(\bar{T}_{air} - \bar{T}_s) \quad (2.54)$$

Then equation 2.45 becomes,

$$Q = (h_{air} A_{total} + h_d A_{total} h_{fg} b)(\bar{T}_{air} - \bar{T}_s) \quad (2.55)$$

Combining equation 2.44, 2.46, and 2.55 yields,

$$Q = \frac{\bar{T}_{air} - \bar{T}_{ref}}{\frac{1}{h_{ref} A_{t,in}} + \frac{(D_{out} - D_{in})}{k(A_{t,in} + A_{t,out})} + \frac{R_c}{A_{t,out}} + \frac{R_f}{A_{t,out}} + \frac{1}{\eta_{ms} A_{total} (h_{air} + h_d h_{fg} b)}} \quad (2.56)$$

On the other hand, the specific enthalpy of moist air can be written as,

$$h_{air} = c_{p,dryair} T_{air} + \omega_{air} (h_{fg} + c_{p,v} T_{air}) = c_{p,air} T_{air} + \omega_{air} h_{fg} \quad (2.57)$$

Hence,

$$\begin{aligned} h_{air,in} - h_{air,out} &= c_{p,air} (T_{air,in} - T_{air,out}) + (\omega_{air,in} - \omega_{air,out}) h_{fg} \\ &= (c_{p,air} + b h_{fg}) (T_{air,in} - T_{air,out}) = c_{p,air,eq} (T_{air,in} - T_{air,out}) \end{aligned} \quad (2.58)$$

where $c_{p,air,eq}$ is an equivalent specific heat capacity of air accounting for both sensible and latent heat exchange.

Neglecting the second term, which is the enthalpy contained in the condensate water and is very small, on the right side of equation 2.43, and substituting equation 2.58, equation 2.43 is converted to,

$$Q = \dot{m}_{air} c_{p,air,eq} (T_{air,in} - T_{air,out}) \quad (2.59)$$

Equations 2.25, 2.56, and 2.59 provide the heat transfer and energy balance equations for a wetted segment, and are similar in the forms to those under dry surface condition. Therefore the ϵ -NTU method for both isothermal and finite capacity fluid flow can also be applied to the combined heat and mass transfer problem in dehumidification process, provided that the UA value and heat capacity C_{air} of the air stream over the segment are defined respectively as

$$UA = \frac{1}{\frac{1}{h_{ref} A_{t,in}} + \frac{(D_{out} - D_{in})}{k(A_{t,in} + A_{t,out})} + \frac{R_c}{A_{t,out}} + \frac{R_f}{A_{t,out}} + \frac{1}{\eta_{ms} A_{total} (h_{air} + h_d h_{fg} b)}} \quad (2.60)$$

$$C_{air} = \dot{m}_{air} c_{p,air,eq} \quad (2.61)$$

It is worthwhile to note that the constants a and b in relating the humidity ratio and temperature of the moist air as shown in equations 2.52 and 2.53 have to be guessed first by assuming the temperature of the condensate surface with its associated saturated air humidity ratio, given the inlet air condition. With the heat transfer rate calculated using the ϵ -NTU method, the outlet air temperature is known, and the outlet air humidity can be calculated with equation 2.52. Then the temperature and humidity ratio at the condensate surface in equation 2.45

are recalculated. The constants a and b are to be updated until no considerable variation is observed.

2.11 Air Side Mass, Energy Flow and Pressure Drop

During heat (and mass) transfer, the air side condition including enthalpy, temperature and humidity also change along the flow path. The mass, energy, and humidity conservation between the neighboring segments are as follows (Figure 2.11).

For staggered tube arrangement,

$$\dot{m}_{air,k} = 0.5(\dot{m}_{air,i} + \dot{m}_{air,j}) \quad (2.62)$$

$$\dot{m}_{air,k} h_{air,k,in} = 0.5(\dot{m}_{air,i} h_{air,i,out} + \dot{m}_{air,j} h_{air,j,out}) \quad (2.63)$$

$$\dot{m}_{air,k} \omega_{k,in} = 0.5(\dot{m}_{air,i} \omega_{i,out} + \dot{m}_{air,j} \omega_{j,out}) \quad (2.64)$$

For in-line tube arrangement,

$$\dot{m}_{air,k} = \dot{m}_{air,i} \quad (2.65)$$

$$h_{air,k,in} = h_{air,i,out} \quad (2.66)$$

$$\omega_{k,in} = \omega_{i,out} \quad (2.67)$$

The pressure drop of the air flowing over the heat exchanger is calculated by using appropriate correlations or empirical values, according to the tube configuration, fin pattern, and surface condition (dry or wet).

2.12 Sub-Dividable Segment in Case of Flow Regime Change within the Segment

Normally each segment can be assumed to not undergo any change in flow region. It is either entirely occupied by subcooled liquid, or two-phase evaporation/condensation fluid, or superheated gas. This is the case, when the number of segments in each tube is large. However, in case that the length of a tube is quite large and/or the number of segments is small, the refrigerant flowing in a particular segment may experience flow regime change, with significant change of temperature and heat transfer coefficient. The heat duty should be carefully evaluated by subdividing this segment, and employing individual ε -NTU equation for each sub-segment of the same phase.

Figure 2.12 shows two tubes in which the refrigerant undergoes desuperheating, condensation and subcooling. One tube is located behind the other tube in the airflow direction. Each tube is divided into 3 segments.

The inlet of the refrigerant is gas (quality ≥ 1), and the $\varepsilon - NTU$ equations for the single phase are used to calculate the heat transfer between the refrigerant and the air, along with the outlet refrigerant pressure/temperature/enthalpy, and the outlet air temperature/humidity.

The outlet enthalpy of the refrigerant is checked. If it is less than the saturated vapor enthalpy corresponding to the outlet pressure, it means that there is condensation or even subcooling taking place somewhere within the segment, and the segment needs to be subdivided into at least two sub segments.

The location where the condensation begins, i.e, where the calculated enthalpy is equal to the saturated vapor enthalpy corresponding to the calculated pressure, is calculated as following.

Comment [RR17]: Do not use questions in a thesis, just say that this questions needs to be addressed!

Supposing at a fraction x of the length of the segment the condensation starts, then the following equations must be satisfied,

$$C_{unmixed} = x\dot{m}_{air} C_{p,air} \quad (2.68)$$

$$C_{mixed} = \dot{m}_{ref} C_{p,ref} \quad (2.29)$$

$$NTU = x \frac{UA}{C_{min}} \quad (2.69)$$

Calculating the heat exchange effectiveness ϵ as outlined in equation 2.33 or 2.35, the outlet temperature of the refrigerant or air can be known, for

$$C_{max} = C_{unmixed} ,$$

$$\epsilon = \frac{T_{in} - T_1}{T_{in} - T_{airin}} \quad (2.70)$$

$$\text{for } C_{max} = C_{mixed} ,$$

$$\epsilon = \frac{T_{air1} - T_{airin}}{T_{in} - T_{airin}} \quad (2.71)$$

$$x\dot{m}_{air} C_{p,air} (T_{air1}(x) - T_{airin}) = \dot{m}_{ref} (h_{in} - h_1(x)) \quad (2.72)$$

$$h_1(x) = h_{sat,v}(P_1(x)) \quad (2.73)$$

$$P_1(x) = P_{in} - DP(x, P_{in}, h_{in}) \quad (2.74)$$

The above equations reduce to one equation with x being the unknown. This implicit equation is a transcendental equation and a numerical iteration scheme is needed. It is found that the Golden Section method is a robust method to solve for x . (It is normalized to lie between 0 and 1). Once x is solved, the outlet air temperature and the outlet pressure/enthalpy of the refrigerant of this sub segment are known.

The remaining part of the segment: supposing all the remaining part of the segment is in condensation, the $\varepsilon - NTU$ equation for one fluid with infinite heat capacity is used to calculate the heat transfer rate, the outlet enthalpy and pressure of the refrigerant, and the outlet air temperature. If the outlet enthalpy is less than the saturated liquid enthalpy corresponding to the outlet pressure of the refrigerant, the remaining part of the segment needs to be further subdivided into two segments, to figure out where condensation ends and the subcooling begins and to account for the respective changes in heat transfer and pressure drop as described above for the transition from superheated vapor to two-phase flow.

In view of the entire coil, the particularly subdivided segment should be treated as an integrated segment by passing its outlet pressure/enthalpy of the refrigerant of the next segment, and the outlet air temperature to the neighboring 'air-wise' downstream segment. The integrated outlet air temperature is the sub-segment-percentage averaged temperature. When there are three sub-segments,

$$T_{air,out} = \frac{I1}{I} T_{air1} + \frac{I2}{I} T_{air2} + \frac{I3}{I} T_{air3} \quad (2.75)$$

When there are 2 sub segments,

$$T_{air,out} = \frac{I1}{I} T_{air1} + \frac{I2}{I} T_{air2} \quad (2.76)$$

Comment [RR18]: You need to average enthalpies, not temperatures, there may be change in humidity!

When the inlet is liquid, it is similar to the above. When the Inlet is two-phase,

Comment [RR19]: Explain in more details!

check if the outlet enthalpy is less than the saturated liquid enthalpy corresponding to the outlet pressure of the refrigerant, or greater than the saturated vapor enthalpy corresponding to the outlet pressure of the refrigerant.

There are at most two sub segments.

2.13 Solution Methodology

On the refrigerant side, a fractional step method is used wherein the hydraulic equation (pressure/mass flow rate relationship) and energy equation (heat transfer between refrigerant and air) are solved alternatively and repeatedly. In this way, the highly nonlinear system of equations is decoupled and nonlinearity is reduced so that the solver becomes more robust. At the beginning, the

pressure field and mass flow rate of each tube are obtained for the entire heat exchanger assuming no heat transfer between the refrigerant and the air takes place, and the enthalpy of the refrigerant throughout each circuit is assumed to be equal to the inlet enthalpy of each circuit. When solving the heat transfer equation of each tube, the mass flow rate value from the previously solved hydraulic equation is used, the inlet enthalpy is obtained from the currently solved heat transfer equations of the upstream tubes and energy balance equation at the upstream junction. Thus, the energy equations for each tube are successively solved from the inlet tubes of the heat exchangers to the outlet tubes of the heat exchangers based on the information the junction-tube connectivity matrix provides in terms of refrigerant flow direction (inside the tube, it is always solved from the first segment at the inlet of the tube to the last segment at the outlet of the tube).

The hydraulic equations are solved with the Newton-Raphson method. Since there is no analytical expression of the partial derivatives of the mass flow residual at one particular junction with the pressures at each neighboring junction (the partial derivatives with the pressures at those un-neighbored junctions, are zero), a finite difference approach is applied, and the finite difference of pressure is scaled such that infinite or zero value of the derivative is avoided.

Comment [RR20]: Show equation how you do it.

On the air side, initially the air condition (temperature and humidity) facing each segment of each tube in the coil is assumed to be the same as that at the frontal face area. During solution of the energy equation of the refrigerant at each segment, the condition of the air leaving each segment is also calculated. After solving the hydraulic equations of the refrigerant in the entire coil, the air conditions facing each segment are updated, and used in solving the energy equations for the refrigerant side in the next step. These processes are repeated until both the refrigerant and air conditions do not change within a specified tolerance.

Comment [RR21]: What value it typically used?

In summary, Table 2.2 lists the hydraulic equations and energy equations that need to be solved, and Figure 2.13 shows the flow chart of the solution methodology.

2.14 Heat Transfer, Pressure Drop and Fin Efficiency Correlations

Accuracy of performance prediction with computer model is highly dependent on the heat transfer coefficients and pressure drops both on the refrigerant side and the air side, and the fin efficiency. As noted above, they are calculated based on extensive correlations in literature or empirical data at the user's choice when using Coil Designer. As an ongoing process, these correlations are continuously integrated and updated into the program, to meet the increasing needs and

applications of the users. Some of the built-in correlations are provided in the appendix.

The factors that affect the heat transfer coefficients and pressure drop on the air side, include the fin types (plain, wavy, louver, etc), the fin surface condition (dry or wet). Several correlations (Chang, 1997/ 2000, Kim, M, 2002, Kim, N., 1997/1999, Sahnoun, 1992, Wang, 1997) are or will be available in the simulation tool.

The in-tube heat transfer coefficient on the refrigerant side is dependent on the refrigerants (types, pure or mixture) the fluid flow phase (liquid, vapor, condensation, evaporation), the tube diameter, tube inner surface condition (enhanced or not), mass and heat flux of the refrigerant, and range of quality (flow regime such as wavy, annular, stratified, bubbly flow). The evaporation (boiling) heat transfer correlations include those by Gungor (1986), Jung (1989b, 1991, 1993), Kandlikar (1990, 1991, 1997), Klimenko (1988), Lee (2001), Shah (1982). There are also condensation heat transfer correlations built or will be built into the simulation model (Dobson, 1998, Shah, 1989, Soliman, 1968, Triviss, 1973).

The frictional pressure drop of the refrigerant flow is affected by the factors similar to those for heat transfer coefficient. Two-phase pressure drop

correlations include those developed by Didi (2001), Fridel (Smith, 1997), Hahne (1993), Jung (1989a), 1993, Lockhart (1949), Paliwoda (1989, 1992), Tran (2000). There are also different correlations for calculating pressure drop in the bends (Chisholm, 1980, Geary, 1975).

Fin efficiency of plate fins is calculated by sectional method, which is numerically involved, or empirical method with analytical equations. The well-known empirical method by Schmidt (McQuiston, 1994) is currently implemented in the simulation program for fin efficiency calculation.

Table 2.1 Junction-Tube Connectivity Matrix

Junction \ Tube	1	2	3	4	5	6	7	8
1	-1	1	0	0	0	0	0	0
2	0	0	0	0	-1	1	0	0
3	0	-1	1	0	0	-1	0	0
4	0	0	-1	0	0	0	1	0
5	0	0	0	1	0	0	-1	0
6	0	0	0	-1	0	0	0	1

Table 2.2 Summary of System of Hydraulic/Energy Equations

Boundary Conditions	
Refrigerant Side	Air Side
P_{in}, h_{in}, P_{out}	$T_{in}, v_{in}, \phi_{in}$
Hydraulic Equations	
Junction	Tube/Segment
$\sum_{JTA[J][I]=-1} \dot{m}_i = \sum_{JTA[J][I]=1} \dot{m}_i$	$P_{i,k,in} - P_{i,k,out} = \Delta P_f + \Delta P_a + \Delta P_g$
	$\Delta P_f = c \frac{2l}{\pi \rho D^3} \dot{m}_i^2$
	$\Delta P_a = \frac{16\dot{m}_i^2}{\pi^2 d^4} \left(\frac{1}{\rho_{i,k,out}} - \frac{1}{\rho_{i,k,in}} \right)$
	$\Delta P_g = 0.5(\rho_{i,k,in} + \rho_{i,k,out})gl \sin \theta$
Energy Equations	
Refrigerant Energy Conservation at Junction	
$h_{i,in} = h_j = \frac{\sum_{JTA[J][I]=-1} \dot{m}_i h_i}{\sum_{JTA[J][I]=-1} \dot{m}_i}$	
Heat Transfer Between Refrigerant and Air	
$Q = f(\varepsilon, NTU, T_{air,in}, T_{ref,in}), Q = \dot{m}_{air} c_{p,air} (T_{air,in} - T_{air,out}), Q = \dot{m}(h_{ref,out} - h_{ref,in})$	
Air Side Energy/Mass Conservation	
In-line Tube Configuration	Staggered Tube Configuration
$\dot{m}_{air,k} = \dot{m}_{air,i}$	$\dot{m}_{air,k} = 0.5(\dot{m}_{air,i} + \dot{m}_{air,j})$
$h_{air,k,in} = h_{air,i,out}$	$\dot{m}_{air,k} h_{air,k,in} = 0.5(\dot{m}_{air,i} h_{air,i,out} + \dot{m}_{air,j} h_{air,j,out})$
$\omega_{k,in} = \omega_{i,out}$	$\dot{m}_{air,k} \omega_{k,in} = 0.5(\dot{m}_{air,i} \omega_{i,out} + \dot{m}_{air,j} \omega_{j,out})$

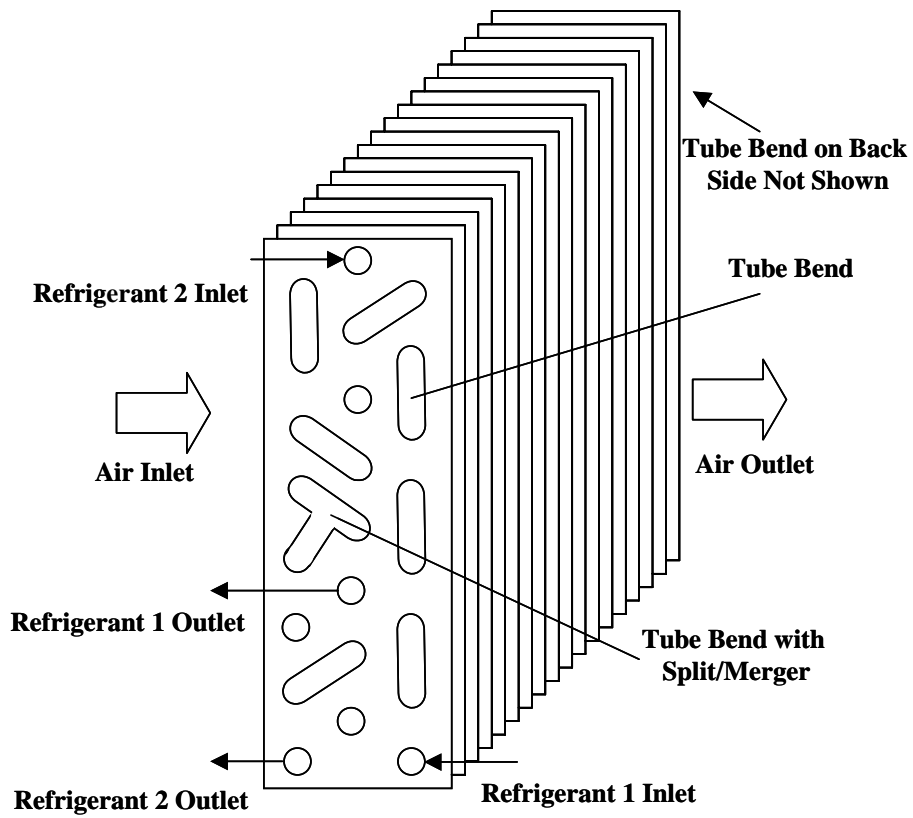


Figure 2.1a Schematic Diagram of a General Cross Flow Heat Exchanger

Comment [RR22]: Also show photograph

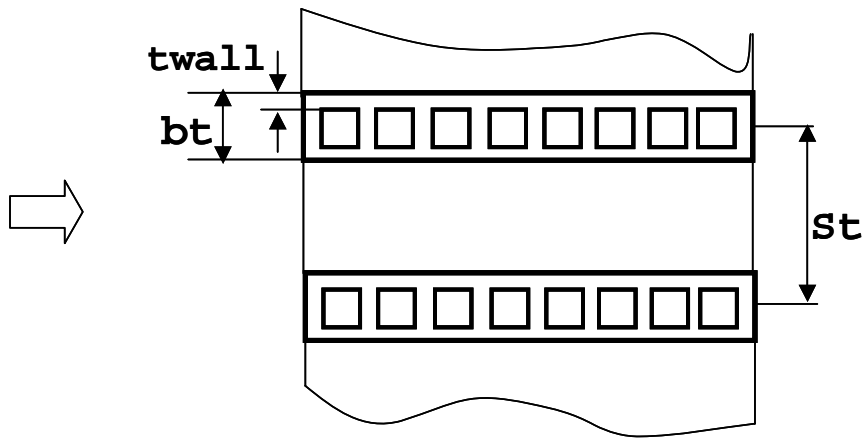


Figure 2.1b Flat Tubes with Microchannels

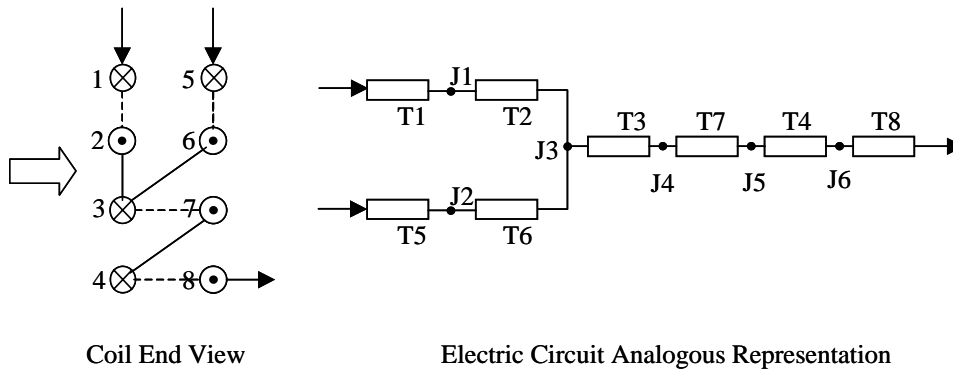


Figure 2.2 Schematic to Explain Junction-Tube Connectivity Matrix (JTA)

Comment [RR23]: this figure does not show a matrix!

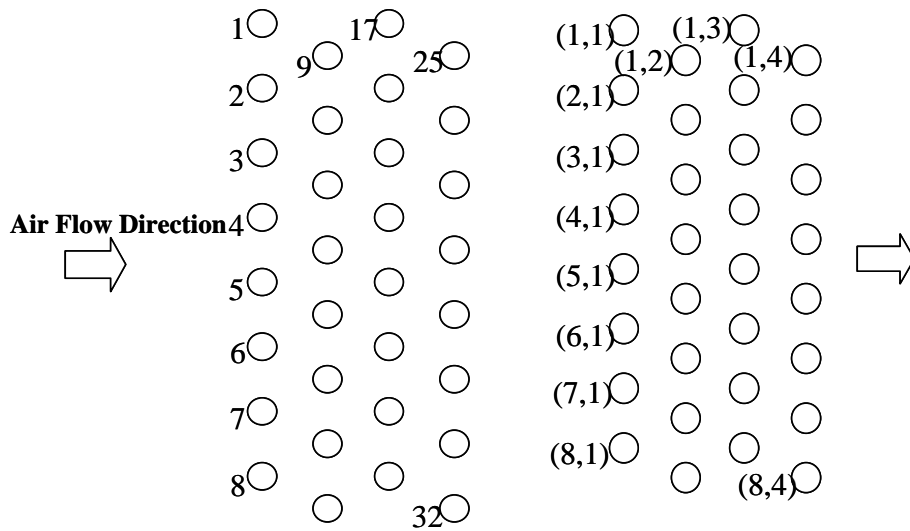


Figure 2.3 Tube Numbering and Location

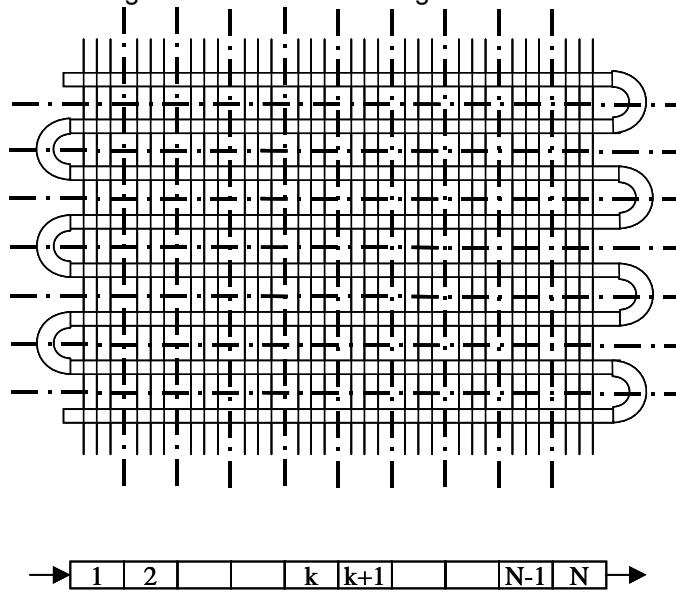


Figure 2.4 Tube Segmentation Example

Deleted: ¶

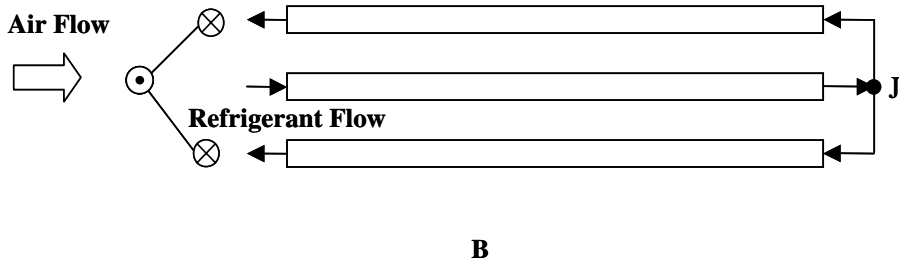
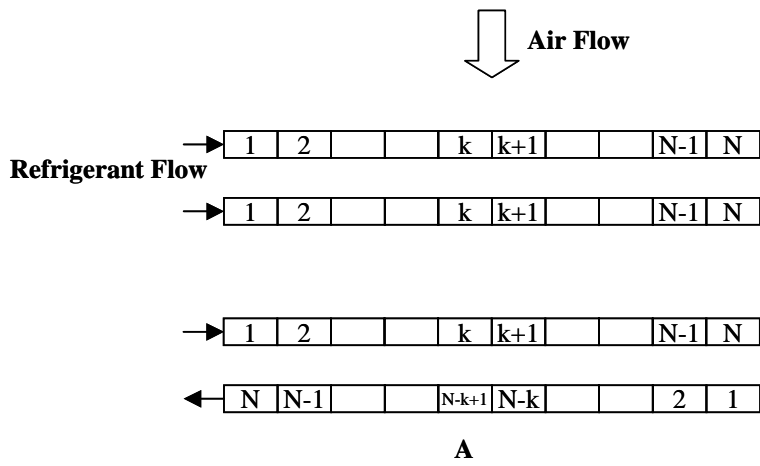


Figure 2.5 Refrigerant Flow Directions inside Tubes

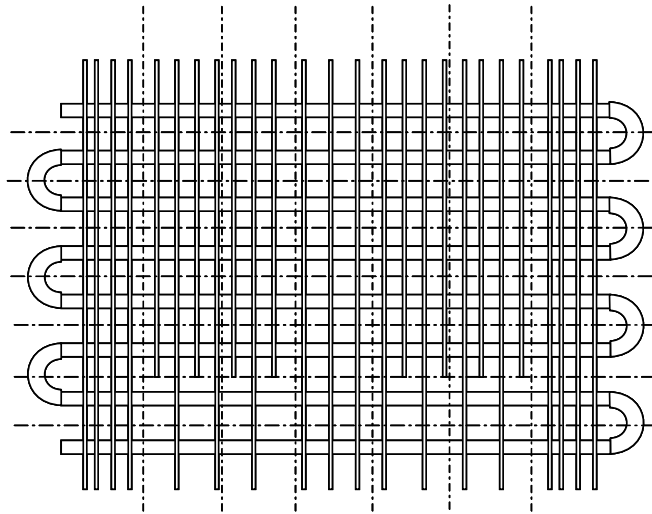


Figure 2.6 Non-uniform Fin Spacing

Comment [RR24]: Delete segment grid, confusing!

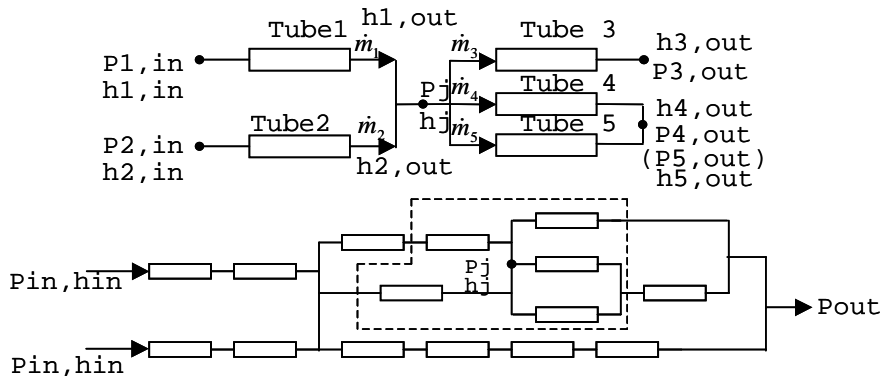


Figure 2.7 Refrigerant Side Mass and Energy Flow in a Tube Network

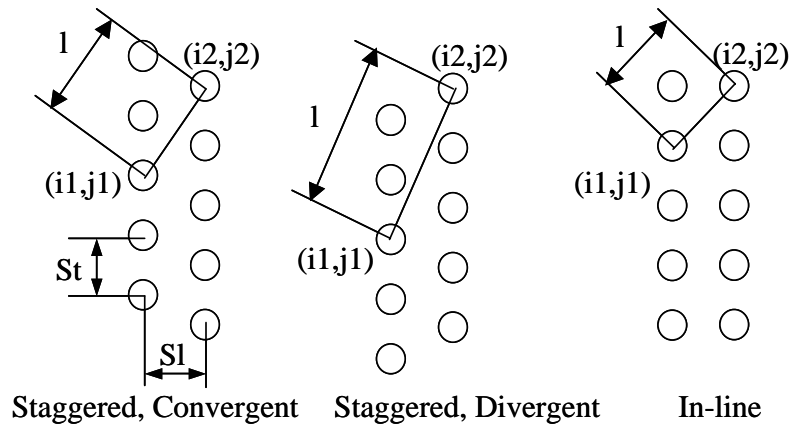


Figure 2.8 Bend Length Dependent on Tube Configuration

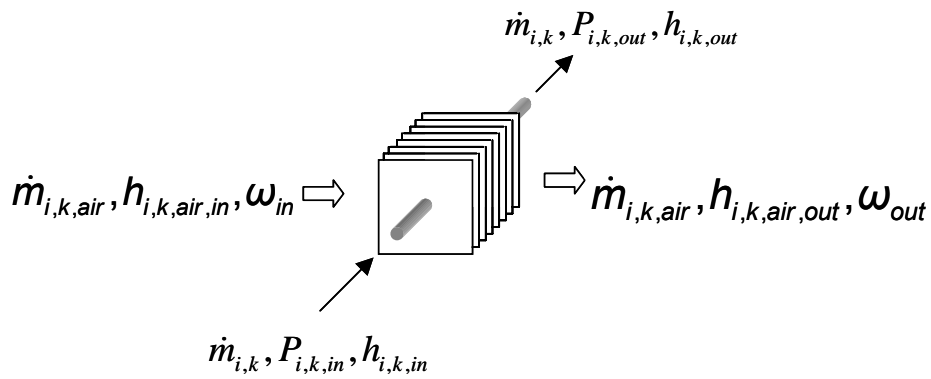


Figure 2.9 Segment as a Single Heat Exchanger

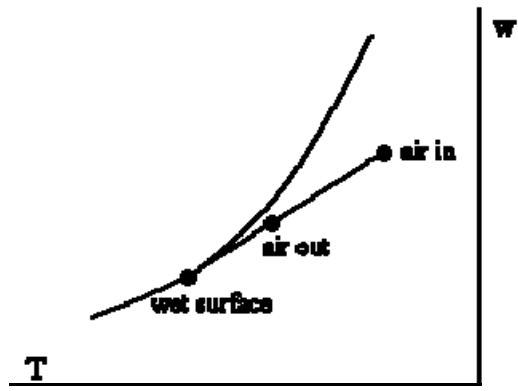


Figure 2.10 Linearized Air Dehumidification Process on the Psychometric Chart

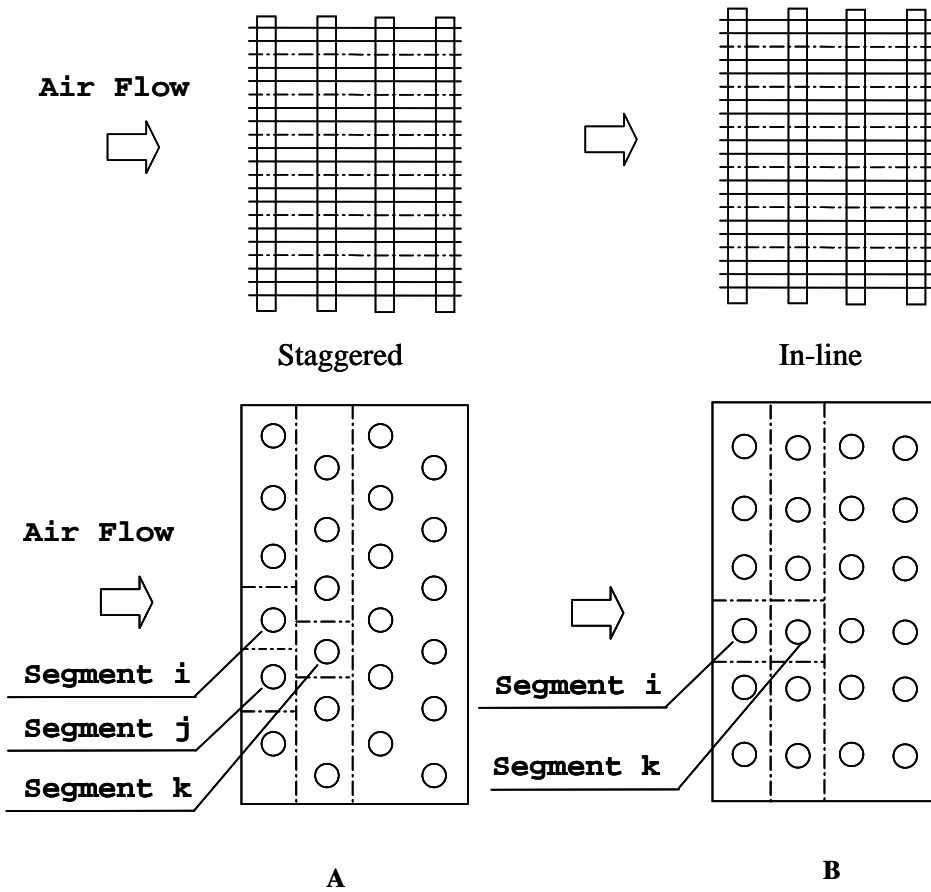


Figure 2.11 Air Side Mass and Energy Flow

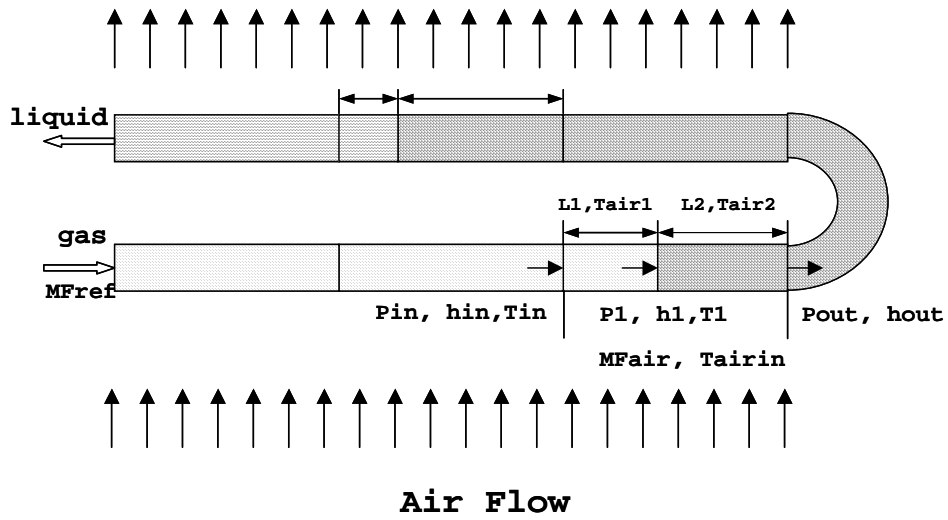


Figure 2.12 Schematic Diagram of Sub-Divided Segment

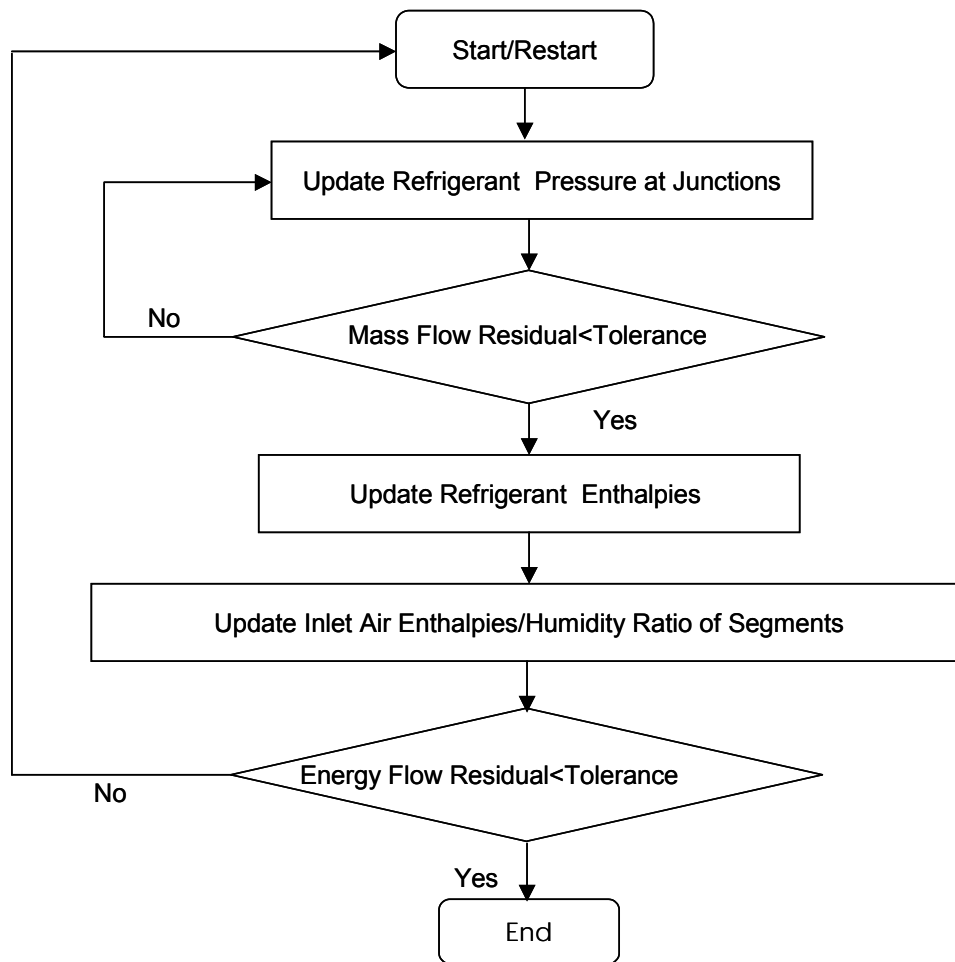


Figure 2.13 Flow Chart of the Solution Methodology

Chapter 3

MODEL VALIDATION

The performance results predicted with the simulation tool are compared against the experimental data collected from the literature, experiments in laboratories (including CEEE), and measurements in companies, for the purpose of model validation. The experimental data represents coils of diverse geometries, varying operating conditions, different working fluids, and includes microchannel heat exchangers.

3.1 Model Agreement with Experimental Data in Literature

McQuiston carried out an extensive set of experiments on plate-fin-tube coils in developing general air side heat, mass and friction coefficient correlations for both wet and dry surface conditions (McQuiston, 1981). The model verification is first conducted by comparing the coil capacity prediction against the test data reported in his paper.

The geometry size specifications and operating conditions are listed in Table 3.1, and the coil circuitry is shown schematically in Figure 3.1. Hot water and chilled water were used to realize dry and wet surface conditions

respectively. Water velocity was maintained high so that the average heat transfer coefficient on the water side was about $210 \text{ W/m}^2\text{K}$.

The air side heat transfer coefficient in the simulation is calculated using the correlation developed by Kim, Youn and Webb (Kim, 1999), and the water side heat transfer coefficient is computed with the Dittus-Boelter equation.

Figure 3.2 shows the comparison of the predicted heat duty with the measured heat duty of the 4 coils under both dry and wet surface conditions. An overall agreement of 10% is found between the simulation results and the experimental data.

Outlet air dry bulb temperature results are illustrated in Figure 3.3, with the simulation predictions within $\pm 3^\circ\text{R}$ of the experimental data, indicating also a good agreement in terms of the sensible heat duty. The upper group of points of Figure 3.3 represents the temperatures when air is heated, whereas the lower group of points corresponds the temperatures when air is cooled.

Error of the simulated outlet air wet bulb temperatures is within $\pm 1\text{--}3.5^\circ\text{R}$ of the experimental data, as shown in Figure 3.4.

3.2 Model Agreement with Experimental Data in Laboratory

3.2.1 A-Type Coil

An experimental study was conducted in the laboratory to compare the effects of the working fluids R22 and R290 on the heat pump performance. An A-type coil shown in Figure 3.5 worked as an evaporator in the cooling mode and as a condenser in the heating mode.

The operating conditions in the cooling mode are specified through ASHRAE test standards A, B, and C. In the heating mode, the outdoor air temperature is maintained at -35°C , -34°C , -29°C , -18°C , -8°C , and 8°C respectively, and the indoor air temperature is kept at 21°C . The geometric data of the coil is obtained by measuring the physical coil after it is uninstalled from the system. The mass flow rate of each inlet tube in the simulation is assumed to be $1/6$ of the total mass flow rate measured before the distributor, since there are 6 circuits in the coil, and each circuit intertwines in the direction of air flow across the coil. As for the air flow direction, it is reasonable to assume the air turns abruptly to flow through the coil perpendicularly by the path of least resistance (Domanski, 1991). In light of this assumption, the air velocity as an input to the model is calculated according to the measured air flow rate in the duct and the coil face area. Table 3.2 shows the overall specifications and operating parameters of this A-type coil.

Seeing the symmetry of the two slabs and refrigerant circuitry in each slab of the A-type coil, identical heat transfer performance is assumed for both slabs. The air outlet temperature as from the simulation is the average of the air exit temperature at each segment of the last row of the coil, for a direct comparison with experimental data.

Kandlikar's correlation for saturated two-phase flow boiling heat transfer (1991), and Dobson's correlation for condensation heat transfer (1998), inside horizontal tubes are used for calculating the refrigerant side heat transfer coefficients in evaporation and condensation respectively. The quality of the refrigerant at the inlet of the coil working as an evaporator is calculated based on measured pressure and temperature at the outlet of the condenser coil, assuming an isenthalpic process in the expansion device.

Figure 3.6 shows the prediction of the air outlet temperature when the coil works as an evaporator in cooling mode. The relatively large error in prediction under ASHRAE test standard A may be attributed to the uncertainty of the refrigerant thermodynamic status at the outlet of the outdoor coil, which may be in two-phase condition, according the experimental data of pressure and temperature.

Figure 3.7 presents the air outlet temperature results when the coil functions as a condenser in the heating mode. The error in the prediction is mostly within 1°C of the experimental data.

3.2.2 Micro-channel Heat Exchanger

Another source of experimental data in the heat pump laboratory is from a gas cooler in a carbon dioxide environmental control unit (Cutler, 2000). The gas cooler consisted of 10 slabs (Figure 3.8). Each slab was made of 34 micro-channel tubes. Each tube had 8 micro channels. Two slabs were mounted in a polypropylene frame side by side, and then stacked in series to the air flow five units deep forming the counter-cross flow setup. The specifications and operating conditions are shown in Table 3.3. The air flow rate, outdoor temperature, and compressor speed were varied in the experimental study, resulting in a number of performance outputs that deserve the verification of the simulation tool.

The carbon dioxide flows in the gas cooler under transcritical condition, for the pressure is beyond its critical pressure of 7.3748 MPa. Gnielinski's correlation (Kakac, 2002, p.96) is used to calculate the heat transfer coefficient of the carbon dioxide, where the characteristic diameter is the hydraulic diameter of the micro-channel in the tube. The air-side heat transfer coefficient is taken from the original test data, seeing no appropriate correlation exists for this particular

configuration of micro-channel heat exchanger with louvered fins between the flat tubes.

The agreement between the measured and calculated outlet temperature of the carbon dioxide is encouragingly good as shown in Figure 3.9, within the range of 0.7K to -1.2K. The air outlet temperature is also predicted with an accuracy of +/- 1K as indicated in Figure 3.10.

3.3 Model Agreement with Test Data of Commercial Products

3.3.1 A Coil for Refrigerator Application

In order to get an empirical equation of the air side heat transfer coefficient on a coil for refrigerator application, a commercial coil as plotted in Figure 3.11 was tested. Water was used as the working fluid inside the tubes. On both the air and water side, the mass flow rates were varied while the temperature difference was maintained nearly the same in each case. In this way, the air side heat transfer coefficient can be determined as a function of only the air velocity for this particular coil. Table 3.4 gives the coil specification and operating range.

The measured heat duty is taken to be the average of the measured heat transfer rate on the water side and air side. The predicted heat duty results are compared in Figure 3.12. Errors in the prediction of heat duty are within +3%/-4% of the measured heat duty. The almost overlapping points in the graph represent

repeated tests for a given pair of mass flow rates of the air outside the tubes and the water inside the tubes, indicating reproductively.

3.3.2 An Integrated Absorber/Condenser Coil

The test data from a company on a coil with 88 tubes and two rows is also used for validation purpose. The working fluids are ammonia water mixtures. Two circuits of this coil are used as a condenser, and four circuits are used as an absorber, with given ammonia mass fraction respectively. These 6 circuits are interlaced to take advantage of the temperature difference between the sections of the circuits to maximize the heat transfer capability. Figure 3.13 shows the schematic of the coil indicating non-uniform air flow distribution and the number of circuits.

The testing data provides the inlet and outlet temperature of each of the 6 circuits, the temperature profile along one of the condenser circuits and one of the absorber circuits, and the pressures at the inlets of the condenser and absorber. The inlet air temperature and velocity are measured at 8 sections of the frontal face of the coil. The total mass flow rates of the absorber and condenser are given as well.

To account for the non-uniform air distribution, each tube is divided into 8 segments, and 4 different air velocity/temperature (from measured data) are

applied to each 2 segment respectively in the tube. From top to bottom of the coil, the air velocity/temperatures of the upper 22 tubes are corresponding to the upper measured 4 sections, and the lower 22 tubes corresponding to the lower measured 4 sections.

The agreement of the simulation results with the measured data is highly dependent on the accuracy of the heat transfer coefficients on the air side and the ammonia water mixture side. An empirical equation to calculate the air side heat transfer coefficient is provided by the coil manufacturer. On the refrigerant side, several methods have been evaluated to determine the inside heat transfer coefficients of the ammonia water mixture in the tube. Correlations available for condensation heat transfer coefficient don't apply to ammonia-water mixtures. The flow pattern map based analytical equation for condensation of vapor mixture, according to the flow pattern (stratified flow and annular flow) and the mass transfer resistance of the mixture in the vapor phase, seems also far away from predicting the heat transfer coefficient satisfactorily. The method of manually tuning up heat transfer coefficient and pressure drop simultaneously for different phases proves to be the most effective method in the validation process.

Figure 3.14 shows the comparison of the simulated temperatures with the measured temperatures along the condenser circuit. Except in the phase change regions, the predicted temperatures are very consistent with the measured

temperature at each point. The heat transfer coefficients in the desuperheating, condensation and subcooling zone were found respectively, and the pressure drop also determined.

Figure 3.15 shows the comparison of the simulated temperatures with the measured temperatures along the absorber circuit. Nearly all the predicted temperatures are within 1°F of the measured temperature at each point. Again the heat transfer coefficients and pressure drops in each zone were found. These values were then used to optimize the coil.

Table 3.1 Specifications and Operating Conditions of the McQuiston Coils

Item	Value
Refrigerant	Water
Tube Length (inch)	12
Tube O.D. (inch)	0.392
Tube I.D. (inch)	0.332
Tube Horizontal Spacing (inch)	0.866
Tube Vertical Spacing (inch)	1
Fin Thickness (inch)	0.006
Fin Pitch (fins per inch)	4, 8, 10, 12
Number of Rows	4
Number of Tubes per Row	5
Face Air Velocity (m/s)	0.5~4
Inlet Air D.B.T (F)	74~83
Inlet Air W.B.T (F)	65~75
Inlet Chilled Water Temp. (F)	35~48
Inlet Hot Water Temp. (F)	138~161

Table 3.2 Specifications and Operating Conditions of the Indoor A-Type Coils

Item	Value
Refrigerant	R22, R290
Tube Length (m)	0.435
Tube O.D. (m)	0.01
Tube I.D. (m)	0.0094
Tube Horizontal Spacing (m)	0.0257
Tube Vertical Spacing (m)	0.0191
Fin Thickness (m)	0.000167
Fin Pitch (fins per inch)	16
Number of Rows	3
Number of Tubes per Row	24
Air Flow Rate (cfm)	1120~1180
Inlet Air D.B.T (°C)	21, 26.6
Inlet Air W.B.T (°C)	15.5, 19.4
Inlet Refri. Temp. (°C)/Quality	25~58/0.15~0.25
Inlet Refrigerant Pressure (kPa)	730~870, 1000~1500
Refrigerant Flow Rate (kg/s)	0.0037~0.038, 0.03~0.06

Table 3.3 Specifications and Operating Conditions of Gas Cooler

Item	Value
Refrigerant	CO2
Tube Length (m)	0.43
Tube Width (m)	0.016
Number of Channels per Tube	8
Channel Size (m \times m)	0.001 \times 0.001
Tube Vertical Spacing (m)	0.01
Fin Thickness (m)	0.0001524
Fin Pitch (fins per inch)	16
Number of Rows	5
Number of Tubes per Row	68
Air Velocity (m/s)	3.16~3.21
Inlet Air D.B.T (°C)	27.6~40.8
Inlet Air Humidity	50%
Inlet Refri. Temp. (°C)	72.4~121.6
Inlet Refrigerant Pressure (kPa)	8226~11627
Refrigerant Flow Rate (kg/s)	0.0551~0.0938

Table 3.4 Specifications and Operating Conditions of A Commercial Coil

Item	Value
Refrigerant	Water
Tube Length (inch)	17.32
Tube O.D. (inch)	0.312
Tube I.D. (inch)	0.272
Tube Horizontal Spacing (inch)	0.75
Tube Vertical Spacing (inch)	0.984
Fin Thickness (inch)	0.005
Fin Pitch (fins per inch)	5
Number of Rows	4
Number of Tubes per Row	5
Air Flow Rate (L/s)	15~35
Inlet Air Temperature (°C)	21
Inlet Water Temp. (°C)	43
Water Flow Rate (kg/hr)	65~122

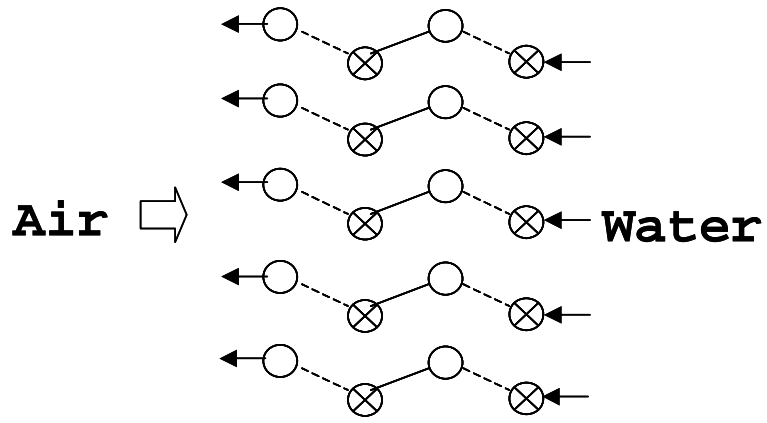


Figure 3.1 Water Coils McQuiston Tested

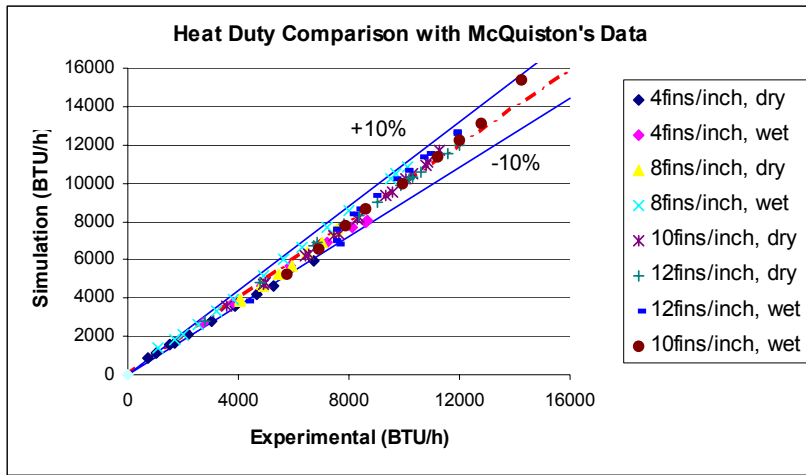


Figure 3.2 Heat Duty Comparison with the Experimental Data of McQuiston's Coils

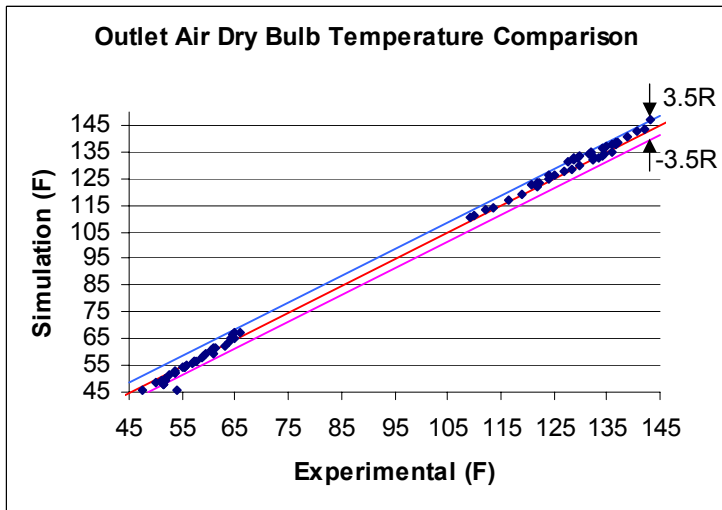


Figure 3.3 Outlet Air Dry Bulb Temperature Comparison with the Experimental Data of McQuiston's Coils

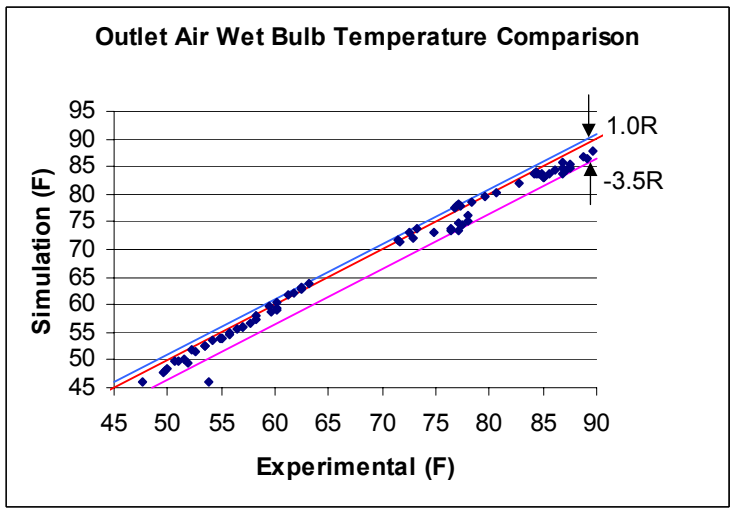


Figure 3.4 Outlet Air Wet Bulb Temperature Comparison with the Experimental Data of McQuiston's Coils



Figure 3.5 An A Type Indoor Coil

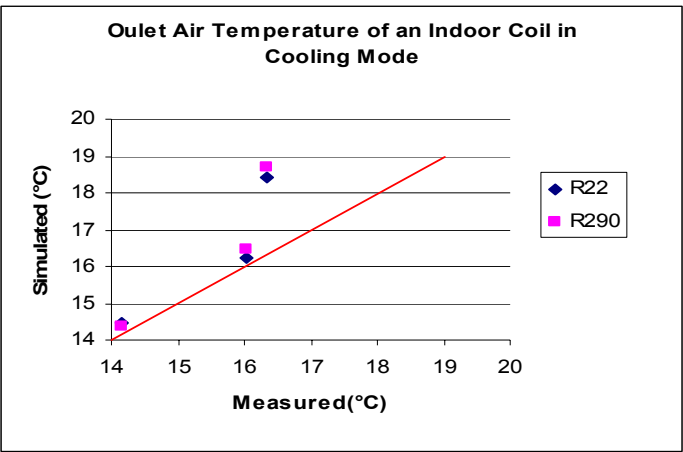


Figure 3.6 Comparison of Outlet Air Temperature of the A Type Coil in Cooling Mode

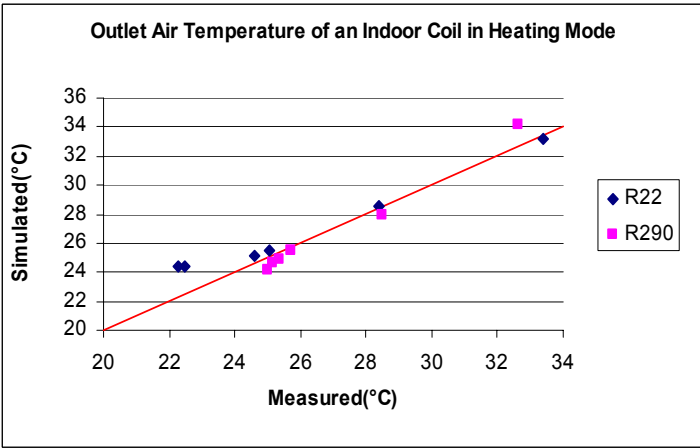


Figure 3.7 Comparison of Outlet Air Temperature of the A Type Coil in Heating Mode

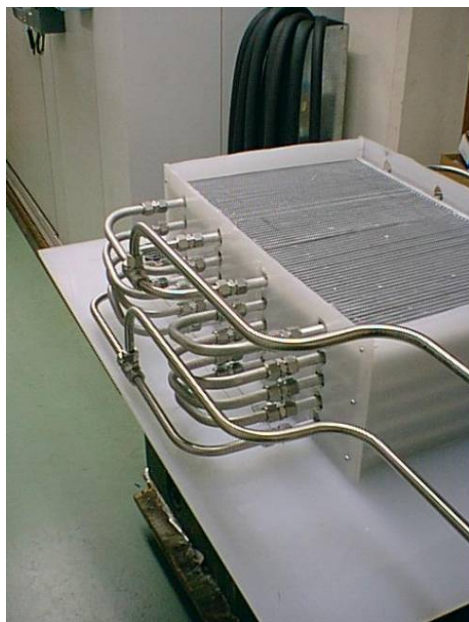
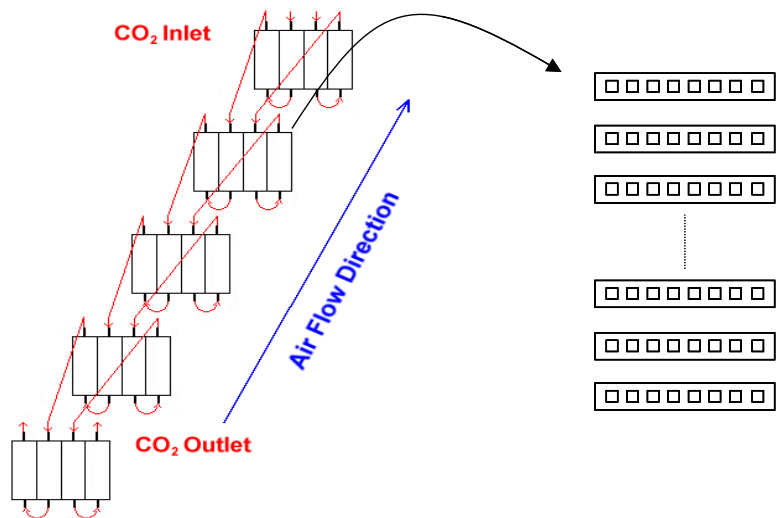


Figure 3.8 A Carbon Dioxide Gas Cooler

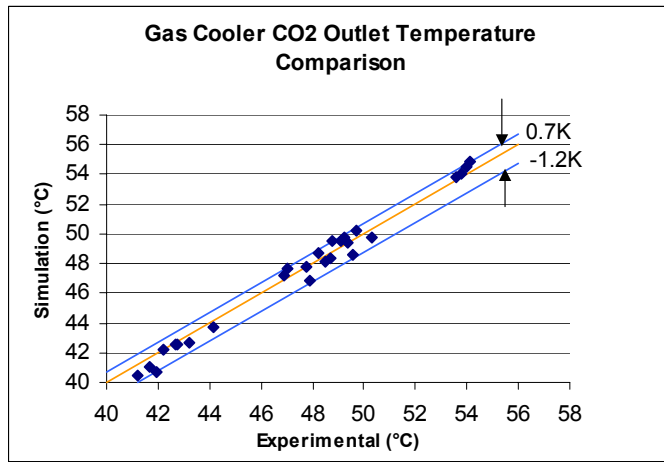


Figure 3.9 Comparison of Carbon Dioxide Outlet Temperature of the Gas Cooler

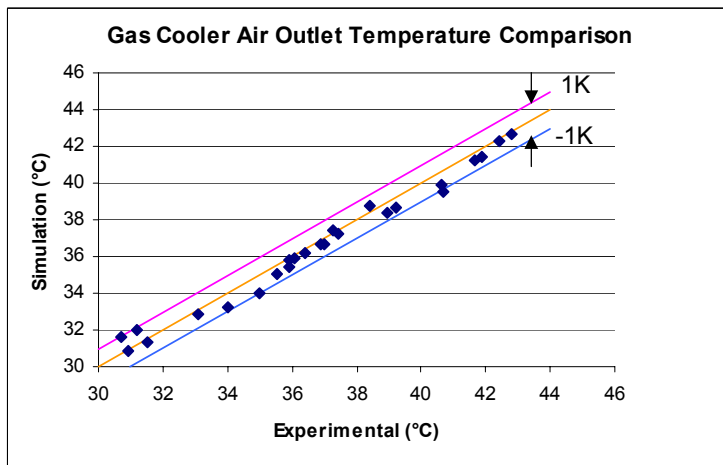


Figure 3.10 Comparison of Air Outlet Temperature of the Gas Cooler

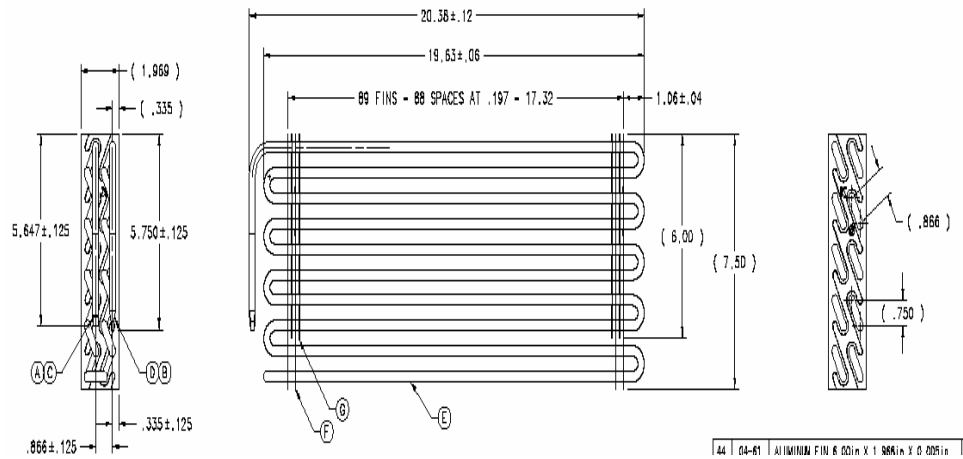


Figure 3.11 A Commercial Coil for Refrigerator Application

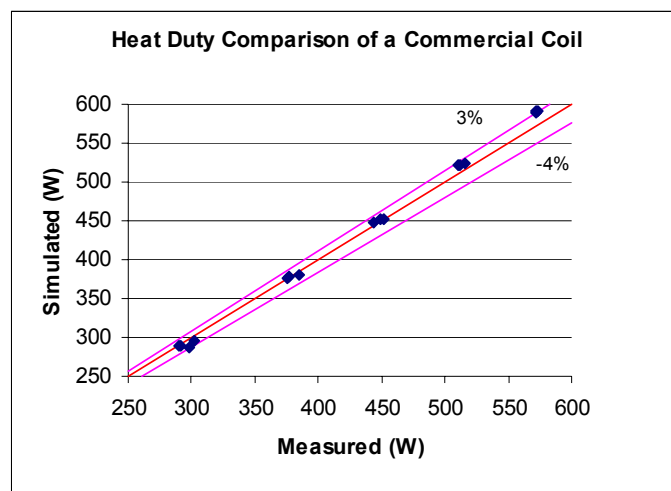


Figure 3.12 Heat Duty Comparison of the Commercial Coil

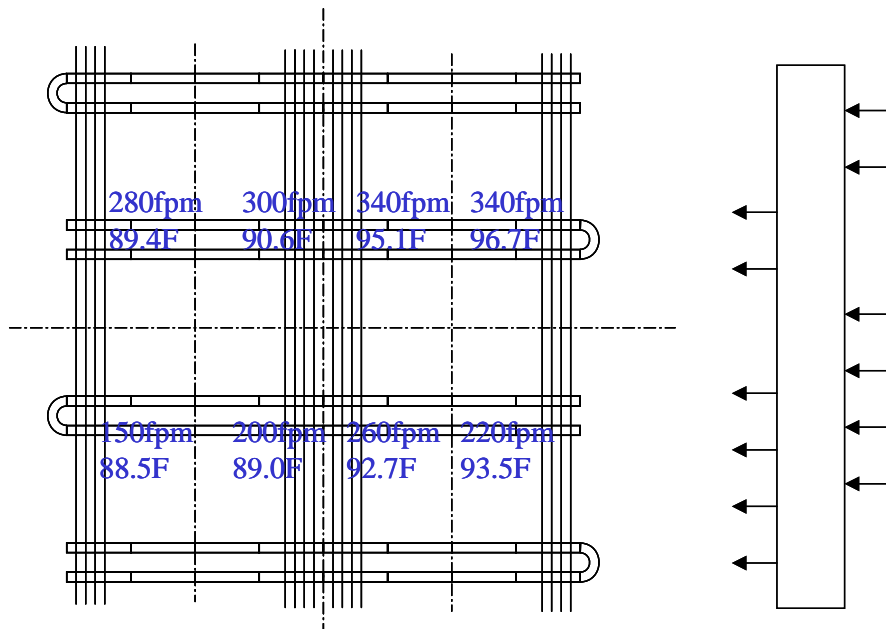


Figure 3.13 An Intertwined Absorber/Condenser Coil

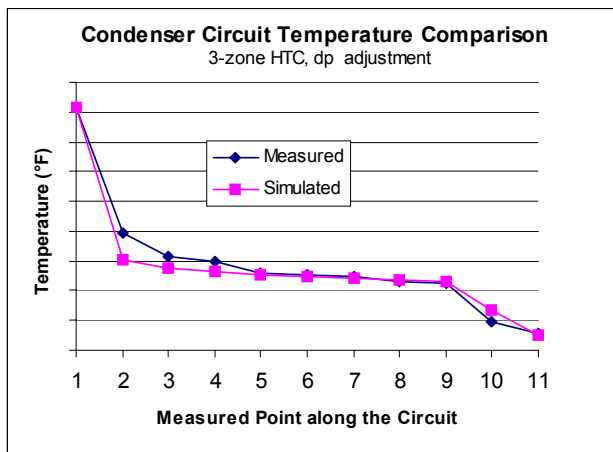


Figure 3.14 Comparison of the Temperatures along the Condenser Circuit

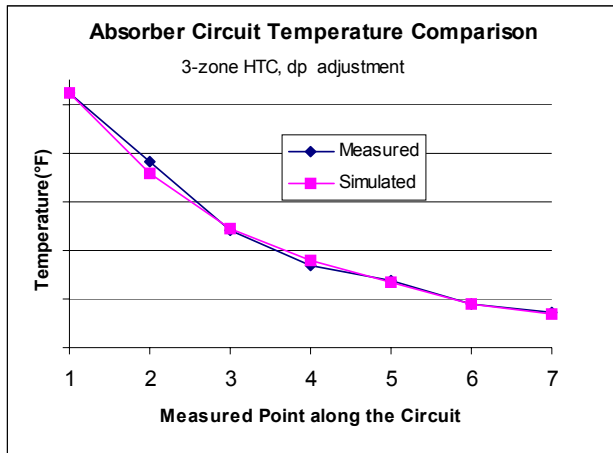


Figure 3.15 Comparison of the Temperatures along the Absorber Circuit

Chapter 4

SIMULATION STUDY

One of the advantages of having a general-purpose design tool for fin-tube heat exchangers is its ability to conduct parametric and circuitry studies under various design, off-design, and operating conditions with different working fluids. Therefore, design alternatives of heat exchangers can be fully explored given the design requirements. This chapter will present the results obtained from the simulation studies with Coil Designer, to show the capability of the design tool in predicting all aspects of heat exchanger performance under a wide variation of design and operating conditions.

4.1 Modeling of a Coil with Arbitrary Circuitry

An arbitrary circuitry is constructed in order to test the capability of the design tool to simulate heat exchanger with tubes connected in an arbitrary manner as shown in Figure 4.1.

Following the solution methodology as described in Chapter 2, Figure 4.2 shows the residual of the air side enthalpies during iterations, which is defined as,

$$\Delta h_{air,res} = \frac{\sum_{i=1}^{N_{tube}} \sum_{j=1}^{N_{seg}} |h_{air,inlet}^{k+1} - h_{air,inlet}^k|}{\sum_{i=1}^{N_{tube}} \sum_{j=1}^{N_{seg}} h_{air,front}} \quad (4.1)$$

where k is the k^{th} iteration on the air side loop of updating the enthalpy facing each segment of each tube beyond the first (frontal) row. After 5 iterations, the tolerance of 10^{-4} has been reached and the entire simulation process is terminated.

Figure 4.3 shows the mass flow rate residual during iterations of solving the hydraulic equations throughout the entire heat exchangers, for each of the air side iteration loop,

$$\Delta \dot{m}_{res} = \max \left| \frac{\sum_{JTA[j][i]=-1} \dot{m}_i - \sum_{JTA[j][i]=1} \dot{m}_i}{\sum_{JTA[j][i]=-1} \dot{m}_i + \sum_{JTA[j][i]=1} \dot{m}_i} \right|_{j=1}^{N_{junction}} \quad (4.2)$$

It can be seen that as the air side iteration loop progresses, the mass flow rate residual at the beginning of each iteration loop decreases, and the iteration number needed to reach the tolerance also decreases. This is due to the fact that the pressure field throughout the junctions is continuously pushed toward the final solution as the repeatedly solved energy equations causes the density field throughout the segments of the tubes of the entire heat exchanger to converge as well.

The ability of the design tool to simulate a coil with arbitrary circuitry is manifested in Figure 4.4. It plots the mass flow rate through each tube respectively. Similar to an electric circuit, tubes connected in parallel decrease the flow resistance, while tubes in series increase the flow resistance, and the mass flow rate through each tube is varied accordingly.

4.2 Model Improvement Results

4.2.1 Subdivided Segments

Chapter 2 has described the modeling of sub-dividable-segment in case of phase change within the segment. Figure 4.5 illustrates this by comparison of the heat duty calculation between the simulation programs with and without implementing sub-dividable segment model. The simulated coil works as a condenser with superheated gas at the inlet and subcooling at the outlet. The air flow is assumed to be uniform facing the front face of the coil, in order to isolate the non-uniform effect on tube segmentation. It is found that by implementing the sub-dividable segment model, the heat duty predicted by the improved simulation program is virtually no more dependent on the number of segments, while without this improvement the predicted heat duty can deviate by approximately 25% of the correct solution.

4.2.2 ϵ -NTU Method versus Arithmetic Average Temperature Difference

Method

Figure 4.6 shows the advantage of using ϵ -NTU method in calculating the heat transfer rate between the air and the refrigerant of a segment, as compared with arithmetic average temperature difference method. The vertical axis represents the refrigerant outlet temperature of the first segment of one tube. While the air side inlet condition is fixed, the refrigerant flow rate is varied over a range. These two methods yield consistent solutions when there is adequate number of segments in a tube. However, the arithmetic average temperature difference method can lead to violation of second law of thermodynamics, if the heat capacity of the air is much larger than that of the refrigerant (vice versa), and the number of heat transfer units NTU ($=UA/C_{\min}$) is large (when there is only one segment in a tube, it implies larger UA value than when there are 10 segments in a tube).

4.3 Examples of Tube-Level and Segment-Level Analysis

4.3.1 Comparison of Cross-counter Flow and Cross-parallel Flow

The cross-counter flow and parallel-flow configured heat exchangers are shown in Figure 4.7. Ammonia/water mixture is used as the working fluid. Figure 4.8 shows the average refrigerant temperature in each row and the average air temperature between each row. The inlet air temperature is indicated at the left side. The inlet refrigerant temperature is shown at the left side for parallel flow

and at the right side for counter flow. As is well established, in a parallel flow configuration, the outlet temperature of the hot streams is never lower than the outlet temperature of the cold streams (air). In counter flow configuration, each tube plays an almost equivalent role in the amount of heat transfer, and the total heat duty of the heat exchanger is considerably larger than that in the parallel flow configuration as indicated in Figure 4.9.

4.3.2 Refrigerant Side Heat Transfer Coefficients at Segments

The variation of the refrigerant side heat transfer coefficient in the flow direction during evaporation is shown in Figure 4.10, where the abscissa represents the 160 segments with each tube divided into 10 segments. Kandlikar's correlation (Kandlikar, 1991) is used to calculate the boiling heat transfer coefficient of the refrigerant. As the mass flow rate decreases, the heat transfer coefficient decreases and the superheated area increases. The shift in the magnitude of the heat transfer coefficients in the two horizontally neighboring tube is because the heat flux in back-row tube is lower than that in the front-row tube.

Figure 4.11 shows the refrigerant temperature profile in the flow direction. There is about 4K drop in temperature from the inlet to the outlet in the two-phase region, due to the effect of the pressure drop of fluid flow. In the

superheated zone, the refrigerant temperature increases rapidly, because of small heat capacity of the superheated gas.

4.3.3 Latent and Sensible Heat Duty at Tubes

Figure 4.12 shows a comparison of the sensible heat with latent heat of each tube in an evaporator consisting of 16 tubes, when air dehumidification occurs on the tube surfaces with 70% of inlet air relative humidity. In the two-phase region from tube 7 to tube 16, the two tubes in the front row, facing warmer and more humid air, have relatively large heat duties. The difference to both latent and sensible heat duty of the tubes in the back row implies the combined effect of the refrigerant temperature and the refrigerant side heat transfer coefficient as illustrated in Figure 4.10 and 4.11. In the superheated zone from tube 1 to tube 6, no condensation of water vapor takes place and heat transfer amount is considerably smaller, due to the relatively high wall/fin temperature of the tubes and lower heat transfer coefficient.

4.4 Non-uniform Air Flow and Fin Spacing

4.4.1 Non-uniform Air Flow

Due to the installation of a fan and fan performance characteristics, distribution of air flow is not uniform in the plane perpendicular to the coil tubes. As introduced in Chapter 2, the design tool accounts for non-uniform air distribution by assigning appropriate air velocity for each segment of each tube in the front row.

The air flow rates associated with the segments of the tubes beyond the front row are calculated according to the air flow rates associated with the segments in tubes of the preceding row.

The effect of non-uniform air distribution on refrigerant temperature distribution is presented in Figure 4.13. While the air flow rate linearly decreases tube by tube from top to bottom of the coil, the temperature of the refrigerant (water) also changes with smaller magnitude from tube to tube. From left to right along the segments in a tube, the temperature gradually decreases in the refrigerant (water) flow direction, since the water is being cooled by the air. However, the water temperature decreases quickly from segment to segment, in the top tubes, and slowly in the bottom tubes.

4.4.2 Non-uniform Fin Spacing

Non-uniform fin spacing is not uncommon, especially in the coils for refrigerator applications. Coil Designer can also account for non-uniform fin spacing by assigning fin spacing to each segment of the tubes in the coil.

Figure 4.14 presents the outlet air temperatures associated with the segments in the tubes at the back row, when the fin spacing increases linearly and the air velocity decreases, from the top to bottom tube by tube. With air stream of higher flow rate entering the tubes with higher fin density, the heat

exchange effectiveness is improved and therefore the outlet air temperature is higher, as compared with the coil with uniform fin spacing as demonstrated in Figure 4.15. Though not conclusive, the heat duty of the coil with non-uniform fin spacing shows a gain of 4% over the coil with uniform fin spacing, provided that the total heat transfer area is the same in both coils, and the air velocity distribution is not affected by the varied fin density.

4.5 ϵ -NTU Relationship Study

The ϵ -NTU relationship for various heat exchanger configurations including cross-flow types has been well addressed in the books of heat transfer. However, it is worthwhile to revisit and confirm it by using the design tool.

In reproducing the ϵ -NTU relationship with the simulation results from the design tool, the “UA” is defined as,

$$UA = \frac{1}{\frac{1}{A_{total} \eta_0 h_{air,aver}} + \frac{0.5(d_o - d_i)}{kA_{tube}} + \frac{1}{h_{refri,aver} A_{tube}}}$$

where the $h_{air,aver}$ and $h_{refri,aver}$ represent average heat transfer coefficients on the air side and refrigerant side respectively.

Figure 4.16 shows the schematic of a cross-counter flow configuration highlighting the number of rows and the number of tubes per row. It is shown in

Figure 4.17 that the effect of the number of tubes per row on the exchange effectiveness is negligible, when the number of rows is fixed. But the number of rows has larger effect on the effectiveness, though as it continues to increase, it will approach the effect of pure counter flow configuration, as seen in Figure 4.18.

A comparison is made of the effectiveness of different configurations of coils in Figure 4.19. Among the three configurations, the cross-counter flow configuration has the largest effectiveness, and the cross-parallel flow configuration least, with the cross-flow configuration in between.

4.6 Effect of Air Flow Rate and Humidity on the Latent Heat Ratio

Figure 4.20 shows the effects of the air flow rate and humidity on the latent heat ratio of a coil functioning as an evaporator. The abscissa represents the air flow rate, and each curve in the figure corresponds to a constant humidity ratio. The air inlet temperature and refrigerant inlet condition are fixed respectively. As the air flow rate increases, the latent heat ratio tends to be smaller, since the larger heat capacity and heat transfer coefficient associated with the increased air flow rate tend to produce higher amount of sensible heat at a higher tube surface temperature. This provides a perspective in optimizing the air flow rates, depending on the applications of evaporators for either air conditioning, dehumidification, or refrigeration.

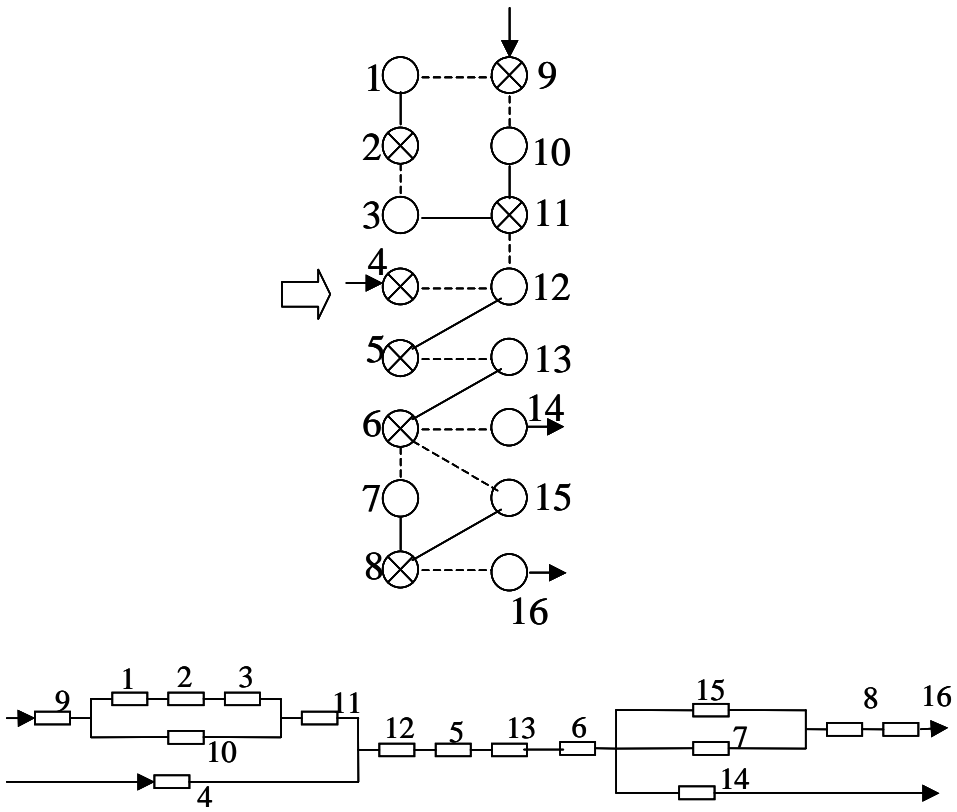


Figure 4.1 A Coil with Arbitrary Circuitry

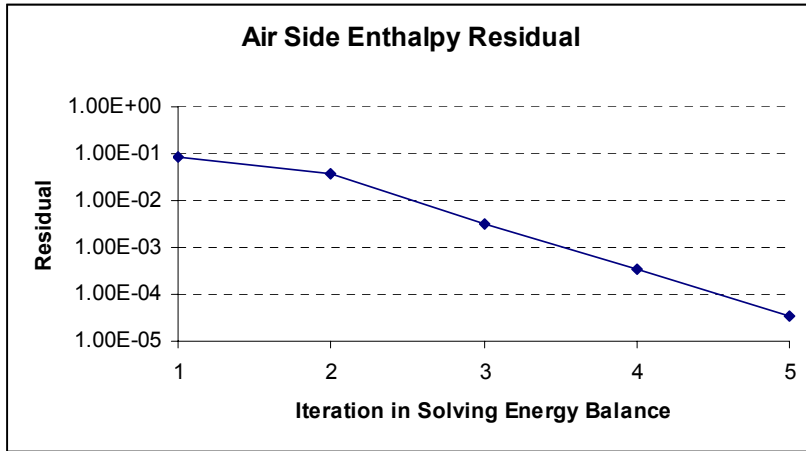


Figure 4.2 Air Side Enthalpy Residual

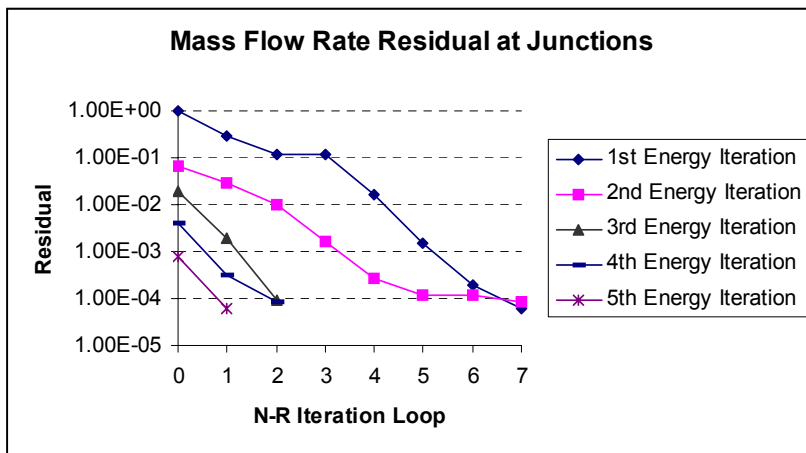


Figure 4.3 Mass Flow Rate Residual at Junctions

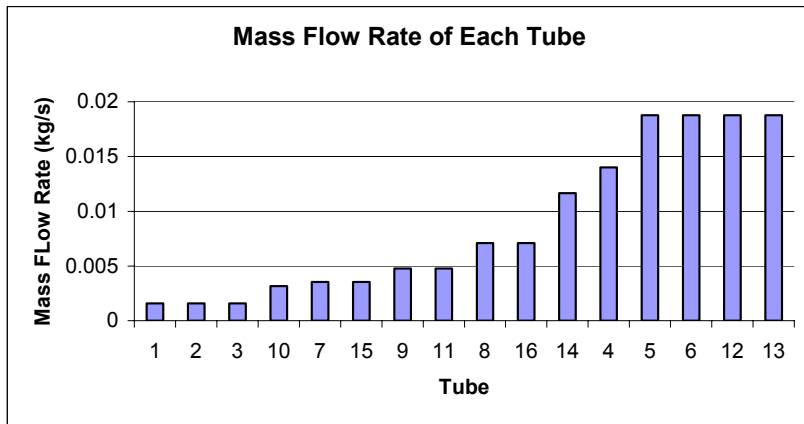


Figure 4.4 Mass Flow Rate of Each Tube in Coil with Arbitrary Circuitry

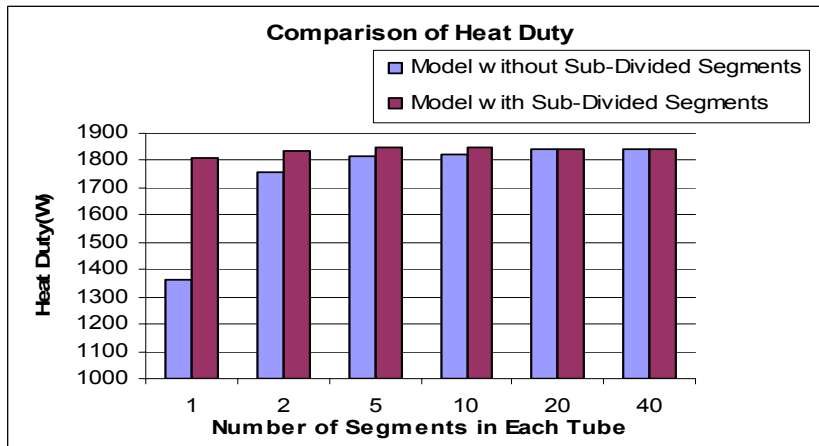


Figure 4.5 Comparison of Heat Duty w/o Sub-divided Segment Model

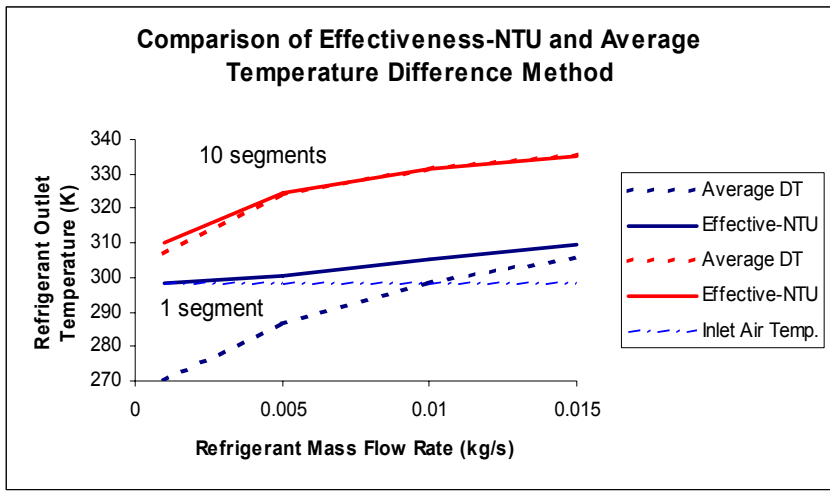


Figure 4.6 Comparison of ϵ -NTU and Average Temperature Difference Method

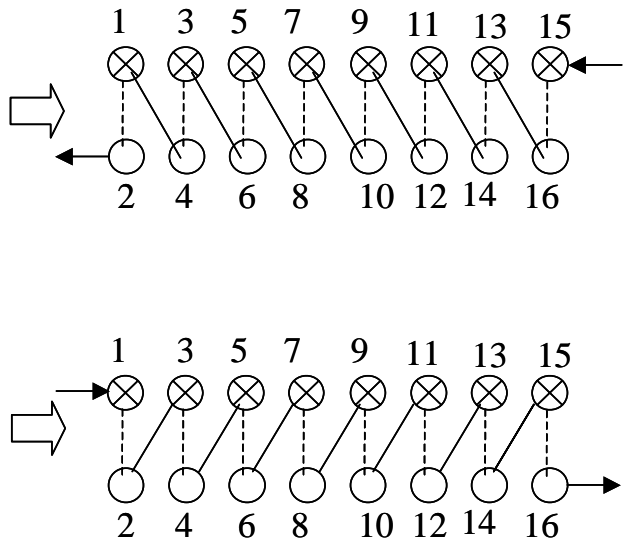


Figure 4.7 Cross-Counter and Cross-Parallel Flow

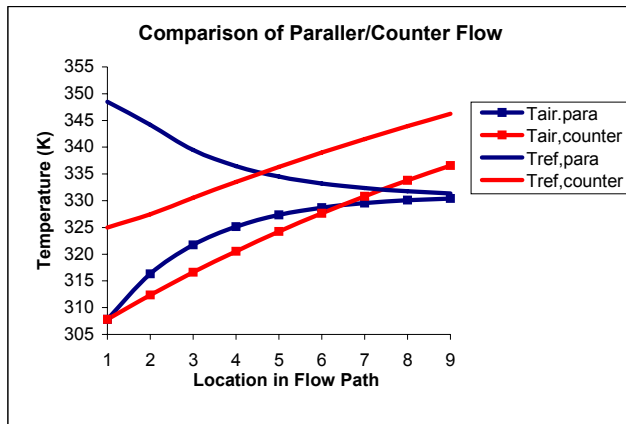


Figure 4.8 Refrigerants and Air Temperature

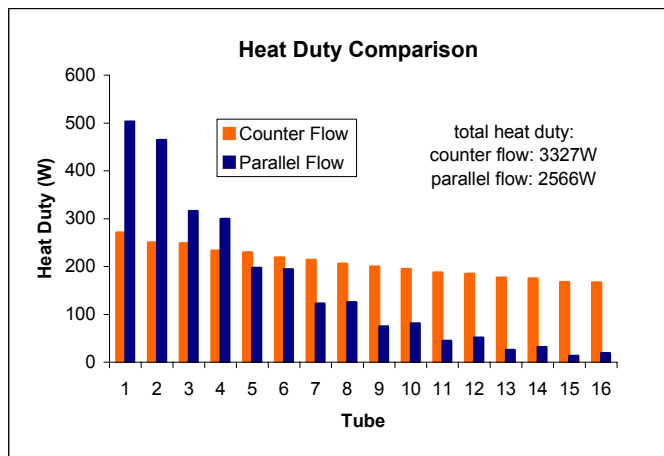


Figure 4.9 Heat Capacity of Each Tube

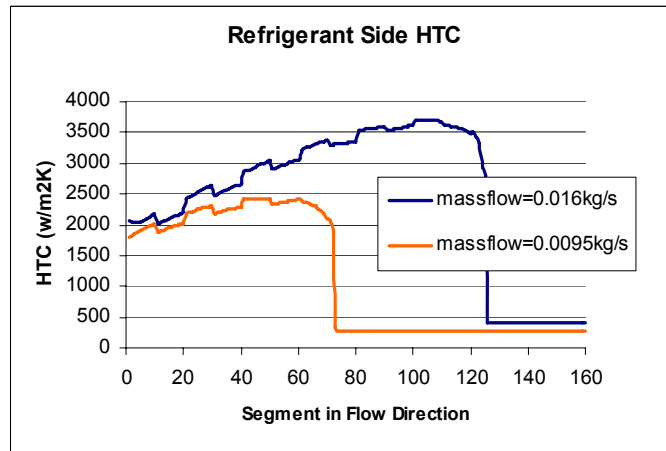
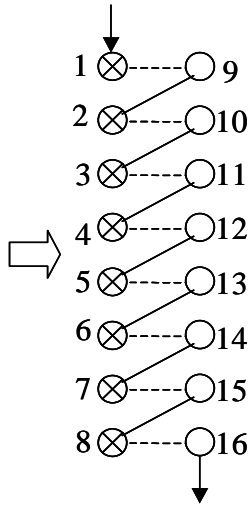


Figure 4.10 Local Heat Transfer Coefficients of Refrigerant Side

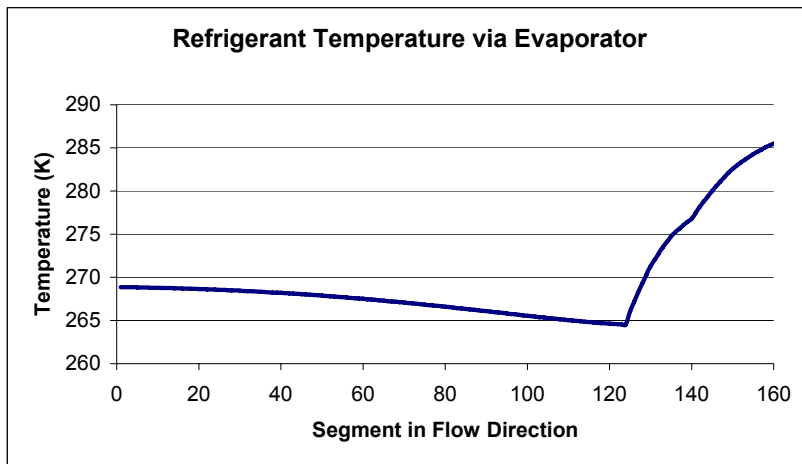


Figure 4. 11 Local Temperature of Refrigerant

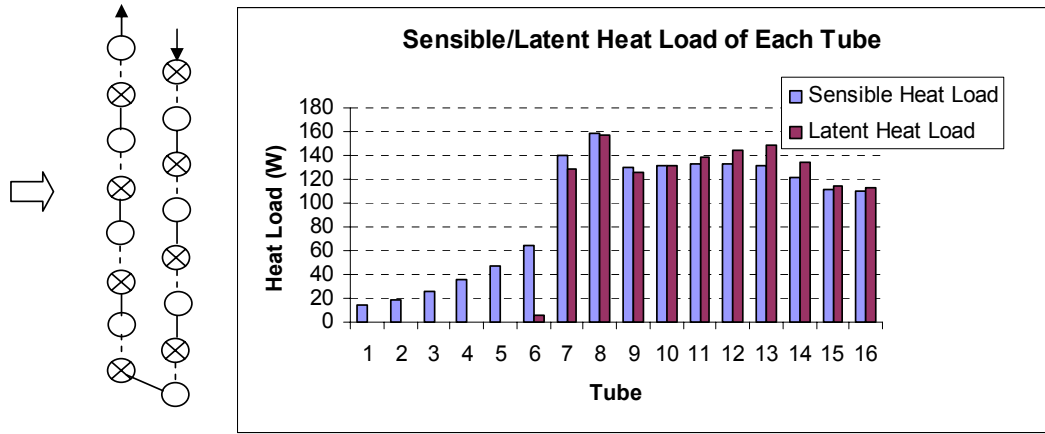


Figure 4.12 Sensible and Latent Heat of Tubes

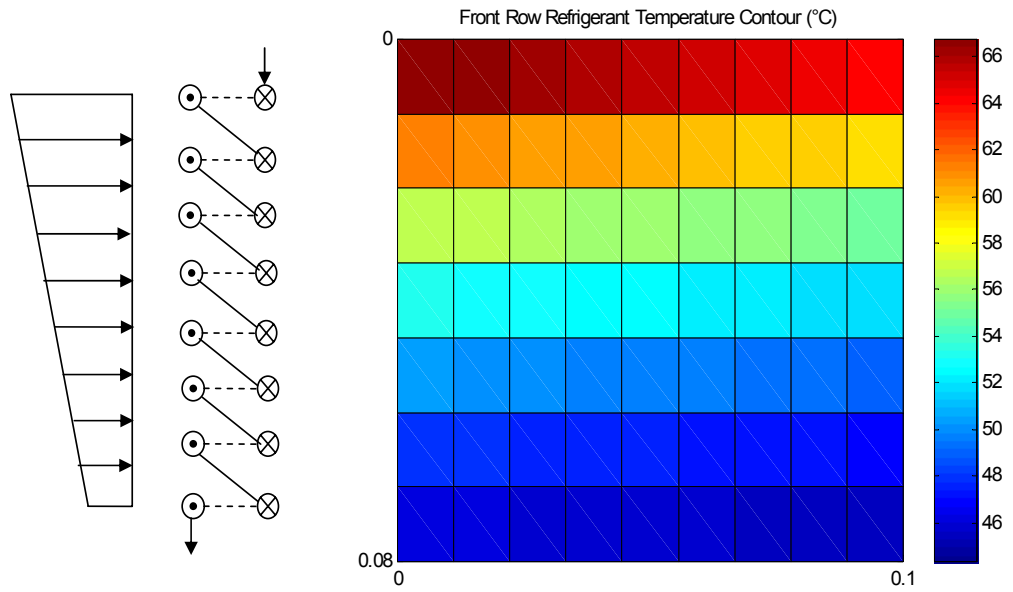


Figure 4.13 Refrigerant Temperature Profile with Non-Uniform Air Flow

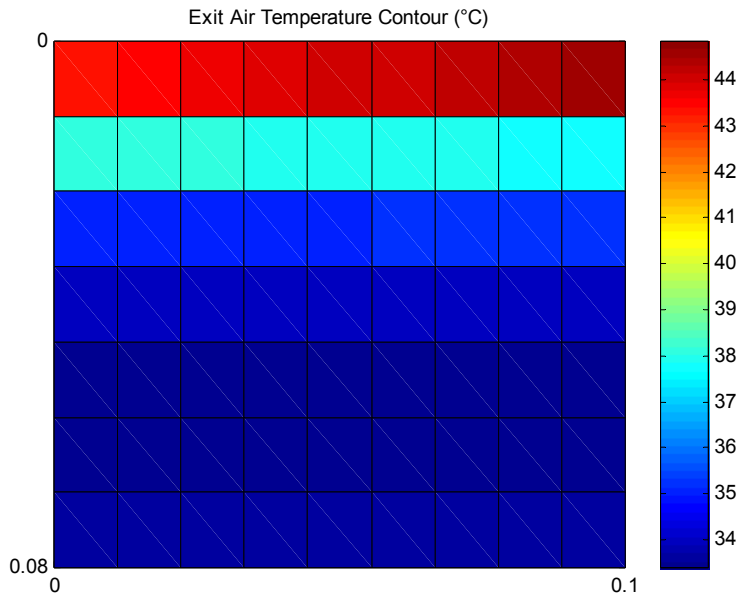
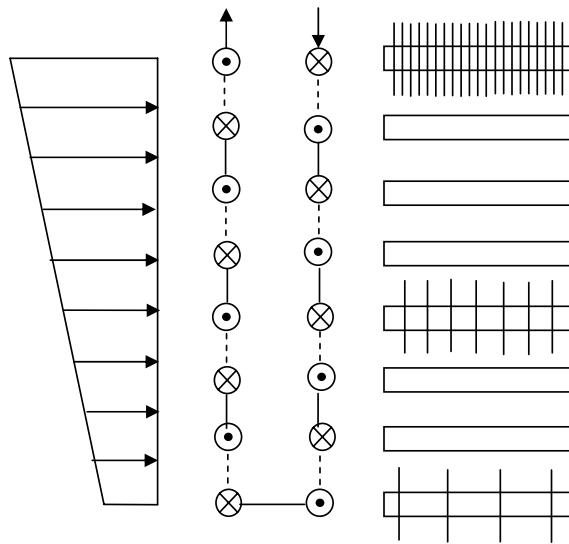


Figure 4.14 Air Temperature Profile with Non-Uniform Fin Spacing

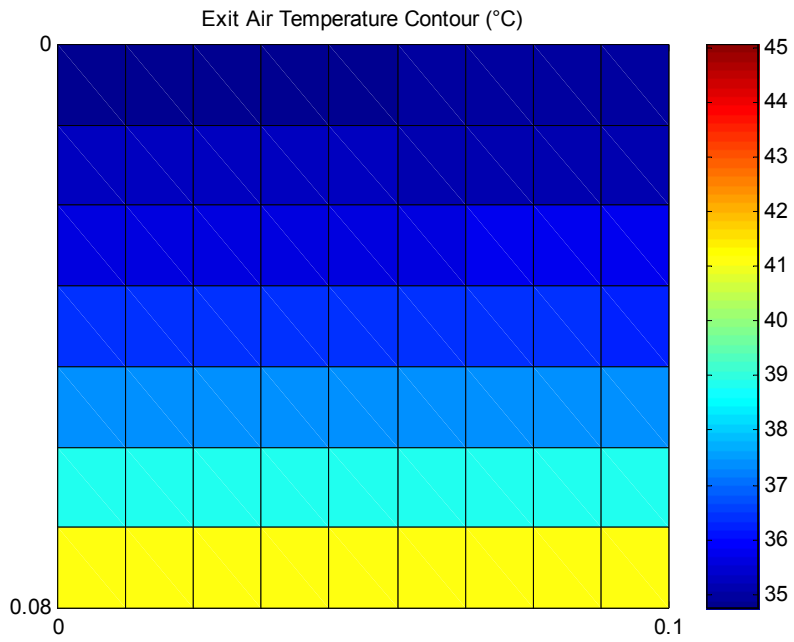
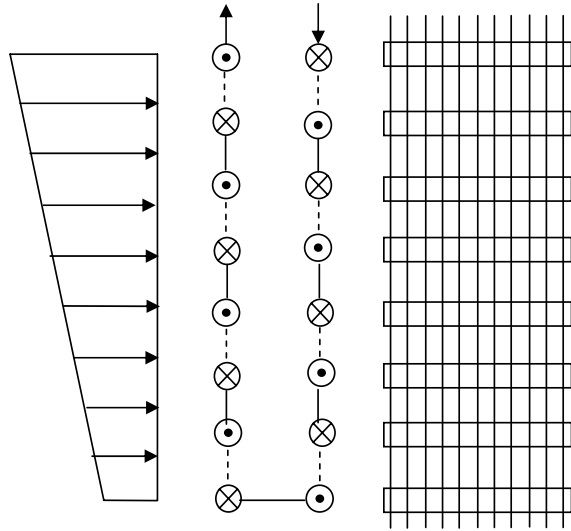


Figure 4.15 Air Temperature Profile with Uniform Fin Spacing

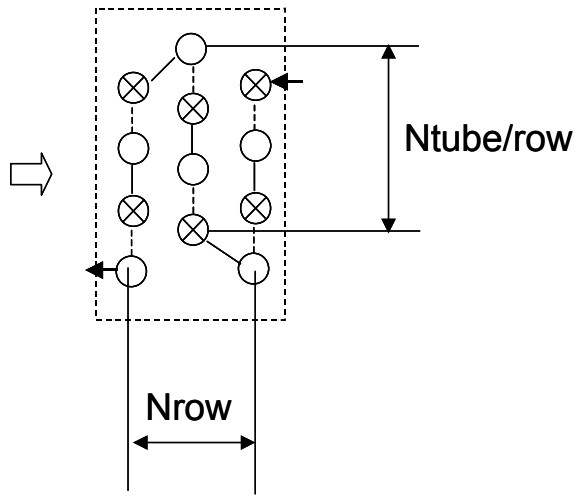


Figure 4.16 Cross-counter Flow Configuration

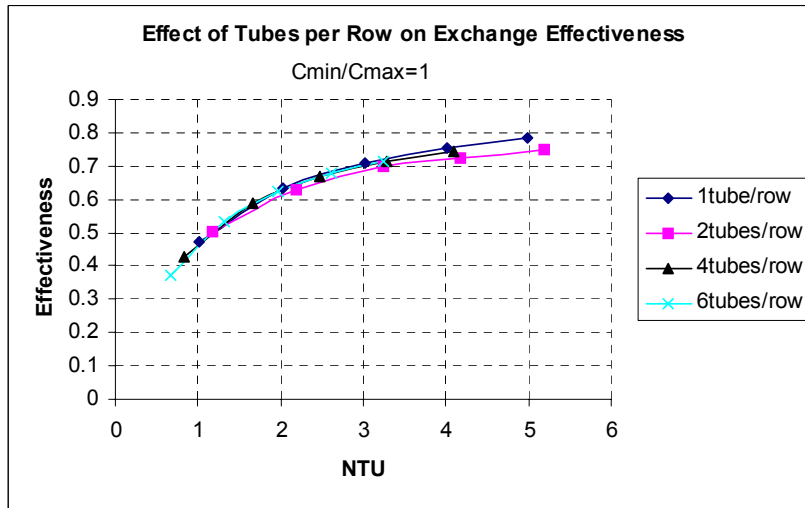


Figure 4.17 Effect of Tubes per Row on Exchange Effectiveness

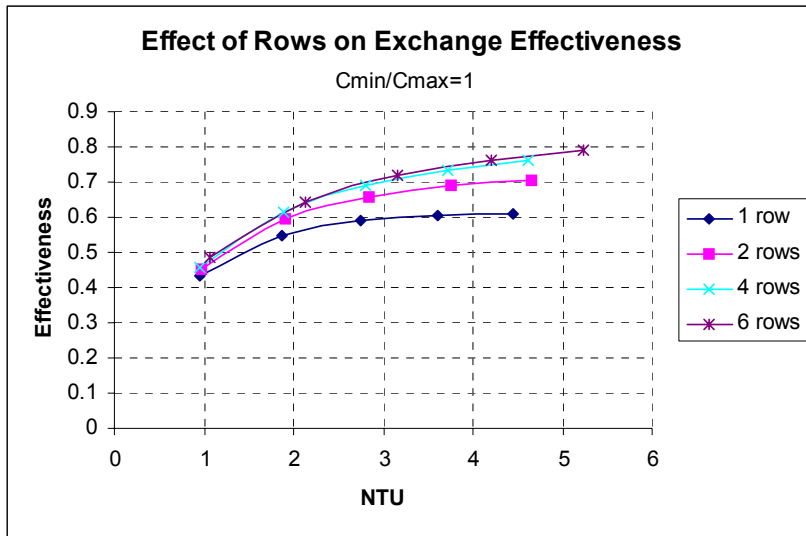


Figure 4.18 Effect Number of Rows on Exchange Effectiveness

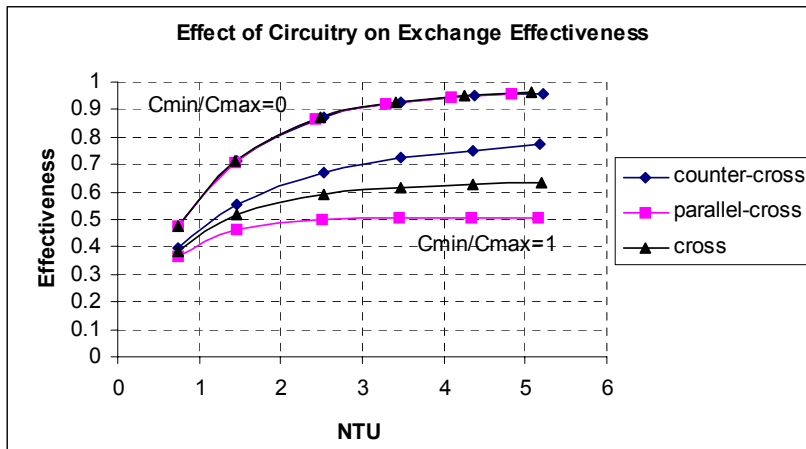


Figure 4.19 Effect of Circuitry (Configuration) on Exchange Effectiveness

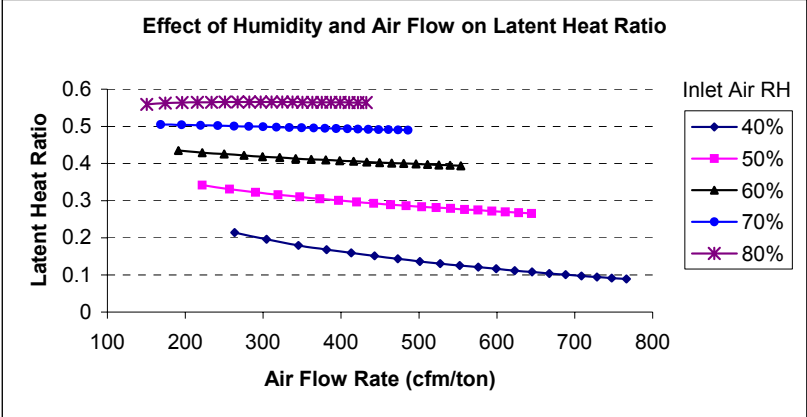


Figure 4.20 Effect of Humidity and Air Flow on Latent Heat Ratio

Chapter 5

DESIGN OPTIMIZATION CASE STUDY

5.1 Introduction

Coil Designer is intended to provide help in design optimization of air-to-refrigerant heat exchangers. An optimal heat exchanger is defined as one that, while satisfying imposed constraints, achieves the required task at the lowest possible cost (Kovarik, 1989). The cost can be defined very diversely depending on manufacturing difficulties and capabilities, material cost, and other parameters. It can be associated with capital expenditure for manufacturing and installation, with energy consumption during operation, and with expense during maintenance. In addition to cost, other parameters or performance can be set as design objectives such as weight, surface area, volume, fan power, or heat transfer rate, to the interests of applications and designers.

A survey of previous work has revealed that, although there are a number of programs for air-to-refrigerant fin-and-tube heat exchangers with increased simulation capabilities, none has as complete a set of features or as comprehensively integrated optimization capability as the tool introduced here.

Fin-and-tube heat exchanger design involves options for both continuous and discrete variables, including variations in tube length, tube diameter, tube spacing, fin thickness, fin spacing, number of rows, and number of tubes per row. A designer can choose from many design options to satisfy the design objectives without sacrificing the performance. However, the number of discrete combinations grows significantly with the number of variables considered and the number of alternatives available for each variable. The design takes place in a multi-dimensional space and intuition on how an optimized design should turn out is quickly lost. Moreover, the computer programs used to evaluate the performance of heat exchangers given necessary input parameters are becoming more sophisticated and involving large number of nonlinear equations without explicit relations. It is computationally prohibitive and practically impossible for the designers to do exhaustive exploration of each design configuration with each design alternative. A computationally efficient optimizer is therefore very necessary and beneficial for such large-scale, combinatorial, black box optimization problem (Tayal, 1999).

Most of the conventional optimization methods and techniques require explicit expressions of the objective functions and constraints as well as gradient information to search the design space. They are mainly intended for optimization problems with continuous variables. Though there are approaches for solving nonlinear optimization problems with mixed discrete-continuous

variables, such as random search methods and those based on the branch-and-bound technique, they either require a large number of function evaluations to locate an optimum solution, or transform the original optimization problem into a large number of sub-optimization problems. Their application is restricted to problems with relatively small search space.

Genetic algorithm are among the probabilistic algorithms dealing with optimization problems. Because of their simplicity, ease of operation, independence of the characteristics of the problem, and parallel and global perspectives, genetic algorithms have been applied successfully in a wide variety of problem domains (Mitsuo Gen, Runwei Cheng, 2000). They offer substantial savings in computational cost and provide global optimal solution or solutions very close to it. They have also been introduced into optimization problems encountered in the thermal/fluid engineering area (Fabbri, 1998, Queipo et al, 1994, Schmit et al, 1996, and Tayal, 1999).

In the following section, a brief introduction to genetic optimization algorithms is described to explain the basic theory involved.

5.2 An Overview of Genetic Algorithms

Genetic algorithms (GA) are search procedures based on the principles of natural genetics and natural selection and the idea of survival of the fittest (Holland, 1975, Goldberg, 1989).

A usual way of applying genetic algorithms to solving optimization problems is to encode a design variable vector into a binary string, or say chromosome. For a problem having n variables, $\bar{x} = (x_1, x_2, \dots, x_n)$, a chromosome contains n sub-strings,

$$\underbrace{1001\dots01}_{x_1} \quad \underbrace{1101\dots00}_{x_2} \quad \dots \quad \underbrace{0001\dots11}_{x_n}$$

If each variable x_i is encoded in l_i bits, the length of chromosome is $\sum_{i=1}^n l_i$. A set of chromosomes representing a set of possible solutions is called a population. Successive populations are called generations.

A sub-string can be decoded into an integer variable k , according to

$$k = \sum_{i=1}^{l-1} b_i 2^{l-i-1} \quad (5.1)$$

where l is the length of the sub-string, and b_i is the value (allele, or gene) of the i^{th} bit. A sub-string can also represent a real variable. First the sub-string is decoded into an integer as described above. Then the integer is mapped from the discrete interval $[0, 2^l - 1]$ to the real interval $[L, U]$ by using the formula,

$$x = \frac{k}{2^i - 1}(U - L) + L \quad (5.2)$$

The general working principle of a GA is described below:

1. Randomly or heuristically generate initial population of n chromosomes
(a discrete set of design variables that is potential solutions to the problem).
2. Obtain the objective function values and constraints (if any). Evaluate the fitness $f(x)$ of each chromosome x in the population.
3. Create a new population by using operators,

Selection:

Select chromosomes from a population according to their fitness. The better the fitness of the chromosome, the larger the chance to be selected and reproduced in the new population or next generation.

Crossover:

With a crossover probability, randomly exchange parts of genes of two parent chromosomes to generate two new chromosomes called offspring. The crossover operator provides new information about the hyperplanes already represented earlier in the population.

Mutation:

With a mutation probability, randomly select gene(s) and alter the value(s) of the gene(s) to generate new chromosomes called offspring. The mutation operator

Formatted: Bullets and Numbering

Formatted: Bullets and Numbering

Formatted: Bullets and Numbering

increases the variability of the population, a safeguard against a premature loss of important genetic information at a particular position.

4. If the stop criterion (e.g. a specified number of generations) is satisfied, stop, and return the best solution in current population. If not, go to step 2.

The above steps of GA search procedure are shown in Figure 5.1. By exploiting the best solution and exploring the search space, the genetic algorithms direct random search in complex landscapes toward the desired area of the solution space.

5.3 Constraint Handling and Multi-Objective Optimization

5.3.1 Constraint Handling

Most of the optimization problems in engineering involve a number of constraints and the optimal solution must satisfy these conditions. A constrained optimization problem can be written as below,

Minimize $f(\bar{x})$

Subject to

$$g_j(\bar{x}) \leq 0, \quad j = 1, \dots, J \quad (5.3)$$

$$h_k(\bar{x}) = 0, \quad k = 1, \dots, K \quad (5.4)$$

$$x_i^l \leq x_i \leq x_i^u, \quad i = 1, \dots, n \quad (5.5)$$

where \bar{x} is a vector of size n . There are n variables, J inequality constraints, and K equality constraints.

In applying genetic algorithms to the above problems, the genetic operators used to manipulate the chromosomes often yield infeasible offspring (chromosomes violating any constraints). Many techniques and methods have been proposed and studied to handle the constraints. They can be classified into the following five categories (Deb, 2000):

1. Methods based on preserving feasible solutions;
2. Methods based on penalty functions;
3. Methods making distinction between feasible and infeasible solutions;
4. Methods based decoders;
5. Hybrid methods;

The most common method used in genetic algorithms to handle constraints is probably the one based on penalty functions, due to its ease to implement and its efficiency. It essentially transforms a constrained optimization problem into an unconstrained one by adding (or subtracting) a certain penalty term to (or from) the objective function for any constraint violation:

$$F(\bar{x}) = f(\bar{x}) \pm \left[\sum_{j=1}^J r_j G_j + \sum_{k=1}^K c_k L_k \right] \quad (5.6)$$

where $F(\bar{x})$ is the new objective function (fitness function) to be optimized, G_j and L_k are functions of the constraints $g_j(\bar{x})$ and $h_k(\bar{x})$ respectively:

$$G_j = \max[0, g_j(\bar{x})]^\beta \quad (5.7)$$

$$L_k = |h_k(\bar{x})|^\gamma \quad (5.8)$$

where β and γ are usually 1 or 2. r_j and c_k are positive constant “penalty factors”. Often the constraints are normalized so that only one penalty factor needs to be used. Equality constraints are normally transformed into inequality constraints in the form:

$$|h_k(\bar{x})| - \varepsilon \leq 0 \quad (5.9)$$

where ε is very small positive tolerance.

In genetic algorithms, the penalty technique is used to keep a certain number of infeasible solutions in each generation so as to enforce the genetic search toward an optimal solution from both sides of feasible and infeasible regions (Gen, Cheng, 2000). The penalty factor affects the balance between information preservation and selective pressure. Both under-penalty and over-penalty should be avoided.

5.3.2 Multi-Objective Optimization

Compared with single objective optimization, there are situations where multiple objective functions need to be optimized simultaneously. However, there does not necessarily exist a solution that is best with respect to all objectives since the objectives are at least partly conflicting and incommensurate with each other. In the multi-objective case, there usually exist a set of solutions, where no improvement is possible in any objective function without compromising at least one of the other objective functions. These solutions are so called “Pareto

optimal solutions”. In reality, a human decision maker can select the most “preferred” from the set of Pareto solutions.

In genetic algorithms, a population of potential solutions is maintained from generation to generation with multiple directional and global search. This makes the genetic algorithms beneficial and effective in exploring the Pareto solutions.

A special issue in genetic multi-objective optimization is how to determine the fitness value of individuals according to multiple objectives. A number of methods have been suggested and tested for fitness assignment. One of them is the Pareto-based approach. This technique explicitly makes use of the definition of Pareto optimality. The fitness of a chromosome is defined in terms of its rank. The method consists of assigning rank 1 to non-dominated chromosomes, removing them from competition; again finding a set of non-dominated chromosomes among the remaining ones in the population, and assigning rank 2 to them and so forth. These rankings are then used in the selection part of the algorithm.

5.4 PGAPack and MOGA

5.4.1 Introduction

PGAPack is a parallel genetic algorithm library that is intended to provide most capabilities desired in a genetic algorithm package, in an integrated, seamless, and portable manner (Levine, 1996). It is featured with easy-to-use interface, multiple choices for selection, crossover, and mutation operators, object-oriented data structure neutral design, parameterized population replacement.

MOGA is based on PGAPack and tailored for multi-objective optimization problems. The main differences between PGAPack and MOGA are in the fitness assignment strategy, and the constraint handling part (Jungkind, 2002).

5.4.2 Key GA Parameters

Due to the probabilistic feature, genetic algorithms do not guarantee global optimality, but are successful in getting very close to the global optimal solution, if not reaching the global optima. The efficacy of a GA is dependent on the customization of parameters to the specific problems. The key parameters affecting the performance of GA include the following,

- Population Size and Population Replacement

The population size is the number of solution strings in a population. It is believed that by increasing the population size, the performance of GA would be improved, though the computational cost also increases. The population

replacement means the number of new strings created via crossover and mutation in each generation, where the remaining strings are the most fit strings from the old population.

- Selection

There are four selection types to choose from: proportional, stochastic universal, binary tournament, and probabilistic binary tournament.

- Crossover

Three crossover types can be specified: one-point, two-point, and uniform crossover. The crossover rate is the probability that a gene undergoes crossover.

- Mutation

The mutation rate is the probability that a gene in a string undergoes mutation. It is normally much smaller than the crossover rate.

- Stopping Criterion

GA is terminated when at least one of the following three stopping criterion is met: 1) Number of generations limit reached, 2) population too similar, 3) no change in the best solutions found in a specified number of generations.

5.5 Single Objective Optimization

5.5.1 Single Objective Optimization without Constraints

To demonstrate the capabilities of the genetic algorithm in finding optimal solutions for heat exchanger design, and to illustrate the process of the genetic algorithm optimization, a case study of single objective optimization without

constrained conditions is carried out. A fin-and-tube coil with single-phase fluid flow is to be optimized with respect to its heat duty. The design variables include circuitry, number of rows, number of tubes in each row, fin spacing, and the entering air velocity. These five variables are represented in a solution vector:

$$\bar{x} = (iCircuitry, N_{row}, N_{col}, s, V_{air}) \quad (5.10)$$

A chromosome of length of 12 bits is constructed to encode this vector. The length of each sub-string is allocated according to how much search space each variable is assigned,

$iCircuitry$: 4 types of circuitries (corresponding to integer variables 0~3),

N_{row} : 8 choices of number of tubes per row,

N_{col} : 4 choices of number of rows,

s : 4 choices of fin spacing, ranging from 0.001m to 0.004m,

V_{air} : 8 choices of air velocity, ranging from 0.5m/s to 3.0m/s.

The above variables are shown figuratively in Figure 5.2.

The reduction of search space for continuous variables (fin spacing and air velocity, in this case) to a set of finite variable values is necessary due to the discretization nature of in the genetic algorithms. The discretization accuracy depends on the number of bits (genes) allocated to each continuous variable.

After initializing the GA parameters and encoding the design variables into a chromosome, the GA calls the “black-box” model CoilDesigner, which returns

the objective function values (and constraint values if any) according to the input design variables.

Figure 5.3 presents the resulting optimized solution string with a graph showing the tendency of the best and average fitness values (heat duty in this study) of the chromosomes as a function of generations during the GA process. The best fitness value is in fact the heat duty output of the "best designed" coil among all the candidate coils in a given population.

It can be seen from Figure 5.3 that after some generations, most of the chromosomes in the population become identical, and the average fitness value is approaching the best fitness value. It is reasonable to expect that if after a certain number of iterations no further improvement of the solution strings can be achieved, then the GA can be terminated at a priori set maximum number of generations. Figure 5.3 also shows that larger population size tends to need less number of generations to reach the optimal solution.

Based on the length of the solution strings, the total number of possible combinations of the design variables (the cardinality of the solution space) is $2^{12}=4096$. However the black-box model CoilDesigner in the GA framework is called only 300 and 220 times for the population sizes of 50 and 20 respectively.

Therefore the computational cost saving by using a GA as compared to an exhaustive search is 92.7% and 94.6% respectively.

It is straightforward that the resulting best solution string corresponds to the maximum (upper limit) number of rows and tubes per row, the largest air velocity, and the smallest fin spacing. The circuitry represented by the sub-string is counter-cross flow as expected. These values of variables certainly yield the maximum heat duty of a coil when no constrained condition exists.

5.5.2 Heat Transfer Surface Area Minimization

The heat transfer surface area governs the overall cost and is a primary concern in the design of a heat exchanger. A case study is conducted for estimation of the minimum area required for a given heat duty.

Table 5.1 provides the specifications of a coil with water as the working fluid, and Figure 5.4 shows the schematic diagram of the coil. This coil is used as a benchmark for design refinement by GA optimization. The variables to be “redesigned” are the vertical tube spacing, horizontal tube spacing, and the fin spacing. The other parameters and operating conditions remain the same. The optimization problem is formulated as below,

Minimize: A

Subject to:

$$Dp_{air} \leq 40Pa \quad (5.11)$$

$$Q = 5692W \quad (5.12)$$

$$0.012 \leq St \leq 0.04m \quad (5.13)$$

$$0.012 \leq Sl \leq 0.04m \quad (5.14)$$

$$0.001 \leq s \leq 0.004m \quad (5.15)$$

By imposing a constraint on the air side pressure drop in equation 5.11, the “redesigned” coil will not require additional fan power input and therefore no extra operating cost. The equations 5.13, 5.14, and 5.15 are the lower and bounds placed on the design variables, referred to as domain constraints, which can be implemented directly when encoding the variables.

Table 5.2 presents the optimized variables together with the minimum area. It is found that compared with the benchmark coil, the heat transfer area of the redesigned coil is reduced by about 25%. While the tube vertical spacing is not changed so much (decreased by just 5%), both the tube horizontal spacing and fin spacing are reduced by more than half of the original design. This parametric effect may be explained as below. The tube vertical spacing governs the frontal face area of the coil and therefore decides the velocity of the air entering the coil. The tube horizontal spacing implies the length of the flow path of air through the coil, and hence affects the air side pressure drop. The fin spacing plays an important role in the magnitude of the surface area of the coil. For a problem of saving surface area under the requirement of given heat duty

and constant air side pressure drop, the “UA” value is essentially constant. How to increase the “U” and decrease the “A”, while keeping the air pressure drop DP below the limit, is the main concern in the parametric design. The typical coil design of considerably less horizontal tube spacing than the vertical tube spacing, in conjunction with very small fin spacing, seems to follow the physical interrelationships among U, A, and DP for a given air flow rate.

5.5.3 Volume Minimization

Compactness of a heat exchanger receives growing interest, due to the emerging needs in the relevant industries. In this case study, the volume of a coil is set to be an objective for minimization, with more variables and more constraints than in the above case.

In this case, the tube diameter, tube spacing, and fin spacing are obtained from data of commercial coils as shown in Table 5.3. The combinations of tube O.D. ranging from ¼” to 1”, and tube spacing ranging from 0.625” to 3” are represented in one of the sub-strings in a solution string, corresponding to integer variables 0~7. The fin pitch ranging from 9 to 25 per inch is represented by another sub-string corresponding to integer variables 0~15.

A schematic diagram of the coil to be optimized in terms of its volume is shown in Figure 5.5. The coil consists of several circuits with the entering water

stream split into several sub-streams. In addition to the tube pattern (O.D., tube spacing) and fin pitch, four other variables are to be optimized, including number of rows N_{col} , number of tubes per row N_{row} , number of sub-streams N_s , and tube length l . The ranges of these variables are defined below,

$$1 \leq N_{col} \leq 8 \quad (5.16)$$

$$1 \leq N_{row} \leq 16 \quad (5.17)$$

$$1 \leq N_s \leq 8 \quad (5.18)$$

$$0.4 \leq l \leq 0.8m \quad (5.19)$$

The water flow rate and air flow rate are 0.1kg/s and 0.6kg/s respectively as fixed operating parameters in this case study. The optimization problem is posed as follows,

Minimize: V

Subject to:

$$Dp_{air} \leq 15pa \quad (5.20)$$

$$Dp_{water} \leq 420pa \quad (5.21)$$

$$Q = 2000W \quad (5.22)$$

$$CoilHeight \leq 0.46m \quad (5.23)$$

$$CoilDepth \leq 0.2m \quad (5.24)$$

With genetic algorithm, this nonlinear single-objective optimization case study with eight variables and five constraints is completed with the results shown in Table 5.4. It is found that the air side pressure drop value of 14.8Pa is

almost meeting the maximum constraint of 15Pa, while the water side pressure drop (173.5Pa) is more than half lower than the given maximum constraint value (420 Pa). This implies that the air side heat transfer resistance is more influential in satisfying the heat duty requirement on the finned-tube coil. Also the resulting height of coil (0.457m) is very close to the constraint maximum value (0.46m), while the coil depth of 0.099m is nearly half of the constraint maximum value of 0.2m. From section 5.5.2 for surface area minimization, it is already found that by reducing the tube horizontal spacing with corresponding high fin density, without changing the coil height, the heat duty requirement can be satisfied given constant fan power consumption. In this case, it results in the volume minimization as well.

5.6 Two-Objective Optimization

5.6.1 Area and Volume Minimization of the Benchmark Water Coil

Under some design scenario, both the total heat exchange surface area and the volume of a coil may be of the designer's interest and set as objectives to be simultaneously minimized. In this section, the benchmark water coil used in section 5.5.2 is to be optimized in terms of the area and volume, with more variables and constraints than described in equations 5.11 through 5.15. The additional variables with their bounds are listed below,

$$1 \leq N_{col} \leq 16 \quad (5.25)$$

$$1 \leq N_{row} \leq 8 \quad (5.26)$$

$$0.005 \leq O.D. \leq 0.02m \quad (5.27)$$

$$0.5 \leq l \leq 2m \quad (5.28)$$

The additional constraints are specified as following,

$$Dp_{water} \leq 240Pa \quad (5.29)$$

$$CoilHeight \leq 0.15m \quad (5.30)$$

$$CoilDepth \leq 0.12m \quad (5.31)$$

From a practical standpoint,

$$St \geq 1.2O.D. \quad (5.32)$$

$$Sl \geq 1.2O.D. \quad (5.33)$$

The above two impractical design constraints are satisfied by setting the objective functions to an extremely large value, if the tube vertical spacing S_t or/and tube horizontal spacing S_l in a set of design variables (corresponding to one of the chromosomes in a population in GA) is/are less than 1.2 times of the tube outer diameter. Since it is a minimization problem, the GA procedure identifies and rejects this infeasible (chromosome) design alternative in the selection operation stage. In another impractical design, the combination of the tube length and the tube diameter is such that the pressure drop of the fluid flowing inside the tube is too high and makes it impossible to find a physically existing thermodynamic state of the fluid at a certain location in the tube. The Coil Designer tool can detect this situation and return a “run error” message to the optimization program for signifying an illegal design.

Figure 5.6 shows the Pareto optima front in the last generation in the GA process. The five red color marked points represent the Pareto solutions corresponding to the two minimized objective functions respectively. To the left side of the front, there are six solutions that dominate the Pareto solutions. However, they are in the infeasible region, violating the design constraints. To the right and upper side, are the solutions that are inferior to the Pareto front.

Table 5.5 presents the optimized variables and the objective values. An interesting observation from Figure 5.6 and Table 5.5 is that in the Pareto optimal solutions, the normalized volume (the percentage of the volume of the benchmark coil) varies widely from 0.34 to 0.94, while the normalized area varies in a much smaller range from 0.752 to 0.844. The explanation for this phenomenon is that under given heat duty condition, there is not much room for the surface area to be changed, but there is much freedom for the volume to be varied for a certain surface area. Table 5.5 shows that the two design configurations with the smallest volumes correspond to the smallest fin spacing and the smallest coil depth (product of tube horizontal spacing and number of rows), while the configurations for the smallest areas not. It is also found that volume minimization and area minimization cannot be realized simultaneously (the reason why multi-objective optimization is needed) at the same design configuration. In other words, they may be partly conflicting with each other. Another interesting observation is that the number of rows (representative of the

coil depth) is 2 in each of the five Pareto solutions, far less than the allowable rows of 8, while the number of tubes in each row (representative of the coil height) is mostly 5, much closer to the maximum tubes of 8 for each row.

5.6.2 Minimal Fan Power and Maximal Heat Duty of a Heat Pipe Heat Exchanger

In a CHP (combined cooling, heating, and power for buildings) research project, the temperature of the process air leaving the desiccant system is considerably higher than that of the ambient air, and the sensible heat within the air can be rejected to the ambient by means of a heat exchanger. In this way, the cooling load imposed on the air handling unit in the cooling system can be reduced and result in energy savings.

In this case study, the temperature of the air exiting the desiccant system is 50°C with a relative humidity of 10%. The air flow rate is 3000CFM. The outdoor air is at 30C. A heat pipe (thermosyphon) heat exchanger made of fin-and-tube coil is proposed for transferring heat between the process air and the ambient air, as depicted in Figure 5.7. The air flows in a duct 0.9m high and 0.616m wide. An additional fan is to be installed in the duct to overcome the pressure drop across the exchanger coil.

The heat pipe heat exchanger consists of an evaporating section in the lower part and a condensing section in the upper part. The hot process air rejects the heat to the working fluid and evaporates it in the evaporating section. The working fluid then condenses in the condensing section and transfers an equivalent amount of heat to the ambient air. The evaporating section and condensing section can be assumed symmetric both in sizing and heat duty performance, and regarded as an evaporator and condenser respectively with the same working temperature of the working fluid in the tubes.

The main design concern is to reduce the process air temperature as much as possible, while minimizing the fan energy consumption. Since the tube length represents the height of the heat exchanger, which is contained in the duct, the tube length can therefore be assumed to be 0.45m for both evaporator and condenser. In predicting the performance of the heat exchanger with the “black-box” model Coil Designer, each tube (heat pipe) can be assumed to undergo phase change process from inlet to outlet. The inlet condition and the mass flow rate of the working fluid in the tube are determined to ensure the quality of the working fluid varies between 0 and 1. The inlet fluid temperature and the two-phase heat transfer coefficient are presumed to be 40°C and 3000W/m²K respectively.

The tube pattern and fin pitch are to be chosen from those listed in Table 5.3. The design of this heat pipe heat exchanger is then posed as a two-objective optimization problem:

Maximize: Q, Minimize: P (fan power)

Optimize: N_{col} , N_{row} , O.D./St/SI, s

Subject to:

$$CoilHeight \leq 0.616m \quad (5.34)$$

$$CoilWeight \leq 36kg \quad (5.35)$$

The optimization results with the GA are shown in Figure 5.8 and Table 5.6 respectively. On the Pareto optima front as shown in Figure 5.8, it is found that after reaching a certain design point, the heat duty improvement is negligible whereas the fan power consumption is increased dramatically. This means that the fan power is proportional to the increased number of rows, while the heat duty is not. Four optimal design alternatives close to certain design point are shown in Table 5.6. The genetic algorithms have an advantage over other optimization methods in yielding multiple optimal solutions, which do not differ, significantly in cost and quality. This benefit provides the designer more flexibility in finalizing a design configuration from a viewpoint of product fabrication and availability.

5.6.3 Minimal Fan Power and Weight Design of a Condenser

A condenser is to be designed with a configuration as shown in Figure 5.5. The working fluid is R22 with inlet pressure 17.7 bar, temperature 70°C, and flow rate of 0.01kg/s. The temperature of the air entering the condenser is 30°C. The required heat transfer rate is 2000W, and the allowable pressure drop of the refrigerant is 300Pa. The coil is to be contained in a limited space of 1.2x0.15x1m. The weight of the coil is set to be one of the objectives to be minimized, since it directly represents the material consumption cost. The fan power is the other design objective for it is associated with both the initial cost and operating cost of the condenser.

In terms of the design variables, this case study is similar to Section 5.5.3, except for an additional variable of the air flow rate. Figure 5.9 shows the Pareto optima with the abscissa representing the weight, and ordinate representing the fan power. It is as expected that larger fan power leads to a smaller coil design, since the air flow rate and the heat transfer coefficient are proportional to the fan power. Table 5.7 gives two example designs from the Pareto solutions, where the heat duty equality constraint is transformed to an inequality constraint by setting the heat duty within 5% of the required.

5.7 Circuitry Optimization of an Interlaced Heat Exchanger

As mentioned in section 3.3.2, the heat transfer coefficient and pressure drop values obtained from the validation of simulation results with the measured data on an integrated absorber/condenser coil, were further used in optimizing the coil, specifically the circuitries.

Circuitry design has a considerable impact on the heat transfer performance of a coil. A preliminary study was conducted on the performance of 5 basic circuitries with water as the working fluid. It is clear from Figure 5.10 that a counter-cross flow circuitry may have the maximum heat duty, since the temperature gap of the working fluid between the air stream wise neighboring tubes allows the air flowing the neighboring tubes to have equivalent heat transfer with the working fluid. This observation can be served as a starting point to optimize the circuitry of a coil.

Ten circuitries have been constructed and the heat duty of each circuitry is calculated using the validated 3-zone heat transfer coefficients and pressure drop values of the absorber and condenser respectively. The inlet air temperature was set to be 95F according to the design condition, and the air velocity profile is set to be the same as the 8-section measurement data. In Figure 5.11, circuitry 1 through 8 is of 88 tubes as the original one (circuitry 11). Circuitry 9 and 10 is of 84 tubes by removing 4 tubes from the original one,

adjusting the air velocity by multiplying a factor of 1.0476 ($=44/42$) to the original velocity profile. The result showed it is possible to remove 4 tubes from the original coil by redesigning the circuitry and adjusting the non-uniformity of the air flow distribution, while not sacrificing the heat transfer rate requirement.

One more try was performed to see how much heat duty and what temperature profile would result of the original circuitry, if the air were uniformly distributed, total air flow rate remaining the same. In Figure 5.12, it seems that both of the condenser circuits cannot be subcooled, though the subcooling degrees of the absorber circuits are a little increased to the limit of the air inlet temperature. The total heat duty has lost 350W.

The circuitry optimization study showed that the non-uniformity of the airflow and arrangement of tubes according to the tube temperature distribution have considerable impacts on the heat exchange performance.

Table 5.1 Specifications of a Benchmark Coil

Item	Value	Item	Value
Ncol	4	Air Flow Rate (kg/s)	0.27
Nrow	5	Water Flow Rate (kg/s)	0.05
O.D. (m)	0.01	Air Pressure Drop (Pa)	40
St (m)	0.03	Water Pressure Drop (Pa)	240
Sl (m)	0.03	Heat Duty (W)	5692
Fin Spacing (m)	0.003	Heat Transfer Area (m ²)	11.08
Tube Length (m)	1	Coil Height (m)	0.15
Tube Thickness (m)	0.0005	Coil Depth (m)	0.12
Fin Thickness (m)	0.00013	Volume (m ³)	0.018

Table 5.2 Area Minimization of the Benchmark Water Coil

Variables	Solution	Minimized Area (percentage of original)
St (m)	0.0285	74.7%
Sl (m)	0.013	
s (m)	0.001387	

Table 5.3 Tube Diameters, Tube Patterns and Fin Pitch Available

O.D. (in.)	St x SI (in. x in.)	Fins per Inch
1/4	1x0.866	9~24
5/16	1x0.625	
3/8	1x0.75	
3/8	1x1	
1/2	1.25x1.083	
1/2	1.5x1.299	
5/8	1.5x1.299	
1	3x2.125	

Table 5.4 Optimization Results for Minimizing Volume of a Water Coil

Variables	Solution	Objective	Value
Ncol	3	Volume (m ³)	0.03
Nrow	12	Constraints	Value
Nstreams	4	Heat Duty (W)	1977.6
O.D. (in.)	5/8	Coil Height (m)	0.457
Tube Length	0.674	Coil Depth (m)	0.099
St (in.)	1.5	Water Pressure Drop (Pa)	173.5
SI in.)	1.299	Air Pressure Drop (Pa)	14.8
Fin Pitch (/in.)	16		

Table 5.5 Area/Volume Minimization of the Benchmark Water Coil

Variables	Pareto Solutions				
Ncol	2	2	2	2	2
Nrow	5	5	4	5	5
O.D. (m)	0.0098	0.0098	0.0103	0.0098	0.0098
Length (m)	1.32	1.76	1.37	1.76	1.32
St (m)	0.029	0.025	0.029	0.024	0.024
Sl (m)	0.029	0.034	0.022	0.039	0.019
Fin pitch (m)	0.0023	0.0033	0.0012	0.0038	0.001
Objectives	Values (percentage of original)				
Area	0.81	0.785	0.814	0.752	0.844
Volume	0.63	0.86	0.38	0.94	0.34

Table 5.6 Heat Pipe Heat Exchanger Optimization Results

Variables	Pareto Solutions			
Ncol	12	12	13	11
Nrow	16	19	16	16
O.D. (in.)	1/2	1/2	1/2	1/2
St (in.)	1.5	1.25	1.5	1.5
Sl (in.)	1.299	1.083	1.299	1.299
Fin pitch (/in.)	13	14	11	16
Objectives	Value			
Heat Duty	14.33	14.43	14.28	14.38
Fan Power	1.95	2.14	1.85	2.13
Constraints	Value			
Weight (kg)	35.35	35.89	35.48	35.77
Width (m)	0.6096	0.60325	0.6096	0.6096

Table 5.7 Design Optimization Results for a Condenser

Variables	Pareto		Objectives	Value	
	Ncol	3		3	Weight (kg)
Nrow	15	14	Fan Power	259.6	139
O.D. (in.)	1/2	5/8	Constraints	Value	
Length (m)	1.013	1.093	Heat Duty (W)	1912.5	1929
St (in.)	1.25	1.5	Height (m)	0.47	0.53
Sl (in.)	1.083	1.299	Depth (m)	0.08	0.098
Fin pitch (/in.)	18	17	DP,refri (Pa)	284	270
Nstreams	3	2			
Air Flow Rate (kg/s)	2.73	2.47			

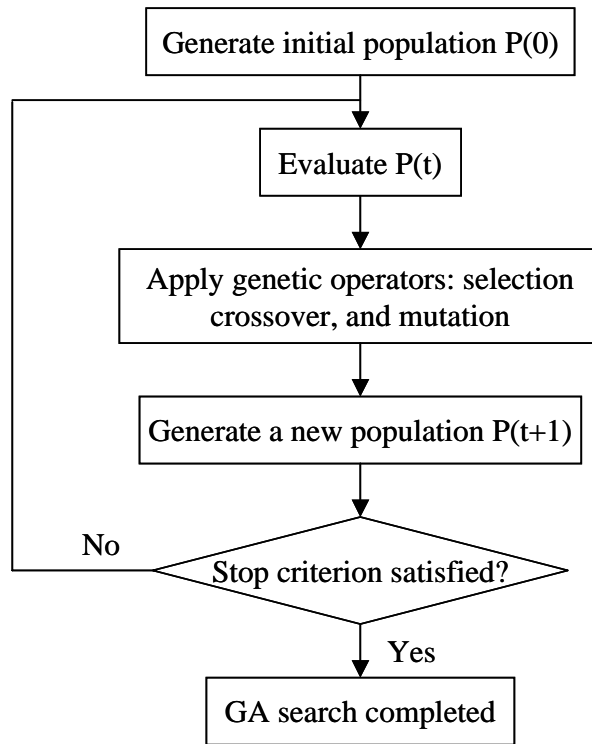


Figure 5.1 Flowchart of Genetic Algorithm

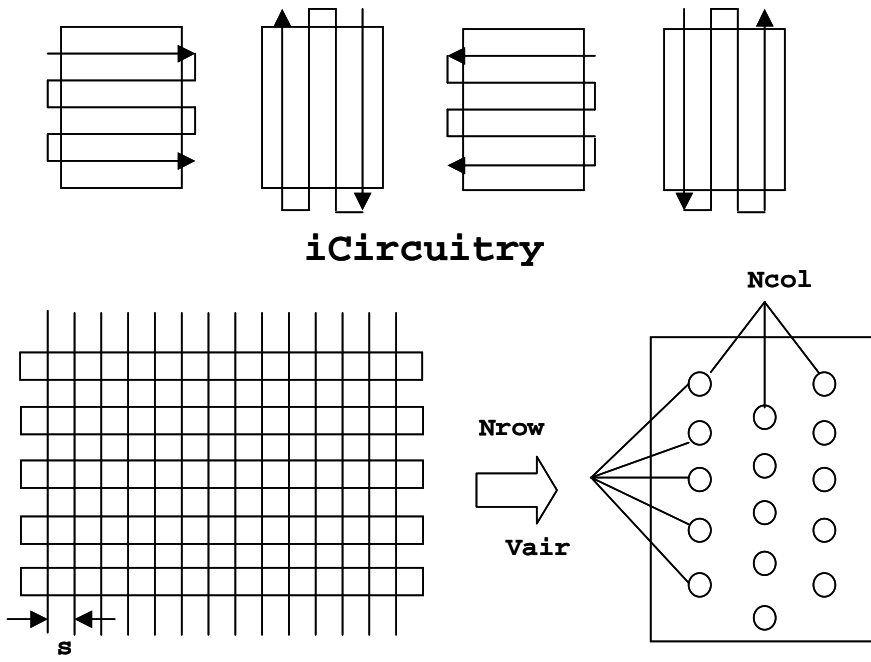


Figure 5.2 Graphic Representations of the Design Variables

Best string

iCir		Nrow			Ncol		s		Vair		
1	0	1	1	1	1	1	0	0	1	1	1

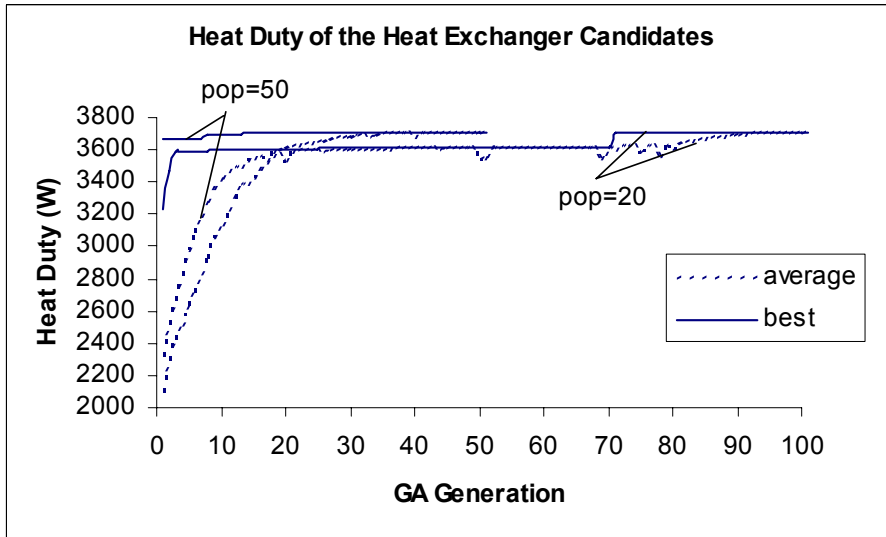


Figure 5.3 Illustration of Genetic Algorithm Process

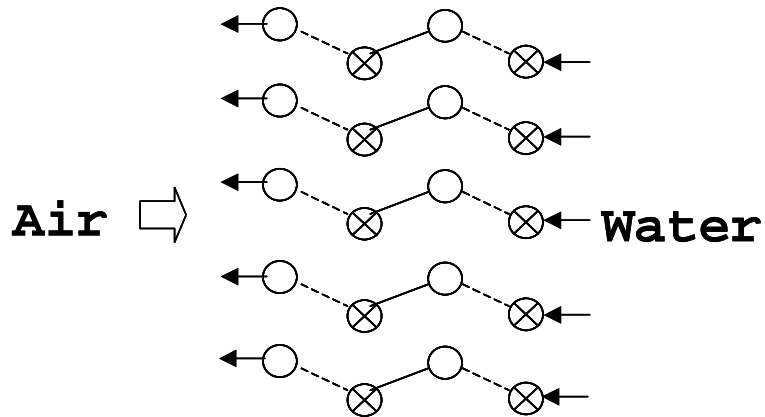


Figure 5.4 Schematic Diagram of a Benchmark Water Coil

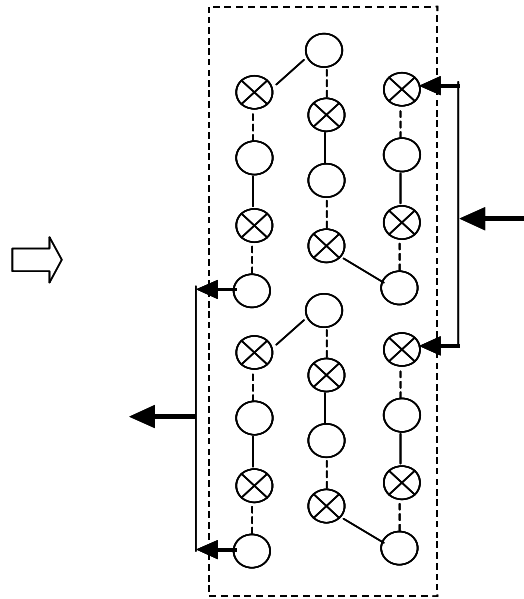


Figure 5.5 Schematic of a Multi-Stream Coil

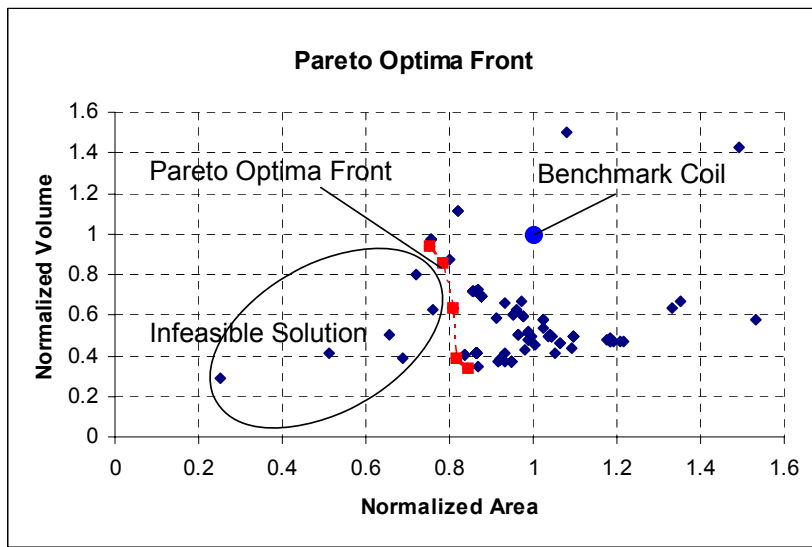


Figure 5.6 Pareto Optima Front in a Population

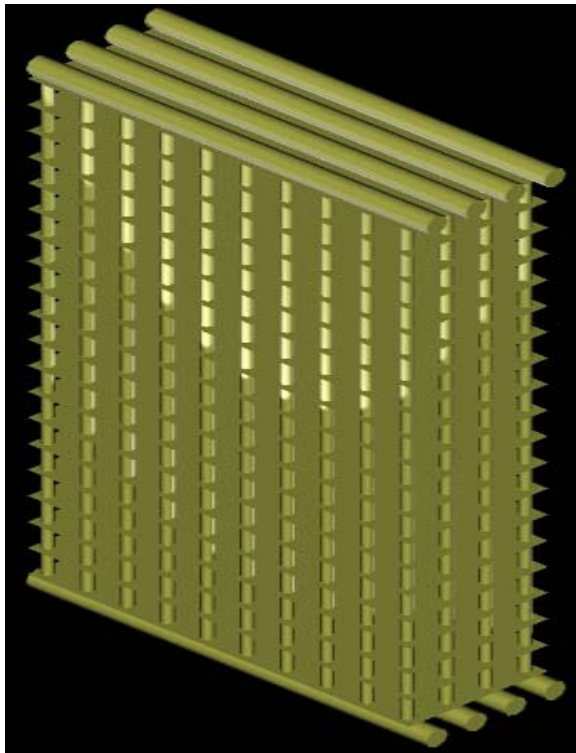
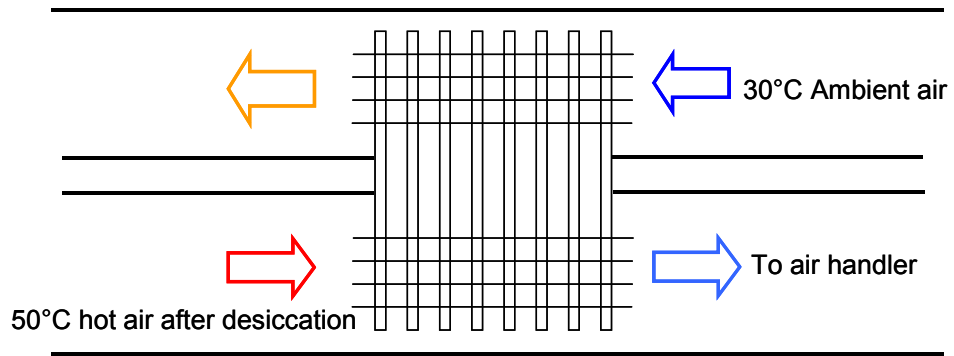


Figure 5.7 Schematic of a Heat Pipe Heat Exchanger

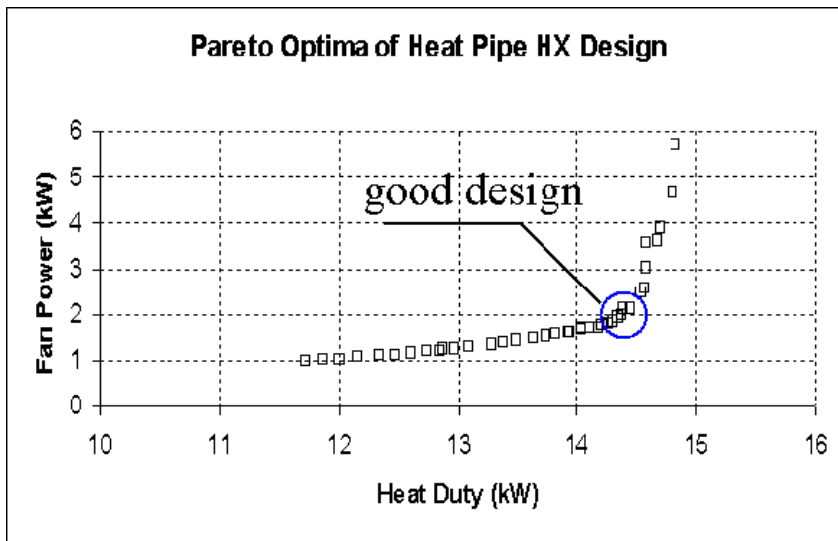


Figure 5.8 Pareto Solutions of Heat Pipe Heat Exchanger Design

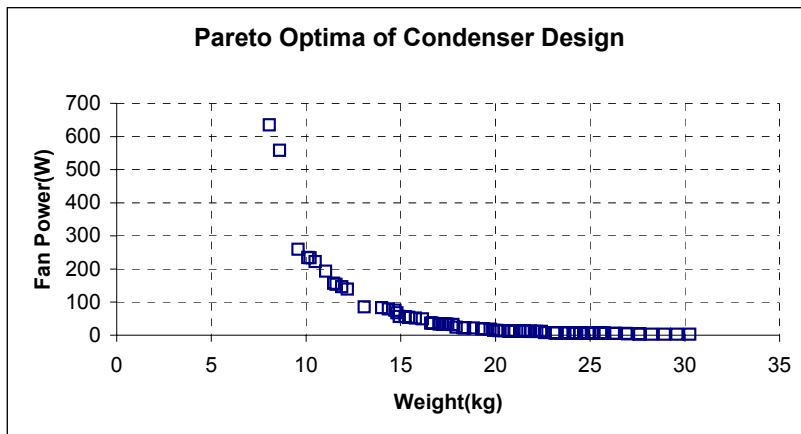
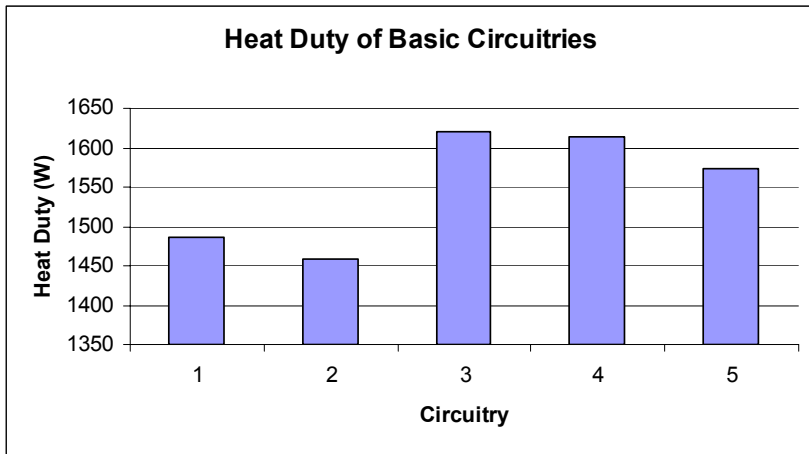
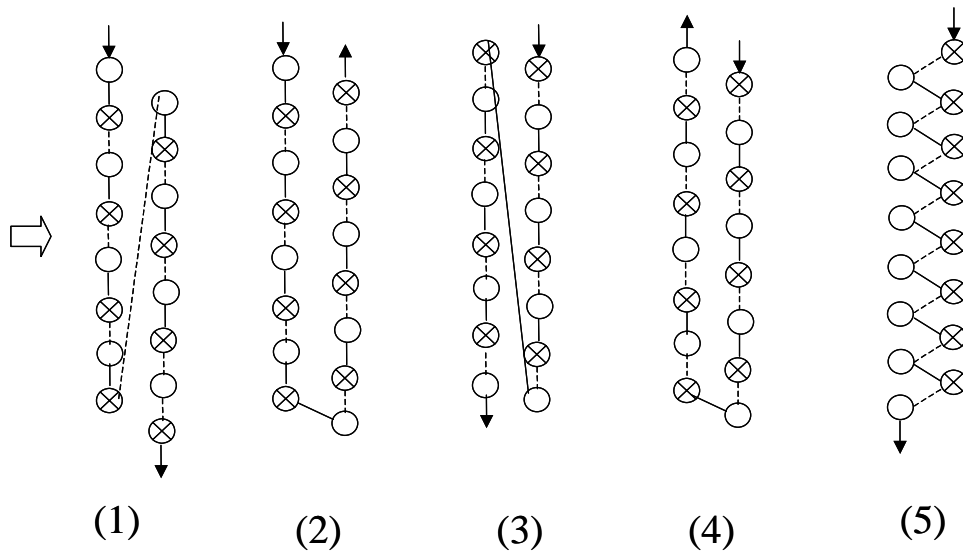


Figure 5.9 Pareto Solutions of Condenser Design



(B)

Basic Circuitry



(A)

Figure 5.10 Basic Circuitry Comparison in Terms of Heat Duty

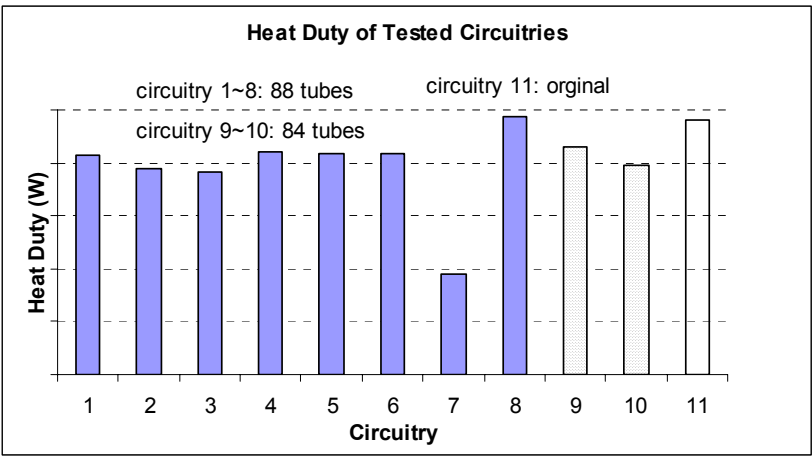


Figure 5.11 Circuitry Optimization on an Interlaced Heat Exchanger

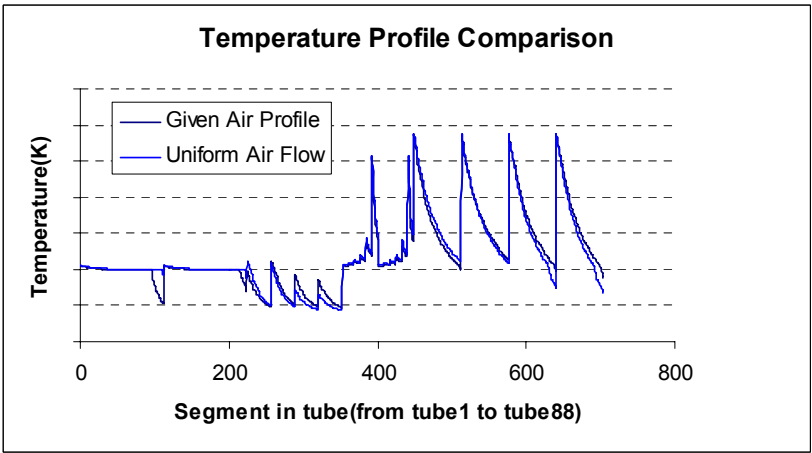


Figure 5.12 Uniform vs. Non-Uniform Air Distribution

Chapter 6

GRAPHIC USER INTERFACE

6.1 Introduction

Many existing simulation packages for heat exchanger design were developed before modern graphical user interfaces (GUI) are available. Simplified circuitry was usually assumed and predefined without flow splits and confluences. Since reducing design cycle time is becoming increasingly important, a software program with user-friendly interface and general-purpose modeling concept is in great need to improve effectiveness and efficiency in design, rating, and analysis of heat exchangers.

CoilDesigner, as a continuously evolving Windows® based software package, is incorporating a graphical user interface featured with,

- Interactive visual-based, object-oriented, comfortable and flexible modeling environment, quick to learn and easy to use.
- Convenience in entering, editing, post processing, with tabular and graphic representation, and management of data.
- Providing comprehensive information, exploring all aspects of heat exchanger design, including thermal and hydraulic performance, cost, weight, surface area, volume, size, and fan power consumption.

- Enabling parametric analysis and graphing to enhance visual interpretation of output information and close examination of any performance irregularities.
- Supporting theoretical analysis with experimentally measured data, and developing custom detailed models.
- Running checks on the plausibility and the format of the entered values, preventing error from occurring during the input stage.

This chapter is a brief description of the graphical user interface of CoilDesigner to highlight its features and capabilities. It does not serve the purpose of documentation and use of the interface.

6.2 Entering Data and Setup of a Heat Exchanger

6.2.1 Geometric Size and Dimensions

Figure 6.1 shows the interface at the beginning of building a heat exchanger model. Typical choice of tube configurations (inline, staggered convergent, or staggered divergent), and number of rows and tubes are to be entered. The prediction of thermal and hydraulic performance, as well as energy/mass balancing on the air side is related to the tube configuration. An example for set up of a micro-channel heat exchanger is shown at the end of this chapter.

A set of parameters for tube sizing and spacing, including diameter, wall thickness, length, and distance between tubes in vertical and horizontal direction,

are shown in Figure 6.2. These are design variables for users to input. A tube is divided into a number of segments in order to account for non-uniform air flow distribution and heterogeneous refrigerant properties.

The input parameters for fins are given in Figure 6.3. Two fin types (wavy, and flat) with an option of dog bone holes are included also. Correlations for heat transfer coefficient and pressure drop calculations are correspondent to the fin types. Other variables are fin thickness, fin spacing, fin-tube contact resistance, and pattern length and projected length (when the fin type is wavy). There are choices for specification of fin efficiency, either by giving a constant value based on experimental data and experience, or by empirical or semi-empirical calculation. When choosing to calculate fin efficiency, a number of different correlations can be applied.

6.2.2 Working Fluids

Various refrigerants including pure fluids such as R134a, R22, water, carbon dioxide, and fluid mixtures such as water-glycol, R404a, R407c, and R410a, as well as ammonia water mixture, are available from the fluid property library of NIST Refprop 7.0 (NIST, 2001), and of AWMix (Tillner, 1998), as shown in Figure 6.4. When new working fluids are being substituted in the HVAC&R industry, this abundant choice of working fluids is especially useful to retrofit existing heat exchangers or design new heat exchangers.

6.2.3 Heat Transfer Coefficients and Pressure Drop

Calculation of heat transfer coefficients and pressure drops on both the refrigerant side and air side largely affects the accuracy in predicting the thermal and hydraulic performance of a heat exchanger. Due to a wide variation in operating conditions and geometries, and complexity in turbulent and two-phase fluid flow and heat transfer, no existing correlation is universally applicable to a particular air- to-refrigerant heat exchange design. Therefore, the GUI offers three options for the user to determine and customize the heat transfer coefficients and pressure drops.

- Built-in correlations

A number of published correlations are implemented in the CoilDesigner program. The user can make an appropriate choice when familiar with the limitation in using these correlations, and aware of his particular modeling scenario, including the kind and flow regime of the working fluids, and geometry conditions of the heat exchangers.

- Fixed Value

In some cases, a constant value based on the user's experience can be sufficiently close to the reality and speed calculations.

- External Library

Experimental or proprietary correlations are not uncommon, especially for a specific range of operating conditions and design configurations. The GUI allows

the user to customize his favorite or proprietary correlations by providing a path to them, compiled in the form of a dynamic link library.

As an example of the user interface, Figure 6.5 is the GUI window for the user to choose the heat transfer coefficient on the refrigerant side, in the three flow regimes of liquid, two-phase, and vapor. Besides, a correction factor for using built-in correlations is incorporated to account for heat transfer surface enhancement or operating condition customization.

6.2.4 Tube Circuitry Design

One of the prominent features of CoilDesigner is its convenience in designing tube circuitry by connecting tube ends in the GUI. Compared with many other heat exchanger simulation packages, and there is no limitation to the number of rows and tubes, and the number of refrigerant inlet and outlet streams. Splits and confluence are allowed by joining more than two tube ends. Multiple refrigerants can be used in interlaced heat exchangers packaged in a single coil.

Figure 6.6 shows the main interface for fin-and-tube coil construction. The left hand view represents the front face area of the coil. Each cell corresponds to the two-dimensional set of air inlet properties including velocity, temperature and relative humidity as shown in Figure 6.9. The number of cells in a row is equal to the number of segments in a tube.

The right hand pane of Figure 6.6 is the tube ends view. To build the circuitry, the user connects tube ends as desired: a dotted line indicates a tube connection on the farther end (away from the user), and a solid line indicates a tube connection on the front end (towards the user). Tube numbering is sequential starting from the first tube row, top to bottom within the tube, and so on. For more convenience in circuitry design, a tube connection editing tool is provided as shown in Figure 6.10, where tube connections can be modified by removing the old ones and adding new ones as desired.

The tubes where the inlet and outlet streams enter or exit can be specified by right clicking over the tube ends and checking properly as shown at the right bottom of Figure 6.6. The stream parameters such as mass flow rate, pressure, temperature, or quality can be entered as illustrated in Figure 6.8.

Setup of microchannel heat exchangers can be implemented in a similar manner as for fin-and-tube coils. The main interface is provided in Figure 6.7.

6.2.5 Unit System

Two units systems, SI and English, are at the user's choice to meet individual needs and customs. Automatic conversion between systems for various physical quantities is also enabled.

6.3 Output Data Processing

After entering input data and setup of the heat exchanger model, the GUI executes the program and calculates solutions with comprehensive information about the design or rating of the heat exchanger. A summary screen of the overall thermal and hydraulic performance, such as the sensible and latent heat duty, flow rates, and pressure drops, are shown in Figure 6.11. The local air and refrigerant properties through the entire heat exchanger are output in tabular form as exemplified in Figure 6.12 for refrigerant quality at each segment. Optionally, all the output data are exportable to a MS Excel spreadsheet as shown in Figure 6.13.

At some stage in the simulation process, by demonstration of results with changing parameters, the “what would happen if” question should be answered quickly. Figure 6.14 is the GUI for the user to choose one or more input variables and step sizes to conduct parametric analysis. As an example, the effect of the tube length on the heat duty output is graphically represented in Figure 6.15.

New HX Wizard

Tube Configuration Parameters

You can choose the tube configuration as inline, staggered (convergent) or staggered (divergent). Here you also have to specify the number tubes in the heat exchanger and the number of segments for each tube. The air mal-distribution and the variable fin spacing is accounted for on a per-segment basis.

Inline Tubes
The tubes are placed in an in-line fashion.

Staggered Tubes (Convergent)
The tubes are placed in an staggered configuration. The first tube in the second column is offset from the top.

Staggered Tubes (Divergent)
The tubes are placed in an staggered configuration. The first tube in the first column is offset from the top.

Number of Rows

Number of Columns

Number of Segments Per Tube

Figure 6.1 Setup of a New Heat Exchanger

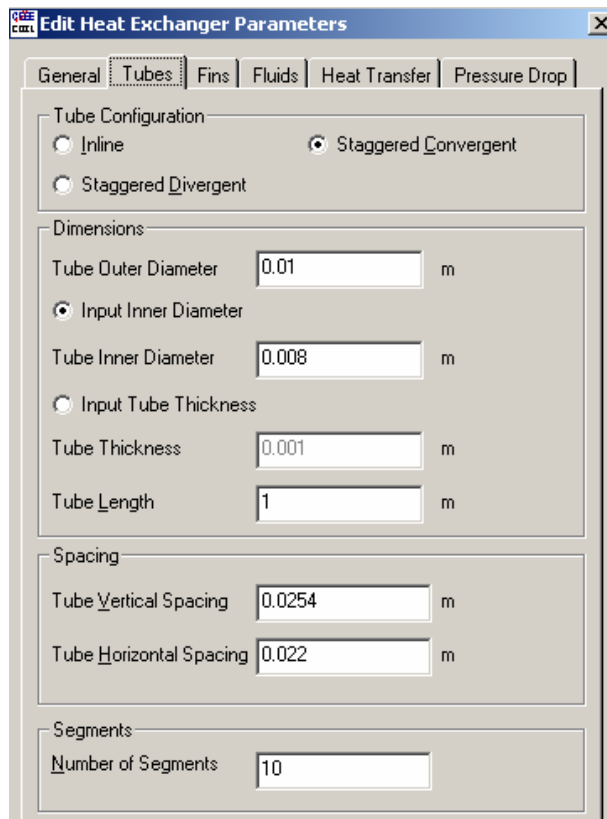


Figure 6.2 GUI for Specifying Tube Parameters

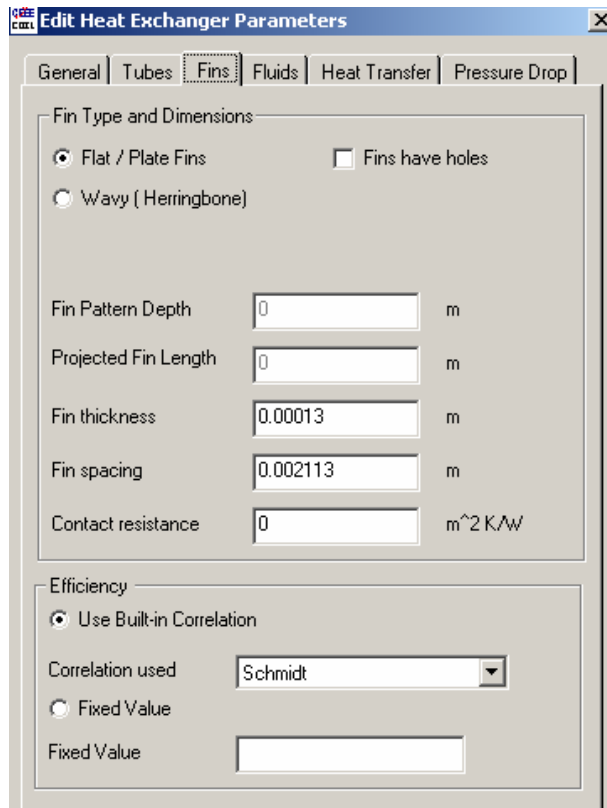


Figure 6.3 GUI for Specifying Fin Types and Parameters

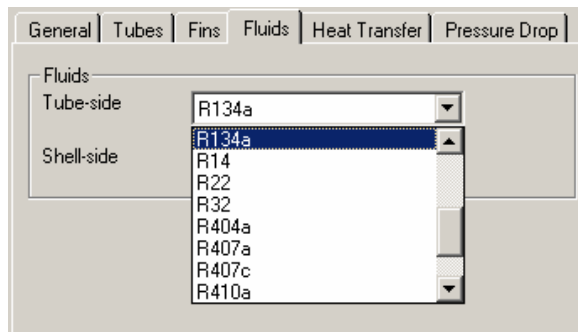


Figure 6.4 GUI for Specifying Working Fluid inside the Tube

Air Side Refrigerant Side

Single Phase - Liquid

Built-in Dittus-Boelter

Fixed Value [] W/m^2K

External Correlation

Correction Factor for Built-in and External Correlations:

[1]

Two Phase

Built-in Jung-Radermacher

Fixed Value [] W/m^2K

External Correlation

Correction Factor for Built-in

[1]

Kandlikar
 Jung-Radermacher
 Shahs' Evaporation
 Gungler-Winterton
 Dobson
 Shahs' Condensation
 Traviss

Single Phase - Vapor

Built-in Gnielinski

Fixed Value [] W/m^2K

External Correlation

Correction Factor for Built-in and External Correlations:

[1]

External Correlation

Path to the external correlation library:

[] Set Library

Figure 6.5 GUI for Choosing Heat Transfer Coefficient (or Pressure Drop)

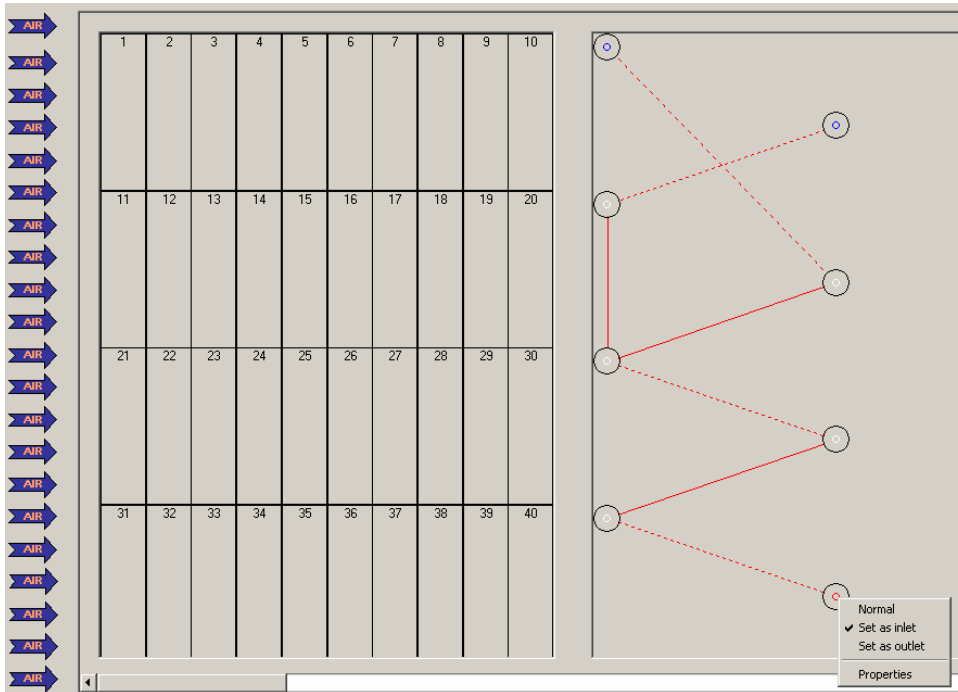


Figure 6.6 The Main Interface for Fin-and-Tube Coil Construction

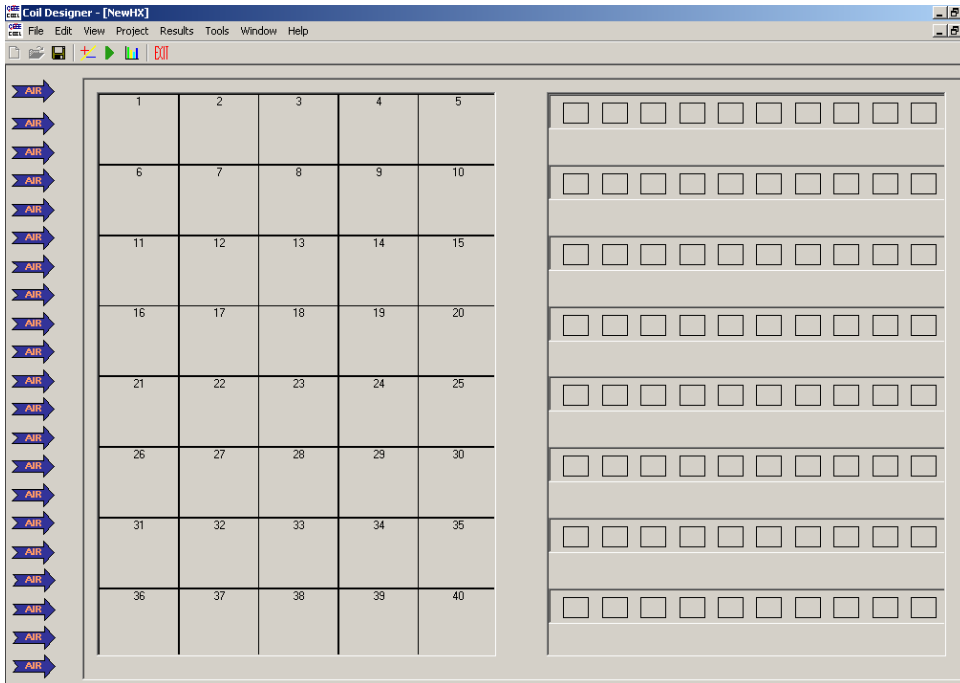


Figure 6.7 The Main Interface for Micro-Channel Heat Exchanger Construction

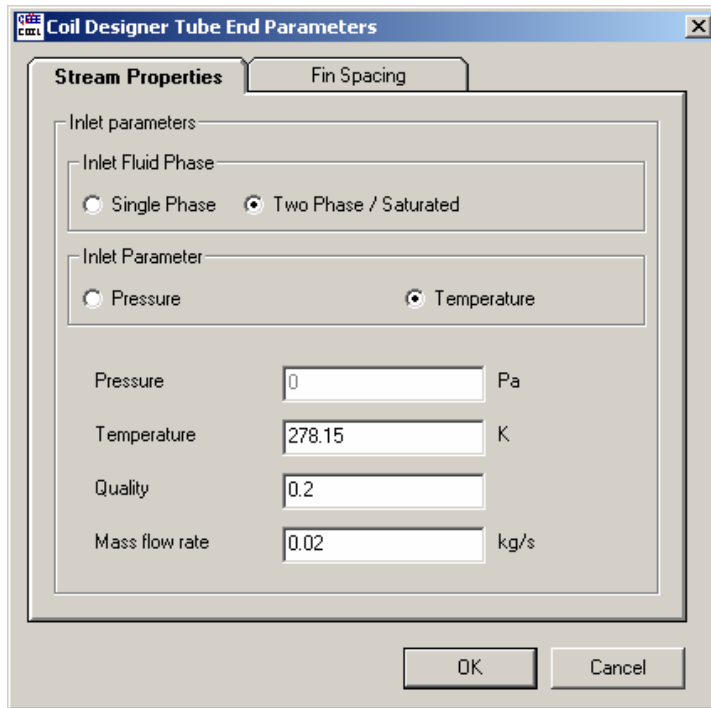


Figure 6.8 GUI for Specifying Inlet Stream Properties

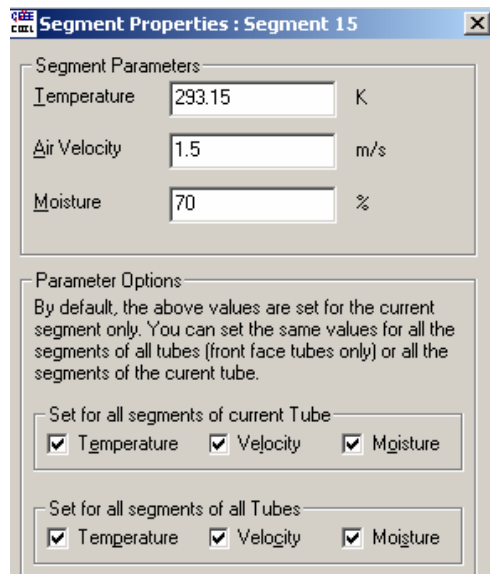


Figure 6.9 GUI for Specifying Inlet Air Properties

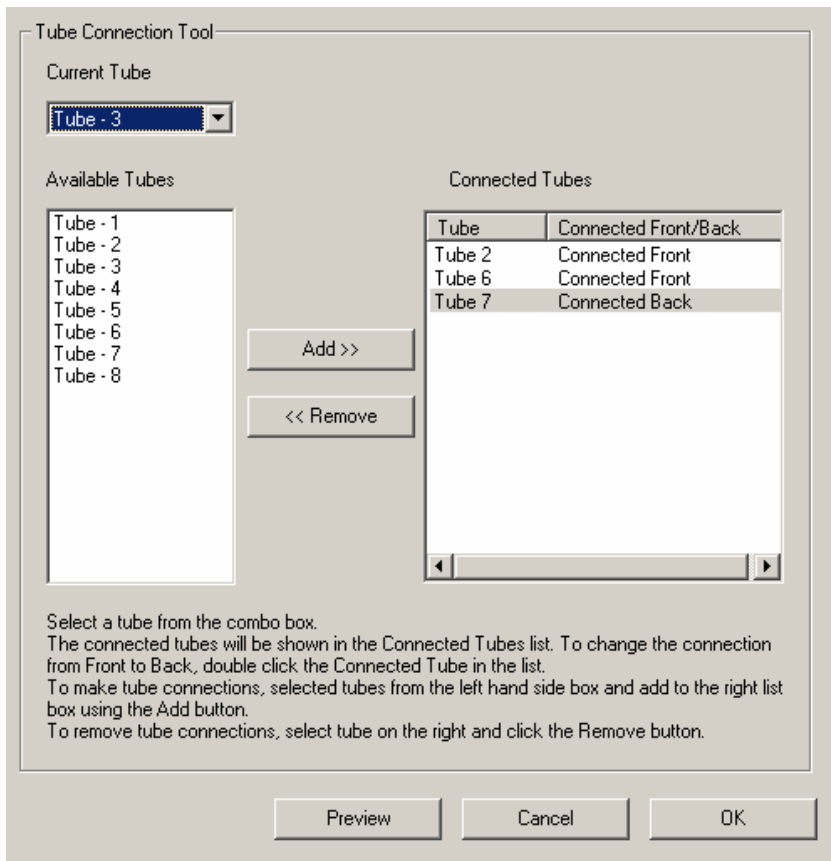


Figure 6.10 GUI for Editing Tube Connection

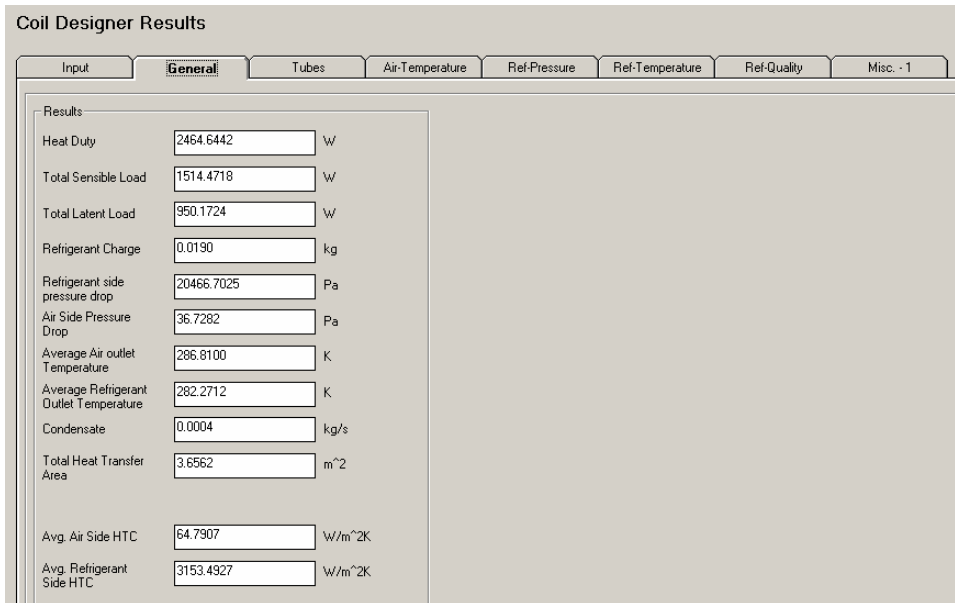


Figure 6.11 Output Window of the Predicted Performance

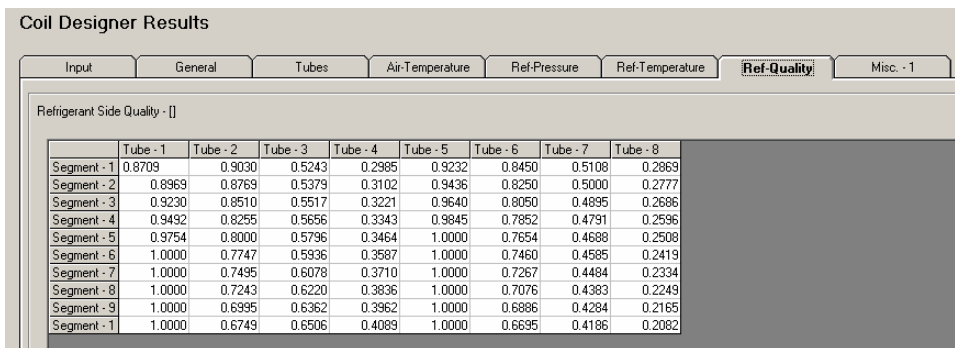


Figure 6.12 Output Window of the Working Fluid Properties (Quality)

	A	B	C	D	E	F	G	H
1	Coil Designer - Results							
2	Project : NewHX							
3								
4	Mass Flow through each tube [kg/s]							
5	Tube-1	Tube-2	Tube-3	Tube-4	Tube-5	Tube-6	Tube-7	Tube-8
6	0.0075	0.0075	0.015	0.015	0.0075	0.0075	0.015	0.015
7								
8	Total heat load for each tube [W]							
9	Tube-1	Tube-2	Tube-3	Tube-4	Tube-5	Tube-6	Tube-7	Tube-8
10	262.4563	381.6761	419.8603	365.1436	177.8226	293.9124	304.5713	259.2017
11								
12	Sensible heat load for each tube [W]							
13	Tube-1	Tube-2	Tube-3	Tube-4	Tube-5	Tube-6	Tube-7	Tube-8
14	171.7039	237.7927	254.8815	230.5074	113.2285	172.4709	177.3323	156.5547
15								
16	Latent heat load for each tube [W]							
17	Tube-1	Tube-2	Tube-3	Tube-4	Tube-5	Tube-6	Tube-7	Tube-8
18	90.75246	143.8834	164.9789	134.6361	64.59406	121.4415	127.239	102.647
19								
20	NewHX - Refrigerant quality/mass-fraction							
21	Tube-1	Tube-2	Tube-3	Tube-4	Tube-5	Tube-6	Tube-7	Tube-8
22								
23	0.870887	0.902951	0.524301	0.298513	0.923234	0.844952	0.510752	0.286854
24	0.896908	0.876935	0.537909	0.310247	0.943568	0.824965	0.500038	0.277704
25	0.923007	0.851002	0.55174	0.322142	0.963988	0.805045	0.489527	0.268625
26	0.949176	0.825473	0.56563	0.334255	0.984453	0.785193	0.479109	0.259637
27	0.975403	0.800036	0.579579	0.346441	1	0.765411	0.468774	0.250753
28	1	0.774695	0.593585	0.358698	1	0.745963	0.458502	0.241941
29	1	0.749456	0.60775	0.371025	1	0.726748	0.448376	0.233392
30	1	0.724323	0.621972	0.383571	1	0.707626	0.438327	0.224913
31	1	0.69949	0.63625	0.396185	1	0.688554	0.428358	0.216536
32	1	0.674886	0.650582	0.408868	1	0.669543	0.418582	0.208232
33								

Figure 6.13 Output to MS Excel Spreadsheet

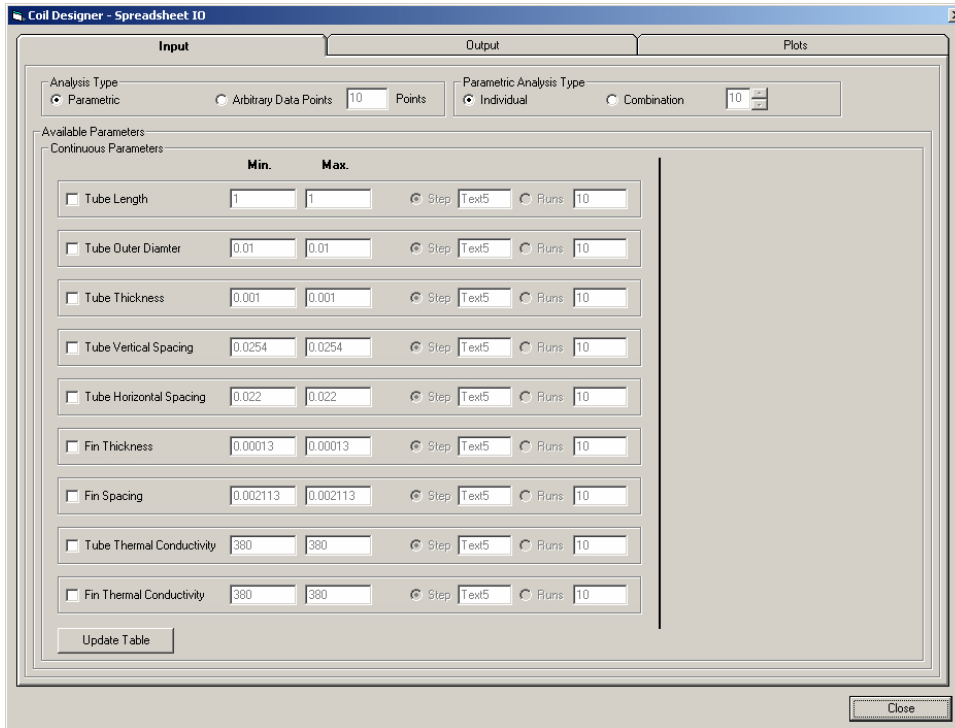


Figure 6.14 Window for Parametric Analysis

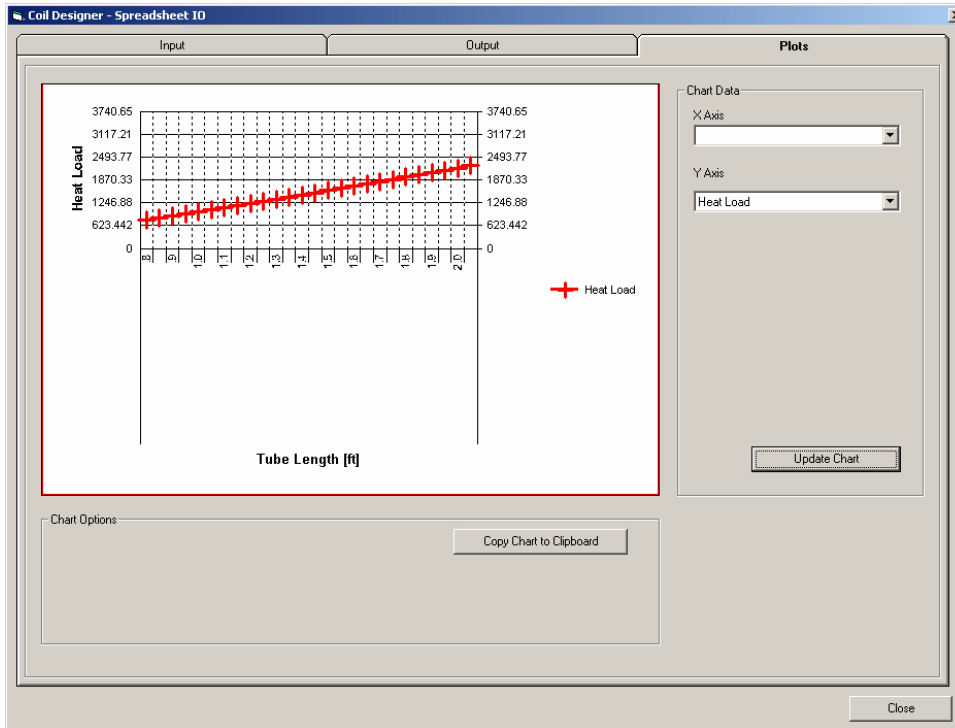


Figure 6.15 Parametric Analysis of the Heat Exchanger Performance

Chapter 7

CONCLUSIONS

The most comprehensive and flexible, general-purpose simulation and design tool for air-to-refrigerants to date was created. The major conclusions derived from this dissertation are summarized next.

7.1 Development of a Comprehensive Simulation Tool

The primary goal of this dissertation is to develop a simulation and optimization tool to design air-to-refrigerant coils based on their thermal and hydraulic performance. Using a general-purpose modeling concept and user-friendly interface, Coil Designer improves speed and efficiency in design, rating, and analysis of conventional finned tube coils and emerging microchannel heat exchangers. It is applicable to design of condensers, evaporators, and heating and cooling coils under any operating condition. Coil Designer is the most comprehensive and advanced design and simulation package for air-to-refrigerant heat exchangers to date. The major features and accomplishments of this project are summarized in the following.

- **Circuitry Design Based on Network Approach**

Comment [RR25]: This paragraph does not talk about convenience

Deleted: ¶

The general-purpose model was established based on a network approach, where a tube in the heat exchanger, the pressures at the inlet and outlet of the tube, and the mass flow rate of the fluid flowing inside the tube or tube segment were analogized as a resistor, electric potentials, and electric current respectively in an electric circuit. With this generalized approach, there is no limitation on refrigerant circuitry design, and mal-distribution of fluid flow through tubes can be addressed. This feature is not available in any other heat exchanger models published so far. To solve the highly nonlinear system of thermal/hydraulic equations resulting from the generic model, a fractional step method to successively approximate physics of heat and fluid flow was developed to enhance the modeling robustness.

- **Accounting for Two-Dimensional Non-Uniform Air Distribution**

Distinguished from other simulation programs of heat exchangers, the heat and fluid flow analysis in Coil Designer is based on a segment-by-segment approach. Each tube is divided into a number of segments. Each segment is considered as a single cross-flow heat transfer unit, and associated with individual air flow rate, temperature, humidity, and refrigerant parameters. Thus the impact of two-dimensional non-uniformity of air distribution across the exchanger, and the local refrigerant behavior, on the heat exchanger performance can be studied.

This segment-by-segment approach can be reduced to a tube-by-tube approach, when there is only one segment in a tube. A further sub-dividable-

segment model was then created in order to account for the significant change of properties and heat transfer coefficients in the single-phase and two-phase regime when a particular segment experiences flow regime change. The effectiveness-NTU method for cross-flow configuration, based on the inlet condition of fluids, was used also for combined heat and mass transfer problem under dehumidification, by defining equivalent thermal resistance and heat capacity.

- **Allow for Multiple Working Fluids in Interlaced Heat Exchangers**

In some special coil design, there are interlaced heat exchangers with different working fluids inside respective subsets of tubes. Coil Designer is capable to model and analyze the performance of this kind of coils.

- **Abundant Choice of Working Fluids**

By integrating fluid property libraries, a wide variety of working fluids become available, including most promising refrigerants and mixtures that are environmentally benign and economically feasible. This abundant choice is especially useful to retrofit existing heat exchangers or design new heat exchangers using substituted refrigerants.

- **Flexibility in Using Correlations**

Up-to-date correlations of heat transfer and pressure drop for both air and refrigerant flow, and of fin efficiency, are built into the program. The designer's propriety correlations or empirical values can also be used. This feature offers the possibility for performance prediction accuracy in designing or rating of heat exchangers constructed of varied fin and tube geometries, using diversified working fluids, and under a wide range of operational conditions.

- **Highly Efficient and Intuitive Graphical User Interface for Engineering Use**

Object-oriented programming techniques were applied in developing Coil Designer to facilitate flexible and customizable modeling environment and building graphic user-friendly interface.

Coil Designer provides interactive, visual-based, and flexible modeling environment. It is user friendly in entering, editing, and post processing of numerical and graphic data. Comprehensive information about heat exchanger design including thermal and hydraulic performance, weight, surface area, volume, and size, is given to the designer. The tabular and graphic representation of performance simulation results provides convenience in comprehensive and detailed parametric analysis.

7.2 Validation of Results from Coil Designer

The prediction results with Coil Designer were compared with experimentally determined data collected from a number of sources, covering a wide range of coil configurations, working fluids, and operating conditions. The simulation tool was shown to be able to predict the heat transfer rate of a variety of coils with good accuracy. The validated heat transfer coefficients and pressure drop values were used to redesign an interlaced heat exchanger.

7.3 Parametric Studies Using Coil Designer

Parametric studies were conducted to confirm the capability of the program in exploring all aspects of heat exchanger performance under a wide variation of design and operating conditions.

A simulation study based on validated and measured data indicated that the two-dimensional non-uniformity of the airflow and fluid flow circuitry have large impacts on the heat exchange performance. It is found from a tentative parametric study that by applying variable fin density design to match the non-uniform air distribution could possibly result in saving of surface area while keeping the same heat transfer capacity.

7.4 Optimization using Genetic Algorithms with Coil Designer

Genetic algorithms were introduced and integrated with the simulation tool to execute heat exchanger optimization case studies for single and multi-objective optimizations. The optimization objectives include optimum circuitry selection, minimized volume, minimized amount of material utilized in the coil while achieving the best possible performance. Genetic algorithms offer over 90% savings in computational cost as compared to exhaustive search in finding the optimal solutions, given any constraints. It is superior to other optimization methods in getting multiple optimal solutions, which do not differ, significantly in cost and quality. This benefit provides the designer more flexibility in finalizing a design configuration from a viewpoint of product fabrication and availability.

Summarizing from optimization case studies, it can be concluded for finned tube heat exchangers, that under given heat duty requirement and fan power consumption, with a design of the tube horizontal spacing considerable less than the tube vertical spacing, in conjunction with necessary corresponding fin spacing, could result in savings of both the surface area and the volume, with more effect in volume minimization.

Chapter 8

FUTURE WORK

The following work and research remain to be performed in order to make the Coil Designer a more advanced and reliable design tool for heat exchanger.

- Integrate more up to date correlations for heat transfer and pressure drop on both the air side and refrigerant side.
- Allow for header design by accounting for its effect on pressure drop and fluid mal-distribution.
- Consider heat conduction between tubes via fins.
- Allow for situation where the air flow direction is not perpendicular to coil face.
- Develop the frosting and defrosting model.
- Develop more rigorous model of dehumidification, addressing the building up mechanism of the condensate in the gravitation-induced flow.
- Integrate CFD tool to analyze both air side and refrigerant side fluid flow and heat transfer.

Appendix

HEAT TRANSFER AND PRESSURE DROP CORRELATIONS

Air-Side Heat Transfer Coefficient

Plain fin and tube

Kim-Youn-Webb (Staggered tube layout)

$$j_{N>3} = 0.163 \text{Re}_D^{-0.369} (\text{St} / \text{Sl})^{0.106} (s / D)^{0.0138} (\text{St} / D)^{0.13}$$

$$j_{N=1,2/N=3} = 1.043 [\text{Re}_D^{-0.14} (\text{St} / \text{Sl})^{-0.564} (s / D)^{-0.123} (\text{St} / D)^{1.17}]^{(3-N)}$$

Wavy plate fin-and-tube

Kim-Yun-Webb

Staggered tube layout

$$j_{N>3} = 0.394 \text{Re}_D^{-0.357} (\text{St} / \text{Sl})^{-0.272} (s / D)^{-0.205} (x_f / p_d)^{-0.558} (p_d / s)^{-0.133}$$

$$j_{N=1,2} = j_{N=3} (0.978 - 0.010N) \quad (\text{Re}_D \geq 1000, N = 1,2)$$

$$j_{N=1,2} = j_{N=3} (1.350 - 0.162N) \quad (\text{Re}_D < 1000, N = 1,2)$$

In-line tube layout

$$j = 0.37 \text{Re}_D^{-0.186} (s / D)^{-0.045} \quad (\text{Re}_D \geq 2000, N = 2,3,4)$$

$$j = 0.238 \text{Re}_D^{-0.528} (s / D)^{-0.635} \quad (\text{Re}_D < 2000, N = 4)$$

$$j_N / j_4 = 1.350 - 0.097N \quad (\text{Re}_D < 2000, N = 2,3)$$

Airside Pressure Drop

Plain fin and tube

Kim-Youn-Webb (Staggered tube layout)

$$\Delta P = \Delta P_f + \Delta P_t$$

$$\Delta P_f = f_f \frac{A_f G_c^2}{A_c 2\rho}$$

$$\Delta P_t = f_t \frac{A_t G_c^2}{A_{c,t} 2\rho}$$

$$f_t = \frac{4}{\pi} \left(0.25 + \frac{0.118}{[St/D-1]^{1.08}} Re^{-0.16} \right) [S_t/D-1]$$

$$f_f = 1.455 Re_D^{-0.656} (St/SI)^{-0.347} (s/D)^{-0.134} (St/D)^{1.23}$$

Wavy plate fin-and-tube

Kim-Yun-Webb

Staggered tube layout

$$f_t = 4.467 Re_D^{-0.423} (St/SI)^{-1.08} (s/D)^{-0.0339} (x_f/p_d)^{-0.67}$$

In-line tube layout

$$f_t = 0.571 Re_D^{-0.601} (s/D)^{-0.82}$$

Refrigerant Side Heat Transfer Coefficients

Kandlikar

$$h_{NBD} = 0.6683 Co^{-0.2} (1-x)^{0.8} h_{i_o} + 1058 Bo^{0.7} (1-x)^{0.8} F_{\#} h_{i_o}$$

$$h_{CBD} = 1.1360Co^{-0.9}(1-x)^{0.8}h_{lo} + 667.2Bo^{0.7}(1-x)^{0.8}F_{fi}h_{lo}$$

Gunger-Winterton

$$h_{tp} = Eh_l + Sh_{pool}$$

$$E = 1 + 24000Bo^{1.16} + 1.37(1/X_{tt})^{0.86}$$

$$S = \frac{1}{1 + 1.15 \times 10^{-6} E^2 Re_l^{1.17}}$$

$$h_l = 0.023Re_l^{0.8} Pr_l^{0.4} k_l / d$$

$$h_{pool} = 55P_r^{0.12} (-\log_{10} P_r)^{-0.55} M^{-0.5} q^{0.67}$$

$$E_2 = Fr^{(0.1-2Fr)}$$

$$S_2 = \sqrt{Fr}$$

Dobson

$$Nu = 0.023Re_l^{0.8} Pr_l^{0.4} \left[1 + \frac{2.22}{X_{tt}^{0.89}} \right]$$

Jung-Radermacher

Pure fluid

$$h_{tp} = Nh_{SA} + F_p h_l$$

$$N = 4048 X_{tt}^{1.22} Bo^{1.13}$$

$$h_{SA} = 207 \frac{k_f}{bd} \left(\frac{qbd}{k_f T_{sat}} \right)^{0.745} \left(\frac{\rho_v}{\rho_l} \right)^{0.581} Pr_l^{0.533}$$

$$F_p = 2.37 \left(0.29 + \frac{1}{X_{tt}} \right)^{0.85}$$

$$h_i = 0.023 Re_i^{0.8} Pr_i^{0.4} k_f / d$$

Mixture

$$h_{tp} = \frac{N}{C_{UN}} h_{UN} + C_{me} F_p h_i$$

$$C_{UN} = [1 + (b2 + b3)(1 + b4)](1 + b5)$$

$$b2 = (1 - X) \ln \left(\frac{1.01 - X}{1.01 - Y} \right) + X \ln \left(\frac{X}{Y} \right) + |Y - X|^{1.5}$$

$$b3 = 0 \quad (X \geq 0.01)$$

$$b3 = (Y / X)^{0.1} - 1 \quad (X < 0.01)$$

$$b4 = 152 (\rho / \rho_{c,mve})^{3.9}$$

$$b5 = 0.92 |Y - X|^{0.001} (\rho / \rho_{c,mve})^{0.66}$$

$$X / Y = 1 \quad (X = Y = 0)$$

$$h_{UN} = \frac{h_i}{C_{UN}}$$

$$h_i = \frac{1}{\frac{X_1}{h_1} + \frac{X_2}{h_2}}$$

$$C_{me} = 1 - 0.35|Y - X|^{1.56}, \quad 0.9 < C_{me} \leq 1$$

Shah evaporation

$$Ns = Co \quad \text{for} \quad Fr_{le} \geq 0.04$$

$$Ns = 0.38Fr_{le}^{-0.3}Co \quad \text{for} \quad Fr_{le} < 0.04$$

$$Fs = 14.7 \quad \text{for} \quad Bo \geq 11 \times 10^{-4}$$

$$Fs = 15.4 \quad \text{for} \quad Bo < 11 \times 10^{-4}$$

$$\psi_{cb} = 1.8Ns^{-0.8}$$

for $Ns > 1.0$

$$\psi_{nb} = 230Bo^{0.5} \quad \text{for} \quad Bo > 0.3 \times 10^{-4}$$

$$\psi_{nb} = 1 + 46Bo^{0.5} \quad \text{for} \quad Bo \leq 0.3 \times 10^{-4}$$

$$\psi_s = \max(\psi_{nb}, \psi_{cb})$$

for $Ns \leq 1.0$:

$$\psi_{bs} = FsBo^{0.5} \exp(2.74Ns^{-0.1}) \quad \text{for} \quad 0.1 < Ns \leq 1.0$$

$$\psi_{bs} = FsBo^{0.5} \exp(2.47Ns^{-0.15}) \quad \text{for} \quad Ns \leq 0.1$$

$$\psi_s = \max(\psi_{bs}, \psi_{cb})$$

$$\psi_s = \frac{h}{h_l}$$

$$Co = \left(\frac{1-x}{x} \right)^{0.8} \left(\frac{\rho_v}{\rho_l} \right)^{0.5}$$

$$Bo = \frac{q''}{Gh_{lv}}$$

$$Fr_{le} = \frac{G^2}{\rho_l^2 g D}$$

Shah condensation

$$\frac{h}{h_{lo}} = (1-x)^{0.8} + \frac{3.8x^{0.76}(1-x)^{0.04}}{(P/P_{cr})^{0.38}}$$

Traviss

$$\frac{hD}{k_l} = \frac{0.15Pr_l Re_l^{0.9}}{F_T} \left[\frac{1}{X_{tt}} + \frac{2.85}{X_{tt}^{0.476}} \right]$$

$$X_{tt} = \left(\frac{1-x}{x} \right)^{0.9} \left(\frac{\rho_v}{\rho_l} \right)^{0.5} \left(\frac{\mu_l}{\mu_v} \right)^{0.1}$$

$$F_T = 5Pr_l + 5 \ln(1 + 5Pr_l) + 2.5 \ln(0.0031 Re_l^{0.812}) \quad \text{for } Re_l > 1125$$

$$F_T = 5Pr_l + 5 \ln[1 + Pr_l(0.0964 Re_l^{0.585} - 1)] \quad \text{for } 50 \leq Re_l \leq 1125$$

$$F_T = 0.707 Pr_l Re_l^{0.5} \quad \text{for } Re_l < 50$$

Refrigerant Side Two-Phase Pressure Drop

Jung-Radermacher

$$\Delta P_{tp} = \frac{2f_{lo} G^2 L}{D \rho_l} \left[\frac{1}{x} \int_0^x \phi_{tp}^2 dx \right]$$

$$\text{where, } \phi_{tp}^2 = 12.82 X_{tt}^{-1.47} (1-x)^{1.8}$$

REFERENCES

- AEA Technology Engineering Software Hyprotech, 2001, HTFS Software Solutions, AEA Technology Engineering Software Hyprotech, Didcot, Oxfordshire OX11 0QR, UNITED KINGDOM.
- ASHRAE, 1997, Handbook Fundamentals, SI Edition.
- Bagalagel, S.M., Sahin A.Z., 2002, "Design Optimization of Heat Exchangers with High-Viscosity Fluids", *International Journal of Energy Research*, Vol., 26, No.10, pp.867-880.
- Bansal, P., Chin, T., 2003, "Modeling and Optimization of Wire-and-Tube Condenser", *International Journal of Refrigeration*, Vol. 26, No.3, pp. 601-613.
- Bejan, A., 1977, "The Concept of Irreversibility in Heat Exchanger Design: Counterflow Heat Exchangers for Gas-to-Gas Applications", *ASME Journal of Heat Transfer*, Vol.99, pp.374-380.
- Bensafi, A., Borg, S., and Parent, D., 1997, "CYRANO: A Computational Model for the Detailed Design of Plate-Fin-and-Tube Heat Exchangers Using Pure and Mixed Refrigerants", *International Journal of Refrigeration*, Vol. 20, No.3, pp. 218-228.
- Bigot, G., Clodic D., 2002, "Tube by Tube Simulation for Global Design of R-407C Evaporators", *Proceedings of 16th International Compressor Engineering and 9th International Refrigeration and Air Conditioning Conferences*.
- Bulck, E., "Optimal Design of Cross Flow Heat Exchangers", 1991, *ASME Journal of Heat Transfer*, Vol.113, pp.341-347.
- Carey, V., 1992, *Liquid-Vapor Phase-Change Phenomena*, Taylor & Francis.
- Chang, Y., Wang, C., 1997, "A Generalized Heat Transfer Correlation for Louver Fin Geometry", *International Journal of Heat and Mass Transfer*, Vol.40, pp. 533-544.
- Chang, Y., Hsu, K., Lin, Y., Wang, C., 2000, "A Generalized Friction Correlation for Louver Fin Geometry", *International Journal of Heat and Mass Transfer*, Vol.43, pp. 2237-2243.

- Chaudhuri, P.D., and Diwekar, U.M., 1997, "An Automated Approach for the Optimal Design of Heat Exchangers", *Ind. Eng. Chem. Res.*, Vol. 36, pp. 3685-3693.
- Chisholm, D., 1980, "Two-phase Flow in Bends", *International J. of Multiphase Flow*, vol.6, pp.363-367.
- Chisholm, D., 1983, "Two-phase Flow in Pipes and Heat Exchangers", Institute of Chemical Engineers.
- Chung, K., Lee, K.S., and Kim, W.S., 2002, "Optimization of the Design Factors for Thermal Performance of a Parallel-Flow Heat Exchanger", *International Journal of Heat and Mass Transfer*, Vol.45, pp.4773-4780.
- Coello, C.A., 2002, "Theoretical and Numerical Constraint-Handling Techniques Used with Evolutionary Algorithms: A Survey of the State of the Art", *Comput. Methods Appl. Mech, Engrg.*, No.191, pp.1245-1287.
- Corberan, J. M., and Melon M.G., 1998, "Modeling of Plate Finned Tube Evaporators and Condensers Working with R134a", *International Journal of Refrigeration*, Vol. 21, No.4, pp. 273-284.
- Cutler, B., 2000, Development of a Carbon Dioxide Environmental Control Unit, M.S. Thesis, University of Maryland.
- Deb, K., 2000, "An Efficient Constraint Handling Method for Genetic Algorithms", *Comput. Methods Appl. Mech, Engrg.*, No.186, pp.311-338.
- Didi, M., Kattan, N., Thome, J., 2001, Prediction of Two-Phase Pressure Gradients of Refrigerants in Horizontal Tubes", *International Journal of Refrigeration*, article in press.
- Dobson, M.K., Chato, J.C., 1998, "Condensation in Smooth Horizontal Tubes", *ASME Journal of Heat Transfer*, Vol.120, pp.193-213.
- DOE, 2001, Annual Energy Review 2000.
- DOE, 1999, A Look at Residential Energy Consumption in 1997.
- DOE, 1998, A Look at Commercial Buildings in 1995.
- Domanski, P.A., 1991, "Simulation of an Evaporator with Non-Uniform One-Dimensional Air Distribution", *ASHRAE Transaction*, pp 793-802, pt 1.

Domanski, P.A., 1999, "Finned-tube Evaporator Model with a Visual Interface", *International Congress of Refrigeration*, 20th. IIR/IIF. Proceedings. September 19-24, 1999, Sydney, Australia, pp1-7.

Domanski, P.A., 2003, "EVAP-COND, Simulation Models for Finned Tube Heat Exchangers", National Institute of Standards and Technology Building and Fire Research Laboratory Gaithersburg, MD, USA

Fabbri, G., 1997, "A Genetic Algorithm for Fin Profile Optimization", *International Journal of Heat and Mass Transfer*, Vol., 40, No. 9, pp. 2165-2172.

Fabbri, G., 1998, "Optimization of Heat Transfer through Finned Dissipators Cooled by Laminar Flow", *International Journal of Heat Fluid Flow*, Vol., 19, pp.644-654.

Fax, D., Mills, R., 1957, "Generalized Optimal Heat Exchanger Design", *Transactions of the ASME*, pp. 653-661, April.

Geary, D., 1975, "Return Bend Pressure Drop in Refrigeration Systems", *ASHRAE Transactions*, Vol. 81, pt.1, pp.250-257.

Gen, M., Cheng, R., 2000, *Genetic Algorithms & Engineering Optimization*, John Wiley & Sons, Inc.

Gunger, K.E., Winterton, R.H., 1986, "A General Correlation for Flow Boiling in Tubes and Annuli", *International Journal of Heat and Mass Transfer*, Vol., 29, No. 3, pp. 351-358.

Hahne, E., Spindler, K., Skok, H., 1993, "A New Pressure Drop Correlation for Subcooled Flow Boiling of Refrigerants", *International Journal of Heat and Mass Transfer*, Vol.36, No.17, pp.4267-4274.

Heat Transfer Consultants, Inc., 2001, STX/ACX, Heat Transfer Consultants, Inc. Pleasant Hill, CA 94523, USA

Hedderich, C., Kelleher, M., Vanderplaats, G., 1982, "Design and Optimization of Air-Cooled Heat Exchangers", *ASME Journal of Heat Transfer*, Vol.104, pp.683-689.

Heun, M.K., Dunn, W.E., 1996, "Principles of Refrigerant Circuiting with Application to Microchannel Condensers: Part1—Problem Formulation and the Effects of Port Diameter and Port Shape," *ASHRAE Transactions*, Vol.102, pp.373-381.

Heun, M.K., Dunn, W.E., 1996, "Principles of Refrigerant Circuiting with Application to Microchannel Condensers: Part2—the Pressure drop Effects and the Cross-Flow Heat Exchanger Effect," *ASHRAE Transactions*, Vol.102, pp.382-383.

Hill, J., Jeter, S., 1991, "A Linear Subgrid Cooling and Dehumidification Model with Emphasis on Mass Transfer", *ASHRAE Transactions*, Vol.97, pp.118-128.

Hwang, W., Kim, B., and Dessiatoun, S., 1996, "Boiling Heat Transfer Correlation for Carbon Dioxide", *Journal of Enhanced Heat Transfer*, Vol. 3, No. 4, pp. 301-309.

Jegede, F., Polley, G., 1992, "Optimum Heat Exchanger Design", *Trans. IchemE*, Vol.70, pp.133-141.

Jiang, H., et al, 2002, "A User-Friendly Simulation and Optimization Tool for Design of Air-Cooled Heat Exchangers", *Proceedings of 16th International Compressor Engineering and 9th International Refrigeration and Air Conditioning Conferences*.

Johnson C.M., Vanderplaats, G.N., Marto, P.J., 1980, "Marine Condenser Design Using Numerical Optimization", *Journal of Mechanical Design*, Vol.102, pp.469-475.

Judge, J., Radermacher, R., 1997, "A Heat Exchanger Model for Mixtures and Pure Refrigerant Cycle Simulations", *International Journal of Refrigeration*, Vol. 20, No 4, pp.244-255.

Jung, D.S., Radermacher, R., 1989a, "Prediction of pressure drop during horizontal annular flow boiling of pure and mixed refrigerants", *Int. J. of Heat and Mass Transfer*, vol.32, pp.2435-2446

Jung, D.S., McLinden, M.O., Radermacher, R., Didion, D., 1989b, "A Study of Flow Boiling Heat Transfer with Refrigerant Mixtures", *International Journal of Heat and Mass Transfer*, Vol. 32 No 9, pp.1751-1764.

Jung, D.S., Radermacher, R., 1993, "Prediction of Evaporation Heat Transfer Coefficient and Pressure Drop of Refrigerant Mixtures", *International Journal of Refrigeration*, Vol. 16, No. 5, pp. 330-338.

Jung, D.S., Radermacher, R., 1991, "Prediction of Heat Transfer Coefficient During Evaporation of Various Refrigerants", *ASHRAE Transactions*, Vol. 97, Part 2, Paper #3492.

Kakac, S., Liu, H., 2002, Heat Exchangers: selection, rating, and thermal design. 2th edition, CRC Press.

Kandlikar, S.G., 1990, "A General Correlation for Saturated for Two-Phase Flow Boiling Heat Transfer in Horizontal and Vertical tubes", *Journal of Heat Transfer, Transactions of ASME*, Vol.112, pp.219-228.

Kandlikar, S.G., 1991, "A model for correlating flow boiling heat transfer in augmented tubes and compact evaporators", *Journal of Heat Transfer, Transactions of ASME*, Vol.113, pp.966-972.

Kandlikar, S.G., 1997, "Boiling Heat Transfer with Binary Mixtures, Part II-Flow Boiling in Plain Tubes", *ASME National Heat Transfer Conference*, Vol.4, pp.27-34.

Kays, W.M., London, A.L., 1984, Compact Heat Exchangers, 3rd edition, McGraw-Hill Book Company.

Kempiak, M.J., Crawford, R.R., 1992, "Three-Zone, Steady-State Modeling of a Mobile Air-Conditioning Condenser", *ASHRAE Transactions*, Vol.98, pt1, pp.475-488.

Kim, M-H, Bullard, C., 2002, "Air-side Hydraulic Performance of Multi-louvered Fin Aluminum Heat Exchangers", *International Journal of Refrigeration*, Vol. 25, pp. 390-400.

Kim, M-H, Bullard, C., 2002, "Air-side Performance of Brazed Aluminum Heat Exchangers under Dehumidifying Conditions", *International Journal of Refrigeration*, Vol. 25, pp. 924-934.

Kim, N.H., Youn, B., Webb, R.L., 1999, "Air-Side Heat Transfer and Friction Correlations for Plain Fin-and-Tube Heat Exchangers with Staggered Tube Arrangements", *Journal of Heat Transfer, Transactions of ASME*, Vol.121, pp.662-667.

Kim, N.H., Yun, J.H., Webb, R.L., 1997, "Heat Transfer and Friction Correlations for Wavy Plate Fin-and-Tube Heat Exchangers", *Journal of Heat Transfer, Transactions of ASME*, Vol.119, pp.560-567.

Klimenko, V., 1988, "A Generalized Correlation for Two-Phase Forced Flow Heat Transfer", *International Journal of Heat and Mass Transfer*, Vol.31, No.3, pp.541-552.

- Kovarik, M., 1989, "Optimal Heat Exchanger", *ASME Journal of Heat Transfer*, Vol.111, pp.287-293
- Kumar, K.P., Venkatarathnam, G., 2000, "Optimization of Matrix Heat Exchanger Geometry", *ASME Journal of Heat Transfer*, Vol.122, pp.579-585.
- Kundu, B., Das, P.K., 1997, "Optimum Dimensions of Plate Fins for Fin-Tube Heat Exchangers", *Int. J. of Heat and Fluid Flow*, Vol.18, No.5, pp.530-537,
- Kuppan, T., 2000, *Heat Exchanger Design Handbook*, Marcel Dekker.
- Lee, H., Lee, S., 2001, "Heat Transfer Correlation for Boiling Flows in Small Rectangular Horizontal Channels with Low Aspect Ratios", *International Journal of Multiphase Flow*, Vol. 27, pp. 2043-2062.
- LeRoy, J., et al, 1998, "Computer Model Predictions of Dehumidification Performance of Unitary Air Conditioners and Heat Pumps under Extreme Operating Conditions", *ASHRAE Transactions*, Vol.104, pt1, pp.773-788.
- LeRoy, J., et al, 2000 "Evaluating the Accuracy of PUREZ in Predicting Unitary Equipment Performance", *ASHRAE Transactions*, Vol.106, pt1, pp.200-215.
- Levine, D., 1996, *Users Guide to the PGAPack Parallel Genetic Algorithm Library*, Argonne National Laboratory.
- Liang, S., Wong, T., and Nathan, G., 2001, "Numerical and Experimental Studies of Refrigerant Circuitry of Evaporator Coils", *International Journal of Refrigeration*, Vol. 24, pp. 823~833.
- Lindsay, D., 2000, *NetworkBuilder Notes*, internal paper, July.
- Lockhart, R., Martinelli, R., 1949, "Proposed Correlation of Data For Isothermal Two-Phase Component Flow in Pipes", *Chemical Engineering Progress*, Vol.45, No.1, pp.39~48.
- London, A., Shah, R., 1983, "Cost of Irreversibilities in Heat Exchanger Design", *Heat Transfer Engineering*, vol.4, pp.59-73.
- McQuiston, F., Parker, J., 1994, *Heating, Ventilating, and Air Conditioning, Analysis and Design*, John Wiley & Sons, Inc., 4th edition, (enthalpy method, Schmidt fin)
- McQuiston, F., 1978, "Heat, Mass and Momentum Transfer Data for Five Plate-Fin-Tube Heat Transfer Surfaces", *ASHRAE Transaction*, pp.266~293.

McQuiston, F., 1978, "Correlation of Heat, Mass and Momentum Transport Coefficients for Plate-Fin-Tube Heat Transfer Surfaces with Staggered Tubes", *ASHRAE Transaction*, pp.294~301.

Mirth, D.R., 1993, Experimental Studies and Mathematical Modeling of Chilled-Water Cooling Coils, Ph.D. Thesis, Purdue University.

Mullen, C., et al, 1998, "Development and Validation of a Room Air-Conditioning Simulation Model", *ASHRAE Transactions*, v 104, n 2, p 389-397.

Murata, K., Hijikata, K., 1997, "Optimization of Two-Phase Flow Evaporator by Varying the Channel Cross Section", *Heat Transfer-Japanese Research*, Vol.26, No.3, pp.143-157.

NIST, 2001, NIST Thermodynamic and Transport Properties of Refrigerants and refrigerant Mixtures-REFPROP Version 7.0, National Institute of Standards and Technology, Boulder, Colorado, USA.

Oliet, C., et al, 2002, "Numerical Simulation of Dehumidifying Fin-and-Tube Heat Exchangers: Modeling Strategies and Experimental Comparisons", *Proceedings of 16th International Compressor Engineering and 9th International Refrigeration and Air Conditioning Conferences*.

Olson, D., Allen, D., 2002, "Heat Transfer in Turbulant Supercritical Carbon Dioxide Flowing in a Heated Horizontal Tube", NIST Report, Gaithersburg, MD 20899.

Oskarsson, S. et al, 1990, "Evaporator Models for Operation with Dry, Wet, and Frosted Finned Surfaces, Part I: Heat Transfer and Fluid Flow Theory", *ASHRAE Transactions*, Vol.96, pt.1, pp.373-380.

Oskarsson, S. et al, 1990, "Evaporator Models for Operation with Dry, Wet, and Frosted Finned Surfaces, Part II Evaporator Models and Verification", Vol.96, pt.2 pp.381-392.

Paliwoda, A., 1989, "Generalized Method of Pressure Drop and Tube Length Calculation with Boiling and Condensing Refrigerants within the Entire Zone of Saturation", *International Journal of Refrigeration*, Vol. 12, pp. 314-322.

Paliwoda, A., 1992, "Generalized Method of Pressure Drop Calculation across Pipe Components Containing Two-Phase Flow of Refrigerants", *International Journal of Refrigeration*, Vol. 15, pp. 119-125.

Pettersen, J., et al, 2000, "Heat Transfer and Pressure Drop for Flow of Super-critical and Sub-critical CO₂ in Microchannel Tubes", Dept. of Refrigeration and Air Conditioning, Kolbjørn Hejes vei ID, Norway, Internal Circulation Report.

Poddar, T.K., Polley, G.T., 2000, "Optimize Shell-and-Tube Heat Exchanger Design", *Chemical Engineering Process*, Sept., pp.41-46.

Press, W., et al, 1999, *Numerical Recipes in C*, Cambridge University Press.

Queipo, N., et al, 1994, "Genetic Algorithms for Thermosciences Research: Application to the Optimized Cooling of Electronic Components", *International Journal of Heat and Mass Transfer*, Vol.37, No.6, pp.893-908.

Ragazzi, Franco, 1995, "Thermodynamic Optimization of Evaporators with Zeotropic Refrigerant Mixtures", *Ph.D. Dissertation*, University of Illinois, Urbana-Champaign.

Ragazzi, F., Pedersen, C., 1996, "Thermodynamic Optimization of Evaporators with Zeotropic Refrigerants Mixtures," *ASHRAE Transactions*, Vol.102, pt2, pp.367-372.

Reid R., Prausnitz, J., Poling, B., 1987, *The Properties of Gases & Liquids*, 4th Edition, McGraw-Hill, Inc.

Reneaume, J., Pingaud, H., and Niclout, N., 2000, "Optimization of Plate Fin Heat Exchangers, a continuous formulation", *Trans. IChemE*, Vol.78, pp.849-859.

Sakamoto, Y., et al, 199, "An Optimization Method of District Heating and Cooling Plant Operation Based on Genetic Algorithm", *ASHRAE Transactions*, Vol.105, pt2, pp.104-115.

Schmit, T., et al, 1996, "A Genetic Algorithm Optimization Technique for Compact High Intensity Cooler Design", *Journal of Enhanced Heat Transfer*, Vol.3, No.4, pp.281-290.

Sahnoun, A., Webb, R., 1992, "Prediction of Heat Transfer and Friction for the Louver Fin Geometry", *ASME Journal of Heat Transfer*, vol.114, pp.893-900.

Sekulic, D., 1986, "Entropy Generation in Heat Exchanger", *Heat Transfer Engineering*, vol.7, pp.83-88

Sekulic, D., Shah, R., Pignotti, A., 1999, "A Review of Solution Methods for Determining Effectiveness-NTU Relationship for Heat Exchangers with Complex Flow Arrangements," *Appl Mech Rev*, Vol.152, No.3.

- Shah, M.M., 1982, "Chart Correlation for Saturated Boiling Heat Transfer: Equations and Further Study", *ASHRAE Transactions*, Vol.88, pt1, pp.185-196.
- Shah, M.M., 1989, "A General Correlation for Heat Transfer during Film Condensation inside Pipes", *International Journal of Heat and Mass Transfer*, Vol.22, pp.547-556.
- Smith, E.M., 1997, *Thermal Design of Heat Exchangers*, John Wiley & Sons.
- Soliman, et al, 1968, "A General Heat Transfer Correlation for Annular Flow Condensation", *ASME Journal of Heat Transfer*, May 1968, pp.269-276.
- Tayal, M., Fu, Y., Diwekar, U., 1999, "Optimal Design of Heat Exchangers: A Genetic Algorithm Framework", *Ind. Eng. Chem. Res.*, Vol. 38, pp. 456-467.
- Threlkeld, J.L., 1970, *Thermal Environmental Engineering*, 2nd ed., Prentice-Hall, Inc.
- Tillner,R, Roth, G., AWMix Dynamic Link Library, version 1.0, 1998.
- Tran. T., et al, 2000, "Two-phase Pressure Drop of Refrigerants during Flow Boiling in Small Channels: an Experimental Investigation and Correlation Development", *International Journal of Multiphase Flow*, Vol. 26, pp. 1739-1754.
- Traviss, D.P., Rohsenow, W.M., and Baron, A.B., 1973, "Forced Convection Condensation in Tubes: A Heat Transfer Correlation for Condenser Design", *ASHRAE Transactions*, Vol.79, pt1, pp.157-165
- Turaga, M., Guy, R., 1985, "Refrigerant Side Heat Transfer and Pressure Drop Estimates for Direct Expansion Coils. A Review of Works in North American Use", *International Journal of Refrigeration*, Vol. 8, pp.134-142.
- Unknown Author, 2002, "Evaluation of Existing Evaporation Heat Transfer Models in Horizontal Micro-Fin Tubes", paper for review to be published.
- Vardhan, A. and Dhar, P.L., 1998, "A New Procedure for Performance Prediction of Air Conditioning Coils", *International Journal of Refrigeration*, Vol. 21, No.1, pp. 77-83.
- Vargas, J.V., Bejan, A., 2001, "Thermodynamic Optimization of Finned Crossflow Heat Exchangers for Aircraft Environmental Control Systems", *International J. of Heat and Fluid Flow*, Vol.22, pp.657-665.

Vargas, J.V., Bejan, A., Siems, D.L., 2001, "Integrative Thermodynamic Optimization of the Crossflow Heat Exchanger for an Aircraft Environmental Control System", *ASME J. of Heat Transfer*, Vol.123, pp.760-769.

Wallis, G., 1969, *One-dimensional Two-phase Flow*, McGraw-Hill Book Company.

Wang, C., et al, 1997, "Performance of Plate Finned Tube Heat Exchangers under Dehumidifying Conditions", *ASME J. of Heat Transfer*, Vol.119, pp.109-117.

Wang, L., Sunden, B., 2003, "Optimal Design of Plate Heat Exchangers with and without Pressure Drop Considerations", *Applied Thermal Engineering*, Vol.23, pp. 295-311.

Witte, L.C., 1988, "The Influence of Availability Costs on Optimal Heat Exchanger Design", *ASME J. of Heat Transfer*, Vol.110, pp.830-835.

Zhang, M., Webb, R., 1999, "Correlation of Two-Phase Friction for Refrigerants in Small-Diameter Tubes", paper for review to be published.

Zubair, S.M., Kadaba, P.V., and Evans, R.B., 1987, "Second-Law-Based Thermodynamic Optimization of Two-Phase Heat Exchangers", *ASME Journal of Heat Transfer*, Vol. 109, pp.287-294.